

Truck Technology Efficiency Assessment (TTEA) Project Final Report

November 2012

Prepared by

Tim LaClair, Zhiming Gao, Adam Siekmann (ORNL)

Joshua Fu, Jimmy Calcagno, Jeongran Yun (University of Tennessee, Knoxville)

Energy and Transportation Science Division

**TRUCK TECHNOLOGY EFFICIENCY ASSESSMENT (TTEA) PROJECT
FINAL REPORT**

Tim LaClair
Zhiming Gao
Adam Siekmann

Date Published: November 6, 2012

Prepared by
OAK RIDGE NATIONAL LABORATORY
Oak Ridge, Tennessee 37831-6283
managed by
UT-BATTELLE, LLC
for the
U.S. DEPARTMENT OF ENERGY
under contract DE-AC05-00OR22725

Table of Contents

List of Figures	iii
List of Tables	vi
EXECUTIVE SUMMARY	vii
1. Project Overview	1
1.1. Partner Roles.....	2
2. Vehicle Efficiency Modeling Methodology and the Tractive Energy Model	3
2.1. Calculation of Energy Savings Due to Vehicle Efficiency Technologies	10
2.2. Validation of the Tractive Energy Method and Concluding Remarks Concerning its Relevance.....	11
3. Preparation of Data Files from the Heavy Truck Duty Cycle (HTDC) Project.....	16
3.1. Data Processing.....	17
3.2. Mass Estimations	21
4. Synthetic Drive Cycle Creation	29
4.1. The concept of a synthetic drive cycle.....	30
4.2. The Drive Cycle Generation (DCGen) Tool for developing a synthetic drive cycle	31
4.3. Validating the Use of a Synthetic Drive Cycle and the Tractive Energy Model for Predicting the Fuel Efficiency Benefits from Advanced Vehicle Technologies	37
5. Tractive Energy Analysis Results Based on the Synthetic Drive Cycle	43
5.1. The synthetic drive cycle corresponding to the overall fleet usage	43
5.2. Tractive energy reductions and fuel savings associated with vehicle efficiency technologies ..	48
5.3. Average fuel savings for the overall fleet usage	51
5.4. Summary of the tractive energy model results for the class 8 tractor-trailer application evaluated	54
5.5. Consideration of the accuracy of using a substitute drive cycle as opposed to the synthetic drive cycle.....	55
6. EPA MOVES (Motor Vehicle Emission Simulator) Model Analysis	57
6.1. Objective	60
6.2. MOVES Modeling Analysis/Discussion.....	60
6.2.1. MOVES mean base rates for running exhaust emissions	60
6.2.2. Emissions calculation procedure using the MOVES method	61

6.2.3.	Comparison of MOVES predictions with measured emissions data from one of the HTDC test trucks	62
6.2.4.	Validation of the synthetic cycle methodology for MOVES simulations: comparison of results using a synthetic drive cycle that represents a full day of measured drive cycle data.....	67
6.2.5.	Evaluation of the emissions reductions from advanced efficiency technologies for the overall HTDC fleet usage using MOVES.....	70
6.2.6.	Comparison of results using an alternative drive cycle with those from the synthetic cycle.....	74
6.2.7.	Comparison of emissions estimates for synthetic and real drive cycles versus the default MOVES drive cycles.....	76
6.3.	Summary and Conclusions of the MOVES analysis.....	79
7.	Recommendations for Future Research.....	81
	APPENDIX – Table of the synthetic drive cycle representing the full usage of HTDC drive data	84

LIST OF FIGURES

Figure 1	Drive cycle example to indicate the periods of tractive energy savings (in black) when aerodynamic drag is reduced for a conventional vehicle.	4
Figure 2	The aerodynamic drag power during periods of positive tractive power for the drive cycle shown in Figure 1. The integral of this power represents the aerodynamic drag contribution to the total driving tractive power.	5
Figure 3	Periods of active braking during the drive cycle.	6
Figure 4	The braking power, which represents the maximum recoverable power with regenerative braking.	6
Figure 5	Comparison between the driving tractive power calculated using the tractive energy method, the engine power estimated from the tractive power, and the measured engine power during a measured drive cycle.	12
Figure 6	Comparison of the calculated tractive energy and the cumulative fuel consumption (measured) during periods of positive tractive power during a measured drive cycle. .	13
Figure 7	Cross-plot of the cumulative fuel consumption and the driving tractive energy results.	14
Figure 8	Comparison of the engine power requirement predicted with the tractive energy model and Autonomie for the first portion of the drive cycle.	15
Figure 9	Comparison of fuel consumption predicted by the tractive energy model and by Autonomie.	15
Figure 10	Comparison of the measured elevation and USGS elevation data for the same route (based on a lookup using the measured position).	20
Figure 11	Comparison of the grade determined from raw elevation data and after filtering, for two time segments.	21
Figure 12	Plot of the tractive energy curves, based on measured engine data and determined from the drive cycle data, as used in the mass estimation. This sample case shows a mass change occurring at about 8 hours that was not properly identified by the automated calculation.	24
Figure 13	Plot of the tractive energy curves after the corrections were completed in the mass calculation.	25
Figure 14	Plot showing the measured weight data during a day with two load changes.	26
Figure 15	Distribution of masses for all segments of travel in the HTDC project.	27
Figure 16	Adjusted mass distribution, based on a 12.65% increase compared to the original mass estimate.	29
Figure 17	Bivariate histogram of the velocity and acceleration for a day of driving.	32
Figure 18	The DCGen tool module 1 interface.	33
Figure 19	Difference and segment histograms during the creation of a synthetic drive cycle.	34
Figure 20	Plot of a single drive segment in DCGen tool program module two, showing the speed and elevation changes.	34
Figure 21	DCGen tool, second module segment search interface.	34

Figure 22	Manually-generated DCGenT synthetic plot.....	35
Figure 23	Manual DCGenT segment data.....	36
Figure 24	Manual DCGenT synthetic histogram.....	36
Figure 25	Driving data used to develop the validation synthetic drive cycle.....	37
Figure 26	Synthetic drive cycle developed from the driving data presented in Fig. 23.....	38
Figure 27	Bivariate histogram of the original driving data and of the synthetic drive cycle developed for the validation.....	38
Figure 28	Original and synthetic histograms shown with the scale modified to highlight the low speed operating conditions.....	40
Figure 29	Relative Fuel Savings estimates based on the tractive energy model for (a) the original drive cycle and (b) the synthetic drive cycle. The variations evaluated were for a mass reduction of 2000 kg, a reduction in C_{RR} by 0.0015 and a 10% reduction in C_d . The efficiency of the regenerative braking system is assumed to be 80%.....	42
Figure 30	Comparison of the speed vs. acceleration distributions for the low, medium and high mass operating conditions.....	44
Figure 31	The main synthetic drive cycle developed for the TTEA project, representing the overall usage of the HTDC fleet.....	45
Figure 32	Comparison of the distribution of the synthetic drive cycle and the original histogram containing all of the data from the medium mass operation.....	46
Figure 33	Modified synthetic drive cycle, with the proper ratio of idle time for the overall average. The cycle duration is 3448 seconds.....	47
Figure 34	Fuel savings estimate for combinations of advanced efficiency technologies for the low mass case.....	49
Figure 35	Fuel savings estimate for combinations of advanced efficiency technologies for the medium mass case.....	50
Figure 36	Fuel savings estimate for combinations of advanced efficiency technologies for the high mass case.....	51
Figure 37	Fuel savings estimate for combinations of advanced efficiency technologies for the combined usage in the HTDC fleet.....	54
Figure 38	Comparison of the histogram for substitute measured drive cycle to that of the overall usage for the HTDC fleet.....	55
Figure 39	Fuel savings estimate using the substitute measured drive cycle.....	57
Figure 40	Measured dynamometer hub speed data from the WVU dynamometer testing with the ORNL4LS drive cycle.....	63
Figure 41	Nitrogen oxide emissions measured during the dynamometer test and the mean base rates predicted by MOVES using speed data from the ECU.....	64
Figure 42	Carbon monoxide emissions measured during the dynamometer test and the mean base rates predicted by MOVES using speed data from the ECU.....	64
Figure 43	Gaseous hydrocarbon emissions measured during the dynamometer test and the mean base rates predicted by MOVES using speed data from the ECU.....	65
Figure 44	Energy consumption measured during the dynamometer test and the mean base rates predicted by MOVES using speed data from the ECU.....	65

Figure 45	MOVES default cycles for average speeds 87.2 km/h (54.2 mph) and 95.6 km/h (59.4 mph)	77
Figure 46	Operating mode bin distribution for the original, synthetic, and MOVES average speed cycles.....	79

LIST OF TABLES

Table 1:	Comparison of results predicted with Autonomie to those from the tractive energy model.....	16
Table 2:	Data contained in the Excel spreadsheet during the calculation of the mass for the case shown in Fig. 10.....	24
Table 3:	Data used for the mass adjustment.	28
Table 4:	Comparison of results for the energy loss factors in the tractive energy model, for the original and synthetic drive cycles from the validation case.	41
Table 5:	Default values for parameters used in the tractive energy analysis.....	42
Table 6:	Summary of idling, separated by mass case.	47
Table 7:	Intermediate results of the tractive energy analysis for the low mass case, using the synthetic drive cycle. The results are based on the default model parameters shown in Table 4.....	48
Table 8:	Predicted driving tractive energy and contributions from energy loss factors for the medium mass case, using the synthetic drive cycle.....	49
Table 9:	Driving tractive energy and contributions from the different energy loss factors for the high mass case, based on the synthetic drive cycle.	50
Table 10:	Distance-normalized tractive energy factors from the tractive energy analysis for each mass case, and the combined result for the full fleet.....	53
Table 11:	Distance traveled in each mass case.	53
Table 12:	The contributions to the driving tractive energy from each energy loss factor for the overall, combined fleet usage, based on the synthetic drive cycle.	53
Table 13:	The contributions to the driving tractive energy from each energy loss factor for the overall, combined fleet usage, based on the synthetic drive cycle.	56
Table 14:	MOVES operating modes	58
Table 15:	MOVES default driving schedules for HD vehicles	59
Table 16:	Comparison of total emissions and energy consumption results from dynamometer measurements and MOVES predictions.....	67
Table 17:	Summary of MOVES predicted emissions for the validation synthetic cycle case, with a comparison of the original and synthetic drive cycle results.....	69
Table 18:	Emissions reductions associated with different advanced efficiency technologies as predicted by MOVES using the synthetic drive cycle representing the HTDC driving data. ...	73
Table 19:	Comparison of MOVES-predicted emissions using the synthetic drive cycle with those calculated using a substitute measured drive cycle.....	75
Table 20:	Comparison of the overall usage synthetic drive cycle and the MOVES default drive cycle based on the average speed of the synthetic cycle.	78

EXECUTIVE SUMMARY

Medium- and heavy-duty trucks and buses are responsible for over 28% of the energy used and emissions generated in highway transportation, and class 8 tractor-trailers operating in long-haul and regional cargo transport are responsible for about 75% of all fuel consumed by commercial trucks. The vehicle miles traveled (VMT) for trucks is expected to increase at a rate significantly outpacing passenger VMT growth, which will result in a steady rise in the percentage of energy consumption (and emissions) attributable to trucks over the coming decades. These facts have sparked significant recent interest in truck fuel efficiency in the transportation community.

Although fuel economy regulations in the United States have historically focused on passenger cars, recent legislation requiring new standards for fuel economy in medium- and heavy-duty trucks aims to increase the efficiency of trucks as well. The development of regulations for truck fuel efficiency is quite challenging, however, since vehicle usage and configurations vary substantially among the very diverse set of trucking applications. Fuel economy is very strongly linked to the particular drive cycles followed by a given truck, as are the gains in efficiency that can be realized by implementing new technologies. As demonstration of this fact, a technology that provides significant fuel efficiency gains for one trucking application may yield little improvement or could even be detrimental to fuel economy in a different trucking application. It is therefore critical that the usage of each application be well understood and carefully evaluated to select the set of technologies that can provide the greatest benefits for each application.

Although it is well known that drive cycle data representative of a vehicle or fleet's usage is crucial for an accurate evaluation of fuel economy benefits or to identify an optimum set of technologies to reduce fuel consumption, detailed drive cycle data of trucks are not readily available for many applications. The Oak Ridge National Laboratory (ORNL) has collected a rather extensive set of truck duty cycle data in an effort to characterize the usage of several trucking applications. During the first phase of ORNL's duty cycle data collection activities, drive cycle measurements were made from six tractor-trailers during normal operations in a regional commercial shipping fleet, operating primarily in the southeastern U.S., for a period of a full year. This data, contained in the Heavy Truck Duty Cycle (HTDC) project database, was analyzed in detail for the current research effort in the Truck Technology Efficiency Assessment project. Based on the high fidelity HTDC duty cycle data, the results of this study are therefore highly representative of tractor-trailer operations for this type of regional, freeway-dominant trucking application.

The TTEA project used data collected in the prior study to develop a drive cycle with the same statistical characteristics for the accelerations, speeds and associated power from the engine as those for the complete set of data from the HTDC database. This drive cycle, which is highly representative of the complete usage of these vehicles, is a synthesis of all of the information contained in the original data set, but the resulting synthetic drive cycle is less than one hour in length and is thus appropriate for use in vehicle performance models or in fuel economy or emissions testing. A rigorous approach and

software tools were developed for generating the synthetic drive cycle, and the methodology was validated against measured fuel consumption data as part of this project.

The mass of the vehicles during each segment of travel was also extracted from the data to determine the load distribution as a function of distance traveled. The drive cycle and load results were then used to quantify the energy use attributed to the multiple energy loss factors associated with heavy duty truck operation and to assess the fuel savings potential of implementing various advanced efficiency technologies. This research employed a vehicle tractive energy analysis to explore measured, real-world drive cycle data in order to quantify the effectiveness of technologies that impact the fuel consumption of heavy duty trucks. A detailed analysis of the complete set of measured drive cycle data was performed to develop a better understanding of how advanced efficiency technologies impact the fuel consumption and emissions of class 8 tractor-trailers in regional truckload operations.

Although the class 8 tractor-trailer application considered for this study is the most well understood of all trucking applications, results from this study still provided a few surprises and interesting results:

1. First, the duration of engine idle operation was 49.9% of the total engine run time for the fleet studied. This idling was responsible for the consumption of approximately 22,000 liters (5830 gallons) of diesel fuel from the six trucks during a year of data collection, which increased the average fuel consumption rate by approximately 1.9 L for each 100 km traveled and corresponds to about 5% of the total fuel consumption for this trucking fleet. The vast majority of the idling (47.2%) occurred during periods exceeding 5 minutes, indicating that stops in traffic were 2.7% of the idling, and the majority of the long term idling took place over several hours at a time. It is estimated that the use of an auxiliary power unit (APU) on each truck could have saved approximately 15,800 L (4150 gallons) of diesel during the year for the six trucks. Engine start-stop technology to reduce idling in congestion and at stop lights, however, would yield relatively small benefits for this trucking application.
2. The tractive energy analysis indicated that about 10% of the tractive energy losses are due to braking or engine braking, which represents a significant quantity of energy available for recovery using a regenerative braking system. Although only some fraction of this energy could be recovered with a hybrid powertrain (so the fuel savings benefit with a hybrid system would be less than the 10%), this magnitude of energy availability is rather surprising for a fleet that operates mostly on freeways with an average driving speed of 95 km/hr (59 mph). It is considered likely that many regional tractor-trailer fleets that drive more regularly in off-freeway operations could likely exceed a break-even point for the benefits of a hybrid system incorporating regenerative braking.
3. It was rather unexpected that the statistical distribution of accelerations and speeds changed very little with changes to the vehicle load. In developing the synthetic drive cycle from the complete set of measured driving data, several load categories were evaluated. The acceleration-speed distributions for low load (<20,000 kg [44,000 pounds]), medium load (10,000 to 28,180 kg [62,000 pounds]) and high loads (>28,180 kg) were all very similar, even though a reduced load enables the trucks to accelerate more quickly due to an effectively higher

power-to-weight ratio. This similarity in drive cycle for all load ranges simplifies the analysis since it is not necessary to have separate drive cycles for different loads.

4. Concerning the distribution of loads carried, it was found that the average mass of the loaded vehicles from this study was only about 24,750 kg (54,500 pounds). It is frequently assumed that tractor-trailer freight operations consist of fully loaded tractor-trailers operating at close to maximum load, but the distribution of loads carried by the study fleet covered the full range from empty to full. This is important not only in quantifying the benefits of efficiency technologies, but also in considering potential policy actions that might be pursued to increase the operational efficiency of our nation's freight delivery.

The tractive energy analysis estimated approximately 6.6% in fuel savings possible, on average, from a 1.5 kg/ton reduction in the coefficient of rolling resistance, a level that is typically achieved when replacing conventional dual tires with new generation wide-base single (NGWBS) tires. For a 10% reduction in aerodynamic drag coefficient, which can be achieved when implementing many of the aerodynamic reduction devices currently available, the fuel savings is estimated to be 3.9%. A mass reduction of 2000 kg, through the use of lightweight materials in the truck construction, is estimated to provide fuel savings of approximately 4.1% assuming that the same loads would be carried. These savings are substantial and can provide not only reductions in trucking operational costs, but can help the nation to reduce its reliance on foreign oil, thereby improving our energy security.

The MOVES analysis conducted in this project confirmed that the synthetic drive cycle methodology provides consistent results to those that would be predicted when using the original driving data. MOVES predictions of the emissions reductions possible with the implementation of various combinations of advanced efficiency technologies showed that sizable emissions reductions are achievable for this vehicle application, particularly for NO_x, PM and CO₂ emissions. Predicted reductions of HC and CO emissions were very limited based on the MOVES results, but it was found that these emissions did not match measured emission levels very well, so these predictions are somewhat questionable.

Although there are certainly differences among class 8 tractor-trailer fleets, this study provides valuable insight into the energy and emissions reduction potential that various technologies can bring in this important application. The synthetic drive cycle developed from a full year of measured data on six trucks from the fleet studied is believed to be quite typical of class 8 tractor-trailer operations.

This study supports the U.S. Department of Transportation (DOT) in its mission to address energy efficiency and conservation, energy security, global climate change in transportation, and related environmental impacts. For the development of truck fuel efficiency standards, in particular, the authors of this report believe that the results of this research will be particularly useful in evaluating the fuel economy and emissions reductions benefits that can be expected in this important class of vehicles. The same analysis approach can also provide further insight in other vehicle applications, and it is hoped that the approach developed in this study will be useful in characterizing vehicle usage and energy savings potential in other trucking applications.

1. Project Overview

This project consists primarily of a detailed analysis of a large data set of duty cycle measurements collected from a class 8 trucking fleet operating in the southeastern United States. The primary objective of the TTEA project was to quantify the potential fuel consumption and emissions reductions that can be achieved using advanced energy efficiency technologies for a regional class 8 trucking operation, including combinations of these technologies. To evaluate the potential fuel savings and emissions reductions that these technologies can bring, a unique analysis approach was followed. First, a synthetic drive cycle that is highly representative of the complete operation of the fleet was developed, based on a statistical evaluation and analysis of the entire set of drive cycle measurements collected during a previous Oak Ridge National Laboratory (ORNL) study. The synthetic drive cycle is appropriate to use both for modeling and testing purposes, and the results when using this cycle should very closely match the performance for the overall trucking fleet since the drive cycle measurements were collected from six trucks during a full year of normal operations in the fleet and are therefore very representative of the fleet's overall operations. To evaluate the energy savings that can be achieved with various energy efficiency technologies, a tractive energy analysis was employed using the synthetic drive cycles developed. An additional result of the analysis of the drive cycle data included a determination of the mass distribution of the vehicles during the fleet's operations, and this distribution was also incorporated in the analysis for assessing the fuel and emissions savings potential for the fleet. The final result of this study is an assessment of the overall potential for fuel savings and emissions reduction that can be expected if any combination of the technologies considered were to be implemented in the fleet. This data and the analysis approach employed can assist the DOT in quantifying the improvements in fuel economy that can be realized in the U.S. trucking fleet through the implementation of specific technology options. Furthermore, this assessment enables a detailed evaluation of the costs associated with implementing the technology needed to achieve specific fuel efficiency targets for class 8 tractor-trailers.

For the emissions evaluations, the U.S. Environmental Protection Agency's (EPA's) MOVES (Motor Vehicle Emission Simulator) model was used to characterize the emissions of the trucks. Parameters that are relevant to the vehicles tested were used in the analysis, and the MOVES model was run using both the default drive cycles in MOVES for class 8 tractor-trailers and the synthetic drive cycle developed in this project, which represents the detailed usage of the fleet. The MOVES model results were also compared directly to emissions measurements that were conducted as part of ORNL's data collection activities in the previous research effort. In this way, the relevance of the MOVES model was evaluated. It is therefore expected that these results can be used by the EPA in making improvements to the MOVES software.

The development of a synthetic drive cycle from extensive drive cycle measurements is a new approach for generating a drive cycle that is highly representative of the overall operations. Due to the manner in which the synthetic drive cycle is generated, the results from an analysis or test when using it will be

extremely similar to those that would be achieved if the complete data set were analyzed or tested. Therefore, when a large data set representative of the overall fleet operations is used as the basis for developing the synthetic drive cycle, the cycle can be used to estimate, with high accuracy, the fuel savings benefits that would be attainable in the fleet if particular technologies are deployed. The accuracy of using a synthetic drive cycle as a substitute for a broader data set that the synthetic drive cycle represents was demonstrated in this project through a validation study that examined a full day's drive cycle. The predicted energy savings based on the 30-minute synthetic drive cycle matched the results from the full cycle to within 1% for each of the evaluations considered. The synthetic drive cycle approach can be used at any scale to develop characteristic drive cycles for any fleet of similar vehicles. The tools developed for this project can be of great benefit to policy makers in evaluating the benefits of advanced vehicle technologies at the national level and for different trucking applications, although specific drive cycle data needs to be available to characterize each application.

The advanced efficiency technologies evaluated for this project include regenerative braking (hybrid systems), aerodynamic drag reduction devices, low rolling resistance tires, vehicle mass reduction, and idle reduction technologies. The method can also be used to quantify and compare fuel savings due to improvements in engine thermal efficiency and reductions in accessory power loads. To evaluate the fuel saving potential of these technologies, the study analyzed existing data that was collected from six tractor-trailers during a period of over one year as part of a DOE-sponsored activity at ORNL (the Heavy Truck Duty Cycle, or HTDC, project) [1]. Inherent in these data are the impact of driver behavior, congestion, and other real-world issues associated with heavy-duty truck operations. Accurate duty cycle data—speed, elevation and load histories as a function of time—are critical to determining fuel economy and emissions, and the fuel savings potential of advanced efficiency technologies also depends very strongly on how the vehicle is driven. Therefore, it is essential that relevant, real-world duty cycle data be used to perform any evaluations regarding fuel savings potential. ORNL's HTDC database is believed to contain the most comprehensive measurement of real-world duty cycle information available and serves as a high-fidelity representative set of duty cycle information for the class 8 regional tractor-trailer application evaluated in this study.

1.1. Partner Roles

The TTEA project was completed as a joint research effort between ORNL and the University of Tennessee, Knoxville (UTK). ORNL, which is the largest Department of Energy (DOE) science laboratory, was the primary technical lead and project manager for the TTEA project, while UTK provided technical and analysis support for the MOVES modeling activities.

ORNL, through its Center for Transportation Analysis (CTA), has extensive background in the collection and analysis of truck drive cycle data and this work extends the analysis of data contained in the HTDC database. For the project, ORNL was responsible for the processing of all drive cycle data files, software development for creation of the synthetic drive cycles, all drive cycle development, and fuel economy modeling using the tractive energy model and Autonomie software. ORNL also conducted additional emissions analysis using measured emissions data and an empirical modeling approach.

The UTK Department of Civil and Environmental Engineering has specific expertise and conducts research in climatic change, environmental impact assessments, transportation and air quality, and vehicle emissions. UTK's primary responsibility in the project was to perform all of the modeling and analysis using the EPA MOVES model, including the comparison of results with measured emissions data.

2. Vehicle Efficiency Modeling Methodology and the Tractive Energy Model

Before moving into the details of the data processing and synthetic drive cycle creation performed for the project, it is instructive to first provide a summary of the tractive energy analysis approach used to evaluate the fuel saving potential of the advanced efficiency technologies of the class 8 tractor-trailers. The full analysis methodology is described in detail in [2], but a general discussion of the method is given below and the fundamental equations used are presented here.

An accurate prediction of the fuel savings achievable in a fleet or for a particular trucking application when various fuel efficiency technologies are implemented can be very challenging, particularly when considering combinations of technologies. Differences in highway vehicle usage can strongly influence the benefits realized with any technology, which makes generalizations about fuel savings inappropriate for different vehicle applications. For this reason, it is critical that any evaluation of the fuel efficiency benefits that can be achieved when implementing advanced vehicle technologies must be based on a usage that is very representative of the fleet or application under consideration. For this project, a tractive energy analysis is used to estimate the potential for reducing fuel consumption when advanced efficiency technologies, including combinations of these technologies, are employed. The analysis uses relatively simple assumptions to generate a first order estimate of the fuel savings that can be realized when basic parameters of the vehicle configuration are changed, as occurs with the implementation of fuel efficiency technologies. The intention of this analysis approach is to identify the classes of technologies that have the greatest potential for improving fuel economy, and when the model is used with a drive cycle that is highly characteristic of the overall usage of a fleet or for a given application, the results provide a means to quantify the fuel savings that can be expected for that fleet or application when a particular technology or set of technologies is implemented. This can also serve as a starting point for performing cost evaluations to select technologies (and ultimately specific products) that can yield the greatest efficiency gains in the most cost-effective manner.

While a vehicle is driving, the power required at the wheels (referred to as the tractive power) is determined from the combination of all forces acting on the vehicle. The instantaneous power from the engine consists of the driving tractive power plus any power transmission losses in the drivetrain of the vehicle and the mechanical power consumption of the accessories that are driven by the engine, such as the air conditioning system, engine fan, alternator, etc. In most cases, and especially for trucks, the driving tractive power represents a dominant portion of the engine power, and the other power inputs can be represented with reasonable accuracy simply by using an average value for the accessory power and a constant value for the drivetrain efficiency. If more precise information is available and it is

relevant in evaluating a particular technology, more detailed data regarding the power consumed by individual accessories can be included in the model, but in most cases the tractive contributions to the overall power requirements are what one wishes to evaluate.

It should be understood that most fuel efficiency technologies operate by reducing various energy losses that are inherent in the vehicle operation. For example, aerodynamic drag reduction devices such as fairings, trailer skirts etc. provide a more streamlined vehicle profile, thereby reducing the drag forces that oppose the vehicle's forward motion. The drag reduction causes the driving tractive power requirement to be lessened, and fuel consumption would thus be reduced for the same drive cycle. Not all periods or types of driving provide the same benefits from a technology, however, and in effect, each technology functions by reducing energy losses over a specific portion of the drive cycle. In the case of aerodynamic drag, for example, higher speeds generate greater savings for a given drag coefficient improvement, and there are no tractive energy savings impacting the fuel consumption for a conventional vehicle (without regenerative braking) during the periods of operation when the vehicle is decelerating. This is because engine power output, beyond engine idling, is only required during periods of positive tractive power, and during braking the only effect that a reduction in the aerodynamic drag causes is that a greater braking force is needed to provide the same rate of deceleration. For the drive cycle shown in Fig. 1, therefore, a reduction in aerodynamic drag will generate a reduction in fuel consumption only for those periods shown in black. Figure 2 shows the power associated with the aerodynamic drag over the same periods for this drive cycle. The integral of this power gives the total aerodynamic drag contribution to the driving tractive energy requirement for the drive cycle.

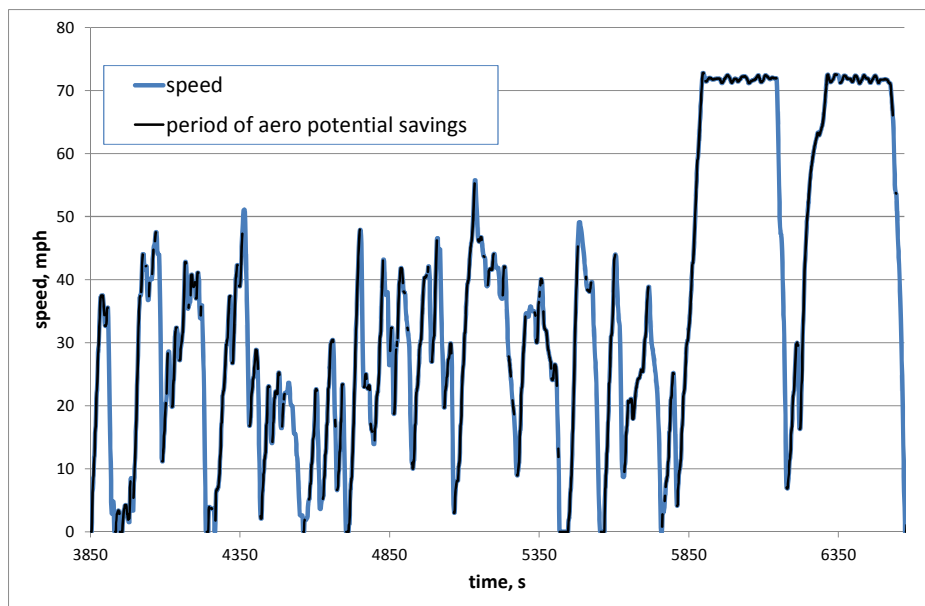


Figure 1 Drive cycle example to indicate the periods of tractive energy savings (in black) when aerodynamic drag is reduced for a conventional vehicle.

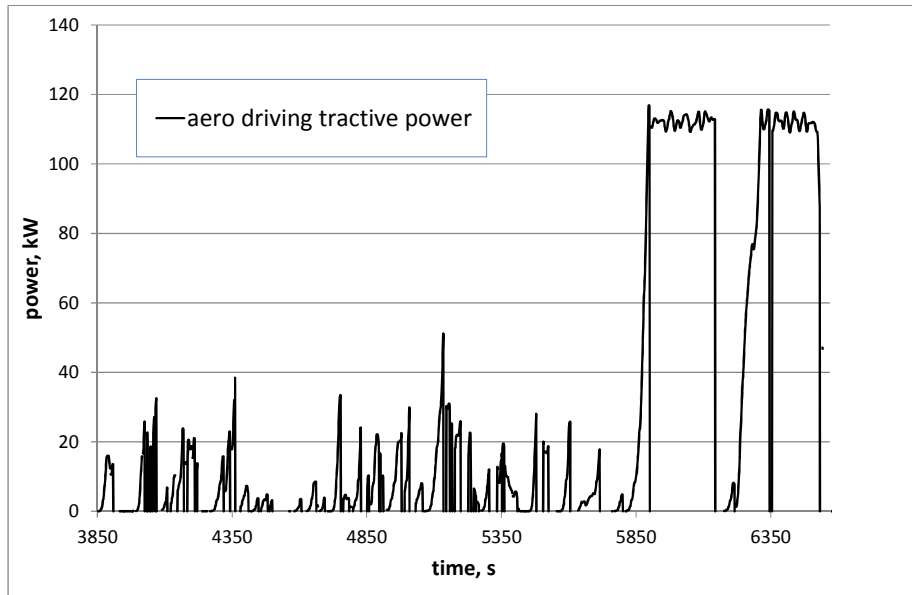


Figure 2 The aerodynamic drag power during periods of positive tractive power for the drive cycle shown in Figure 1. The integral of this power represents the aerodynamic drag contribution to the total driving tractive power.

If a hybrid system with regenerative braking is employed on a vehicle, then some portion of the energy that would be dissipated by the brakes in a conventional vehicle is recovered and stored by the regenerative braking system, and this stored energy will be used at a later portion of the drive cycle to reduce the tractive power required from the engine. This reduces the total driving tractive energy required from the engine, thereby reducing the fuel consumption for the drive cycle. In this case, we see that tractive energy savings are generated during the periods of braking as opposed to periods of driving tractive power for the regenerative braking system. The portion of the drive cycle that regenerative braking functions over is thus complementary to that of the aerodynamic drag (or tire rolling resistance) for a conventional vehicle. Figure 3 shows the portion of the drive cycle in which regenerative braking acts to recover tractive energy, and Fig. 4 shows the power associated with these braking periods, which represents the total available energy that can be recovered by the regenerative braking system.

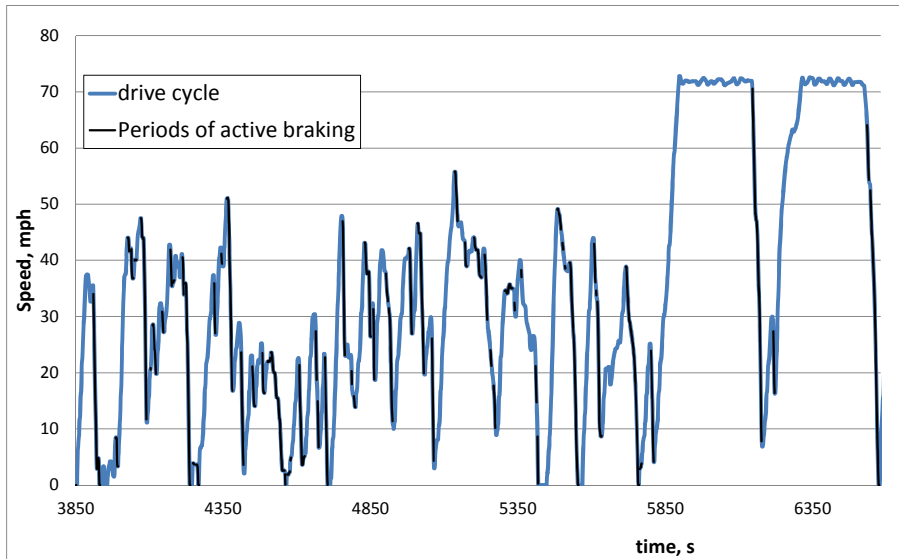


Figure 3 Periods of active braking during the drive cycle.

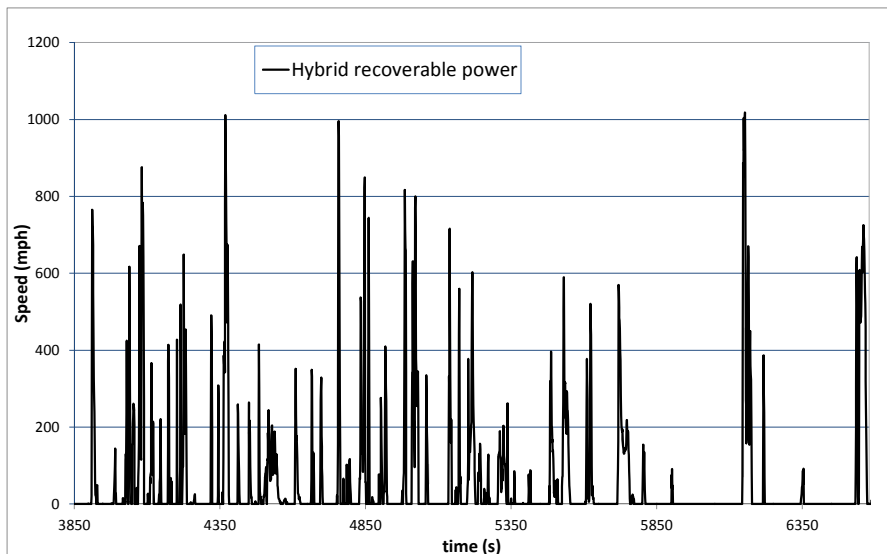


Figure 4 The braking power, which represents the maximum recoverable power with regenerative braking.

If regenerative braking is used in combination with rolling resistance or aerodynamic drag reductions, then more power is available for the regenerative braking recovery during the braking portions of the drive cycle than would be present without the aerodynamic or rolling resistance improvement. By properly tracking each of the energy losses over the entire drive cycle and accounting for the power from each energy loss term during periods of both positive (driving) tractive power and negative (braking) tractive power, the contributions from each energy loss factor to the total mechanical energy required from the engine can be quantified in detail. When the total contribution of each loss factor to the total driving tractive energy is known, it is straightforward to quantify the savings that can be generated if a technology is used that reduces that energy loss factor.

The instantaneous power associated with each loss factor is calculated based on the physics associated with the corresponding energy loss that takes place. For example, the power associated with aerodynamic drag is calculated from the coefficient of drag C_d , the vehicle frontal area A_f , and the speed v using the relationship $\frac{1}{2}\rho v^3 (C_D A_f)$, where ρ is the air density. To distinguish between the periods of driving and braking tractive power, one needs to only consider if the net force at the wheels is positive or negative. The tractive power requirement is positive (driving) if

$$\frac{dv}{dt} > -g \sin \theta - \frac{F_{aero} + F_{RR}}{m} \quad (1)$$

and is negative (braking) if the inequality is reversed. Equality occurs when the vehicle is coasting, so the comparison shows whether the current acceleration is greater or less than the instantaneous coasting acceleration, which can be positive, negative or zero depending on the magnitudes of the aerodynamic and rolling resistance forces, F_{aero} and F_{RR} , respectively, and the grade (given by $\sin \theta$, where θ is the angle relative to horizontal of the roadway). Note that g appearing in Eq. (1) is the gravitational constant and m is the mass of the vehicle. When the vehicle coasts, the tractive energy does not change even though the energy associated with the rolling resistance and aerodynamic drag continue to accumulate. During these periods, the combined potential and kinetic energies will decrease by the same amount as the energy losses from the rolling resistance and aerodynamic drag. To simplify the accounting of the energies, it is simplest to consider the periods of coasting as contributing to the driving tractive energy. This approach was followed for the tractive energy analysis, although there is very little impact on the results since it is very rare to have strict equality when performing calculations with numerical data.

The *net* tractive energy change for any period of driving includes the dissipative energy losses from rolling resistance and aerodynamic drag as well as the net change in kinetic and potential energies experienced. The result is

$$\begin{aligned} \Delta E_{trac} &= \frac{1}{2}m(v_2^2 - v_1^2) + mg(h_2 - h_1) + \Delta E_{aero} + \Delta E_{RR} \\ &= \Delta E_{kinetic} + \Delta E_{potential} + \Delta E_{aero} + \Delta E_{RR} \end{aligned} \quad (2)$$

The driving tractive energy over the complete drive cycle, which is closely related to the mechanical energy output required from the engine, is therefore obtained by summing the tractive energy changes over all of the segments in which the tractive power is driving:

$$E_{trac,drive} = \left[\frac{1}{2}m \sum_{i,non-braking} (v_{e,i}^2 - v_{s,i}^2) + mg \sum_{i,non-braking} (h_{e,i} - h_{s,i}) + E_{aero,drive} + E_{RR,drive} \right] \quad (3)$$

where $v_{s,i}$ and $v_{e,i}$ are the speeds at the start and end of each time segment i for which the tractive power is driving, and $h_{s,i}$ and $h_{e,i}$ are the elevations at the start and end of each driving tractive power segment. The summations are performed over all of the segments where the tractive power is non-negative.

The contribution to the driving tractive energy from the tire rolling resistance is given by

$$E_{RR,drive} = \int_{t_{drive}} P_{RR} dt = C_{RR} mg \sum_{non-braking} \Delta s_i \quad (4a)$$

where the integration of the power associated with the rolling resistance is performed over the periods when the tractive power is non-negative (Eq. (1)). This result uses the basic linear relationship that the rolling resistance force, $C_{RR} mg$, is proportional to the load carried by the tires, where an average coefficient of rolling resistance, C_{RR} , is used to characterize all of the tires on the vehicle. The summation on the right hand side of the equation is the total distance traveled during the periods of driving tractive power. The rolling resistance contribution to the braking tractive energy is given using the same equation, but with the integration performed over the periods when the tractive power is negative. The result is simply

$$E_{RR,braking} = C_{RR} mg \sum_{braking} \Delta s_i. \quad (4b)$$

The aerodynamic drag contribution to the driving tractive energy is given by

$$E_{aero,drive} = (C_D A_f) \int_{t_{non-braking}} \frac{1}{2} \rho v^3 dt \quad (5a)$$

and as in the case for the rolling resistance, the braking tractive energy contribution from aerodynamic drag is determined simply by integrating over the periods of braking tractive power as opposed to the non-braking periods:

$$E_{aero,braking} = (C_D A_f) \int_{t_{braking}} \frac{1}{2} \rho v^3 dt \quad (5b)$$

The force required for braking (taken as a positive value) is equal to the absolute value of the tractive force during the periods of braking tractive force, and is obtained from a basic consideration of the forces acting on the vehicle,

$$F_{brakes} = - \left(m \frac{dv}{dt} + mg \sin \theta + F_{aero} + F_{RR} \right). \quad (6)$$

The braking energy over the drive cycle is calculated by integrating the braking power, and the final result is given by

$$E_{brakes} = - \left[\frac{1}{2} m \sum_{i,braking} (v_{e,i}^2 - v_{s,i}^2) + mg \sum_{i,braking} (h_{e,i} - h_{s,i}) + E_{aero,braking} + E_{RR,braking} \right]. \quad (7)$$

The summations are performed over all of the segments where the tractive power is negative. The energy consumed by the brakes is not included explicitly in the driving tractive energy, Eq. (3), but vehicle braking acts as a dissipative force, in a manner similar to rolling resistance and aerodynamic drag, that results in additional tractive energy being required to travel the distance traversed over the drive cycle. Dissipative braking actually increases the energy required from the engine since subsequent

acceleration is necessary to attain the speed prior to braking (on flat ground at least) and the braking energy therefore, paradoxically, contributes to the driving tractive energy. It is easily shown using Eqs. (3) through (7) that the total driving tractive energy can be expressed as the sum of the driving and braking contributions of aerodynamic drag and rolling resistance plus the braking energy:

$$E_{trac,drive} = E_{RR,drive} + E_{RR,braking} + E_{aero,drive} + E_{aero,braking} + E_{brakes}. \quad (8)$$

Regenerative braking allows the energy that would otherwise be dissipated to be converted to another form of energy and stored so that it can be used at a later time during the drive cycle. To account for regenerative braking, it is assumed that some fraction of the braking energy could be recovered with a hybrid system, and this fraction is subtracted from the braking losses. (80% is assumed in the results presented for this study, since this is a reasonable round-trip energy efficiency for the conversion from mechanical to electrical energy and back for a generator, battery and motor system. The tractive energy analysis aims to quantify the total energy savings potential when implementing various technologies, and this value is probably representative of an upper limit that might be achievable with any real hybrid system. In any event, it is acknowledged that this approach is rather simplistic, but the actual braking energy recoverable with a hybrid system depends on the size of the motor/generator and the battery, in addition to the power levels dissipated during each deceleration experienced during the drive cycle. In other words, it is dependent on the specific hybrid system used as well as by the actual drive cycle. If the estimated energy savings potential from the tractive energy analysis justifies consideration of the use of a hybrid system for a particular application, then more in-depth analysis should be pursued to determine what characteristics of the system are needed to achieve acceptable results.

With the tractive energy calculated, the total mechanical work required from the engine during the tractive periods is calculated by assuming a constant value of the driveline transmission efficiency, η_{trans} , and a constant accessory power, P_{access} . The engine work associated with the periods of driving tractive power output is therefore given by

$$W_{eng,trac} = E_{trac,drive}/\eta_{trans} + E_{access}. \quad (9)$$

Finally, the conversion of the fuel to mechanical energy is assumed to be provided by an average engine thermal efficiency, η_{engine} , and the heat of combustion, taken to be the lower heating value of the fuel, LHV, is used to determine the volume of fuel consumed. The result for the fuel consumption, as a function of the driving tractive energy is the following:

$$m_{fuel} = \frac{E_{fuel}}{LHV} = \frac{1}{\eta_{engine} LHV} \left(\frac{E_{trac,drive}}{\eta_{trans}} + E_{access} \right). \quad (10)$$

This equation, combined with the driving tractive energy calculation and the tractive energy savings associated with the implementation of technologies, can be used to quantify the fuel savings that is expected from any combination of the technologies. Eq. (10) can also be used to assess improvements in engine efficiency when the impact on the average value of η_{engine} can be estimated, and reductions to the average accessory power requirement can also be evaluated directly and compared with the other technology assessments using this approach. Although this level of evaluation is rather superficial for

evaluating an engine redesign, it does allow the general magnitude of improvements that can be expected for the many technology options and combinations that might be considered to be compared simultaneously. As a final technology that can be considered with the others discussed, idle reduction technologies, such as an auxiliary power unit (APU), can be quantified based on a knowledge of the difference in fuel consumption between the engine when it is idling and the fuel consumption rate of the APU. To evaluate this accurately, the average time fraction of idling for the fleet operation must be known, but this is effectively part of the determination of a characteristic drive cycle, which we address in section 3 of this report.

2.1. Calculation of Energy Savings Due to Vehicle Efficiency Technologies

Once the contributions from the rolling resistance, aerodynamic drag and braking to the tractive energy are calculated, the fuel savings that can be realized with specific technologies that reduce these energy losses can be calculated. The regenerative braking savings potential was discussed above, and different assumptions could certainly be used if particular systems have been characterized more accurately for the regeneration efficiency. Fortunately, the situation is easier for the other terms in the tractive energy calculation, although some knowledge of the magnitude of reduction for the rolling resistance coefficient and the aerodynamic drag coefficient are necessary. The equations used in the tractive energy model are simple but realistic for the rolling resistance and aerodynamic drag, and the estimates for the energy savings are expected to be relatively accurate if the coefficient values used in the model are reasonable. For tire rolling resistance, a common improvement that might be considered is to replace conventional dual tires with new generation wide base single (NGWBS) tires. With existing tire technologies, a typical reduction in the average rolling resistance coefficient for a tractor-trailer when the drive and trailer dual tires are replaced with high efficiency NGWBS tires would be in the range of 0.001 to 0.002 (1 to 2 kg/ton) relative to a typical starting value of 0.007. A reduction of 0.0015 (1.5 kg/ton) for the rolling resistance coefficient is assumed in the results presented in this study. Depending on the initial dual tires being replaced and whether or not high efficiency steer tires will also replace less efficient steer tires, the reduction could be even higher. For a particular case in which specific tires are known, actual rolling resistance coefficient values can be obtained and the reduction in the average rolling resistance coefficient can be calculated fairly precisely. For the reduction in the aerodynamic drag coefficient from various technologies, while detailed characterizations are not readily available for each technology, some values in the literature [3] and the level of fuel savings experienced by users of aerodynamic reduction technologies indicate that coefficient reductions of up to 10% are not unreasonable when implementing devices that are available on the market today. An assumed reduction by 8% from a nominal value for the aerodynamic drag coefficient of 0.62 is assumed for the results presented in this study.

Since the contribution to the driving tractive energy from the rolling resistance or aerodynamic drag is directly proportional to its corresponding coefficient C_{RR} or C_D , respectively, the tractive energy change associated with the technology implementation is also proportional to the corresponding reduction in each of the coefficients. The tractive energy reductions from each factor are calculated individually and the total savings are subtracted from the nominal calculated value of the tractive energy. This approach allows the tractive energy savings to be quantified as a percentage of the total required tractive energy,

which is a very natural and informative way to interpret the energy savings potential. Knowing for example, that the tire rolling resistance can provide, say, an 8% reduction in the total tractive energy establishes the benefits of replacing the tires as being significant and worthy of an evaluation of the cost effectiveness.

The tractive energy calculations can be performed using a single set of parameters representing a baseline vehicle configuration to determine the relative contribution from each energy loss factor, and these can be used in turn to quantify the change in the total tractive energy requirement that will be realized if any of the parameters for the tractive energy factors change. Once the tractive energy calculation is complete, a single calculation that accounts for driveline inefficiencies, the engine thermal efficiency and accessory power requirements can be used to estimate the overall impact on fuel consumption when any combination of the parameters that account for the technologies employed are changed. Finally, the fuel savings from idle reduction technology can be evaluated quite simply based on the difference between the baseline vehicle's idling fuel consumption rate and the rate of consumption when the idle reduction technology is employed (e.g. an auxiliary power unit). This simple approach using the tractive energy method allows fuel savings estimates to be made for any combination of the relevant technologies the savings can be evaluated simultaneously without the need to rerun a model multiple times. It also provides a direct, physics-based evaluation of the fuel savings potential for each technology, which can be used to select technologies that will be most cost effective for providing improved fuel economy.

The simplicity of this approach is a significant strength, but there are of course limitations to what can be achieved. In reality, the efficiency of an engine changes with the engine speed and torque. For the tractive energy model, a single average thermal efficiency value is used to determine the fuel energy required for the engine to generate the tractive energy over the complete drive cycle. Changes to gearing and detailed engine design changes that impact engine efficiency over a range of specific operating conditions cannot be accounted for with this approach and a more precise modeling methodology (such as a vehicle performance simulation using software such as Autonomie or GT Drive) would be necessary to obtain reasonable predictions of the effect of such changes. Nonetheless, even for two vehicles with different engines that are designed to operate in the same application, the space of engine operating conditions (with respect to torque and engine speed) that would be experienced could be expected to be relatively similar when operating over the same drive cycle. This being the case, the general trend for the efficiency maps will likely not differ dramatically, and differences in fuel consumption could still be adequately evaluated using this model based on a characterization of the average thermal efficiency for each engine.

2.2. Validation of the Tractive Energy Method and Concluding Remarks Concerning its Relevance

We now provide a final summary of the utility and capabilities of the tractive energy method to provide additional context. Based on an analysis of a characteristic drive cycle that is highly representative of the operations of a fleet or trucking application, we are able, using the equations presented in this section, to compare the fuel savings potential from the following technologies, or from any combination

of these technologies: aerodynamic drag reduction, rolling resistance reduction, regenerative braking, mass reduction, engine efficiency improvements, reduction of the power from the vehicle accessories, and idling reduction. While the precision of the fuel savings estimates using only this model does differ among the different technologies, as noted in discussions above, the results from this assessment can be very instructive to identify those technologies that can yield the greatest reduction in fuel consumption. It should be emphasized that the tractive energy method relies strongly on a drive cycle evaluation, and in order to obtain the most meaningful results, it is important that the drive cycle evaluated be relevant to the application or fleet under consideration.

Now that we have presented the equations for the tractive energy calculation, a bit of validation concerning the accuracy of the method and its appropriateness for estimating fuel savings potential seems appropriate. It is first noted that estimating the engine power based on the tractive power requirement calculated from the drive cycle is quite accurate, even with the relatively simple assumptions used in the model. Figure 5 compares the measured power (the product of engine torque and engine speed) during a drive cycle plotted with the driving tractive power calculated using the tractive energy method and the estimated engine power, which is determined using Eq. (9). For this comparison, the instantaneous power values are evaluated, not just the total energy terms. While the equations for the power calculations were not presented here, they are quite straightforward to derive from the equations presented and the complete derivation is available in reference [2].

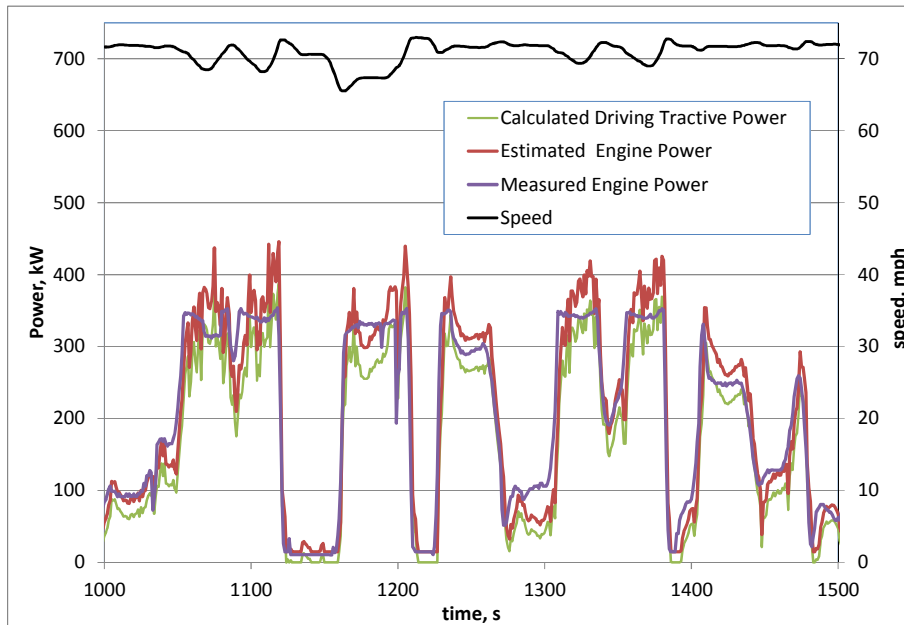


Figure 5 Comparison between the driving tractive power calculated using the tractive energy method, the engine power estimated from the tractive power, and the measured engine power during a measured drive cycle.

The tractive power by itself is reasonably close to the engine power, but by accounting for the transmission efficiency and a typical accessory power, the estimated engine power result is even closer to the measured engine power. It is evident from this comparison that the estimated engine power

trends and overall magnitude are very well matched to the actual measured power from the truck’s engine during the drive cycle. The parameters used in the evaluation were held constant in all cases for this study (except for the vehicle mass, which was determined separately for each segment of driving). Several different cases were evaluated to verify that the predicted power levels were reasonable, and the results prevented are quite typical, even without making any modifications to the parameters of the model for individual cases. This clearly shows that the driving tractive power (and the driving tractive energy, by extension) provides a very good representation for the actual engine power. It is noted that the six tractors tested in the HTDC project were “sister vehicle configurations” of the same type, with the only differences between them being the tires (NGWBS vs. dual tires) and manual vs. automatic transmissions. It is nonetheless quite impressive that the predicted engine power is so well represented with the simple model.

The measured cumulative fuel consumption is next compared to the driving tractive energy during the drive cycle. The two curves are shown separately in Fig. 6, and it is clear that the shapes of the two curves are quite similar during the drive cycle.

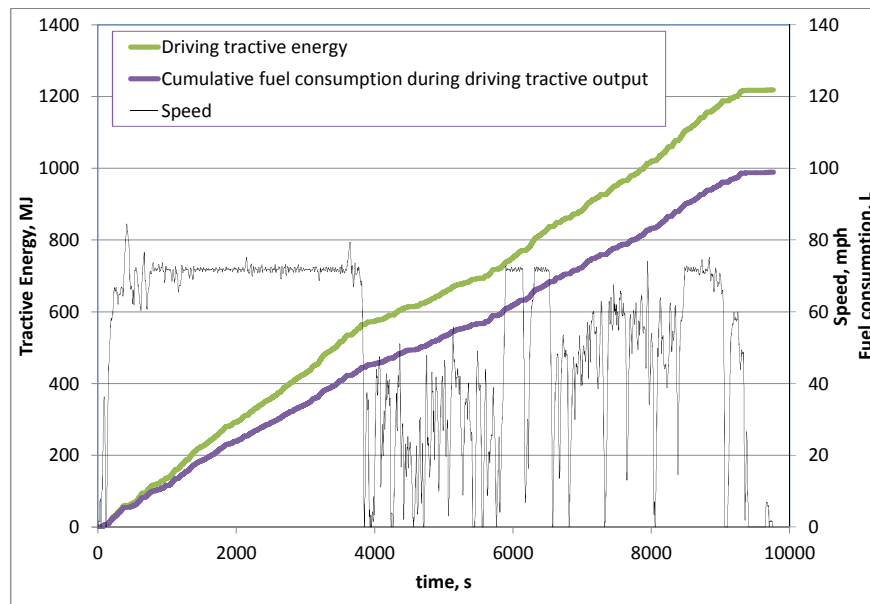


Figure 6 Comparison of the calculated tractive energy and the cumulative fuel consumption (measured) during periods of positive tractive power during a measured drive cycle.

In Fig. 7, we cross-plot the two curves, and it is clear that the correspondence is quite linear between the two variables, even with the very diverse driving conditions experienced during the drive cycle. This confirms that the tractive energy is indeed the primary factor responsible for the fuel consumption from the truck, and this one-to-one correspondence between tractive power and fuel consumption indicates that if the driving tractive energy is reduced (by means of a change in the vehicle configuration), then the fuel consumption will decrease in a linear manner. This result is a very strong validation of the tractive energy method.

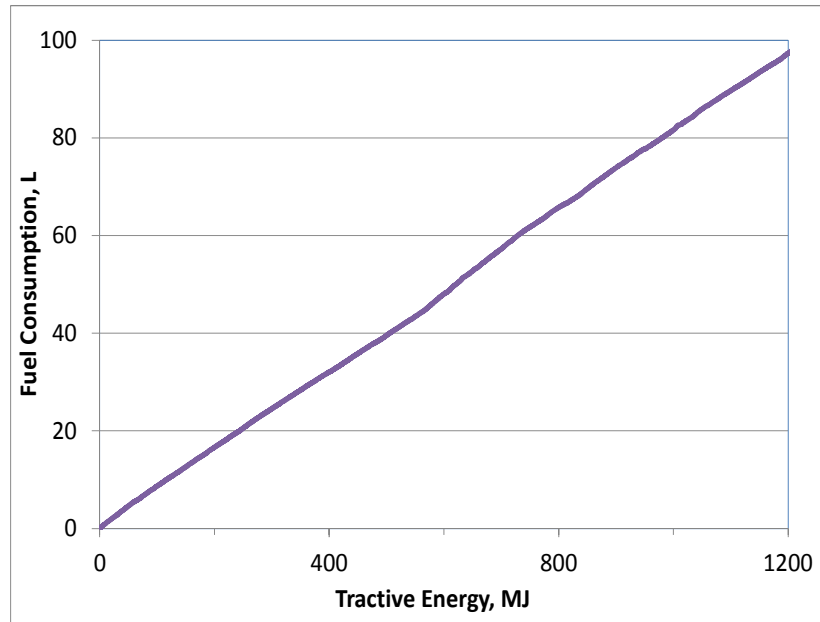


Figure 7 Cross-plot of the cumulative fuel consumption and the driving tractive energy results.

As a validation of the fuel savings predicted by the tractive energy model, ORNL has run several vehicle fuel consumption simulations using Autonomie. Autonomie is a plug-and-play vehicle simulation tool to assess fuel consumption based on a vehicle representation that includes specific engine map fuel consumption data, a complete specification of the drivetrain and a model to simulate driver shifting and acceleration performance [7]. It estimates fuel consumption by applying a detailed physical representation of all of the major powertrain components on the vehicle, and links the forces required to propel the vehicle with an engine map, which characterizes the fuel consumption of the engine as a function of engine speed and torque. An Autonomie vehicle model has been developed at ORNL to represent the vehicles used in the HTDC study. A heavy duty diesel engine map available in Autonomie was used in the model, but the engine parameters were tuned to be representative of the 15-liter, 6-cylinder Cummins ISX 475 diesel engine that was present on the HTDC test vehicles. The transmission in the model is a 10-speed manual transmission, which is also representative of those tractors with a manual transmission used in the study.

For one of the drive cycles that has been analyzed in detail with the tractive energy approach, a complete Autonomie truck model was created that uses the same set of baseline vehicle parameters as the tractive energy model. The parameter variations used in the tractive energy analysis were repeated in the Autonomie simulations in order to validate the energy savings estimates of the tractive energy method against the more detailed model. Figure 8 shows a comparison of the engine power predicted by both models for a portion of the drive cycle, while Fig. 9 is a comparison of the cumulative fuel consumption for the entire cycle. The fuel consumption predicted with the tractive energy model shows some slight deviations from the Autonomie prediction during periods when the driving style changes significantly. This is a result of a more detailed thermal efficiency in the Autonomie model that varies with engine load, whereas the tractive energy model assumes a constant thermal efficiency. Nonetheless, the results from both models match extremely well.

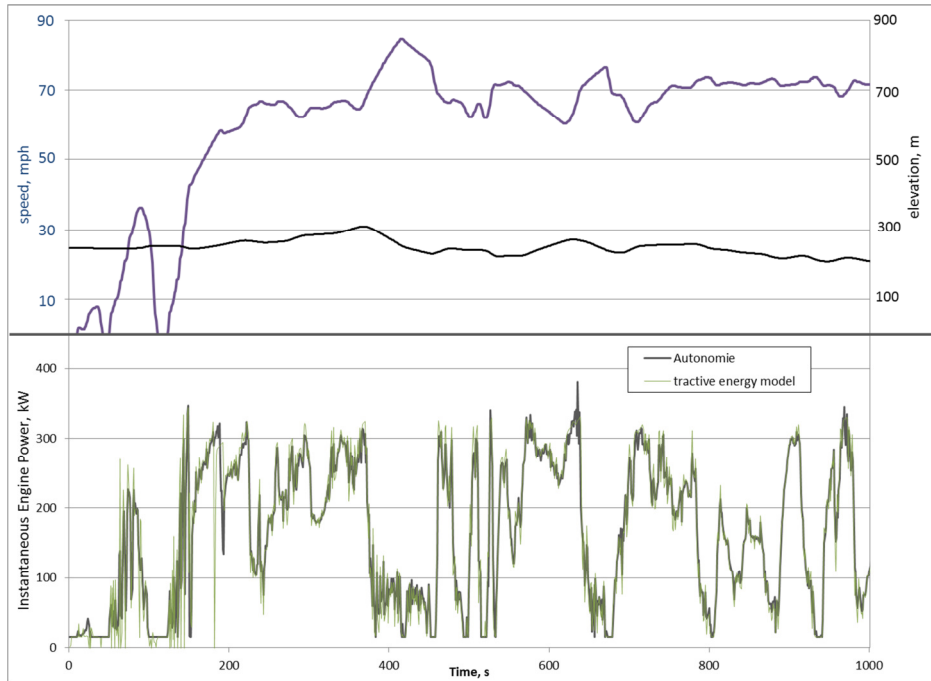


Figure 8 Comparison of the engine power requirement predicted with the tractive energy model and Autonomie for the first portion of the drive cycle.

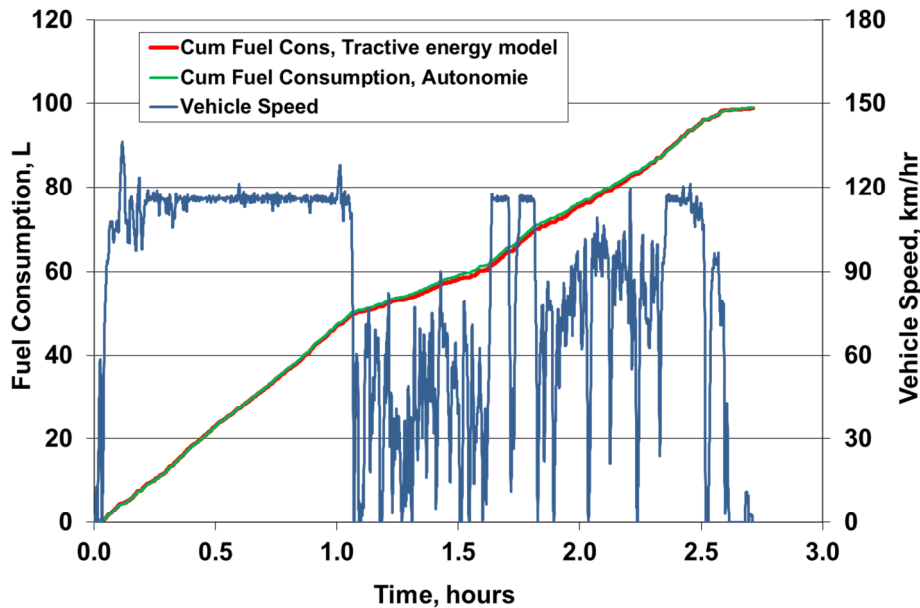


Figure 9 Comparison of fuel consumption predicted by the tractive energy model and by Autonomie.

Table 1 shows a comparison of the energy savings predicted by the Autonomie and Tractive Energy models. The first part of the table is the total energy required from the engine over the drive cycle, while the second part is the fuel consumption. Results are shown for several vehicle configurations, corresponding to parameter changes intended to represent the implementation of various vehicle efficiency technologies.

Table 1: Comparison of results predicted with Autonomie to those from the tractive energy model.

Cumulative Engine Energy Output (MJ)	Tractive Energy Model		Autonomie	
Baseline*	1462.18	% change from base	1435.47	% change from base
20T-Mass	1431.96	-2.1%	1407.28	-2.0%
$C_{RR}=0.0055$	1394.40	-4.6%	1371.18	-4.5%
$C_d=0.52$	1392.29	-4.8%	1368.32	-4.7%
$C_{RR}=0.0055$ & $C_d=0.52$	1325.54	-9.3%	1304.86	-9.1%
20T-Mass & $C_{RR}=0.0055$ & $C_d=0.52$	1297.59	-11.3%	1278.49	-10.9%

Fuel consumption (L/100km)	Tractive Energy Model		Autonomie	
Baseline*	46.32	% change	44.94	% change
20T-Mass	45.38	-2.0%	44.12	-1.8%
$C_{RR}=0.0055$	44.14	-4.7%	43.08	-4.1%
$C_d=0.52$	44.07	-4.9%	42.99	-4.3%
$C_{RR}=0.0055$ & $C_d=0.52$	42.10	-9.1%	41.15	-8.4%
20T-Mass & $C_{RR}=0.0055$ & $C_d=0.52$	41.15	-11.2%	40.40	-10.1%

*Baseline configuration: 21,000 kg, $C_{RR}=0.007$, $C_d=0.58$

The tractive energy model predictions match those of the Autonomie model quite well in terms of the percent savings predicted from each technology. The differences in the engine energy output are within a small fraction of a percent between the two models for all of the parameter variations evaluated and the fuel economy prediction is also reasonable, although the tractive energy model was found to overestimate the benefits somewhat when using the default thermal efficiency value of 0.42. The combination of cases provides a slightly higher error since the differences are cumulative. Nonetheless, this is a very good validation of the tractive energy model's ability to estimate fuel savings associated with advanced efficiency technologies. For this evaluation, the more complicated hybrid system was not considered since an accurate model of the hybrid powertrain for the heavy-duty truck would require a rather substantial effort, and this was not included in the scope of the present project.

3. Preparation of Data Files from the Heavy Truck Duty Cycle (HTDC) Project

This section describes the processing of data files from the Heavy Truck Duty Cycle (HTDC) project that were used to develop the characteristic drive cycle used for the analysis in this project. A brief summary of the HTDC project and data collection is also provided.

The primary data collection for the HTDC project [1] involved conducting a field operational test in which naturalistic driving data was collected and stored from six test vehicles. This testing was performed after initial development and proveout of a data acquisition system (DAS) and instrumentation that could withstand normal operation in a commercial vehicle over extended periods and would be able to operate with no human interaction for initialization on vehicle startup at the beginning of each day or at the beginning of each route. The data collection system consisted of four primary system components:

the DAS, a vehicle self-weighing system, a weather station, and a GPS-based vehicle position and motion system. Measurements were also recorded from the vehicle's data bus, by direct connection from the DAS to the vehicle common area network (CAN). The resulting DAS was capable of collecting 60 channels of data and storing it internally in its dynamic memory. A working fleet (Schrader Trucking of Jefferson City, Tennessee) was selected for partnership in the project, and six tractors and ten box trailers (access was provided gratis by Schrader Trucking) were instrumented in the fall of 2006 using the HTDC DASs. The tractors were 2005 Volvo VNL sleeper cabs, equipped with Cummins ISX 475 engines. The fleet is a dry van truckload (TL) carrier with a regional usage. The first vehicle instrumented was closely monitored in the field for 30 days to evaluate and resolve any issues with the equipment, installation, driver distraction, and software prior to beginning the field operational test.

The drive cycle data collection for the HTDC project began in October 2006 and continued until November 2007. The six instrumented heavy trucks cumulatively hauled freight over more than 690,000 miles, primarily in the southeastern United States within a 500 miles radius of the fleet's base of operation in Jefferson City, Tennessee. During the field operational test, 60 channels of data were recorded at a rate of 5 Hz (5 samples for each data channel every second) any time that the engine was running on each test truck for a twelve-month period, resulting in the collection of 290 GB of raw data. The data collected during the field operational test is believed to be the most comprehensive real-world data set for Class-8 long-haul performance known to exist. The data collected during the FOT included speed, fuel consumption, road grade, location, and weather conditions.

After the drive cycle data collection was completed, one of the trucks tested in the HTDC project was delivered to West Virginia University (WVU), where it was emissions tested for several drive cycles on their Mobile Chassis Dynamometer and Mobile Emissions Measurement System (MEMS) [4]. Data from both the drive cycle measurements and the emissions testing were used for the current project.

3.1. Data Processing

This section documents the procedures followed in processing the measured drive cycle data prior to beginning the primary analysis. The data files were first cleaned, filtered and formatted for input into the drive cycle analysis tool.

A total of 1711 files, each representing one day of driving on an individual truck, were processed. The raw data from the HTDC project were available in text files with each channel stored in a separate column, and each row of data representing a separate time interval. The original data was measured every 0.2s, but it was decided for performing the drive cycle analysis to process the data at a lower frequency of 1 Hz since the velocity and elevation signals, which are most important for the drive cycle development, do not change substantially over time periods shorter than 1 second. Nonetheless, in pre-processing the files that served as inputs to the drive cycle analysis tool, the higher frequency data was retained in case there would be a need for any other purposes.

The channels that were included for performing the present analysis include the time, engine torque, elevation, engine speed, fuel rate, latitude, longitude, and speed. The measured fuel rate data and location information were not used in the main analysis, but they were included to permit additional

evaluations in the event they would be needed. The engine speed and torque data were included to allow the measured power to be determined, since this data was necessary for calculating the vehicle mass, as described in the next section of the report.

The original HTDC data files were always divided at the start of a new day, that is at 12:00 a.m., if the vehicle was running at this time. If the speed was non-zero at the start or end of any file, i.e. if the truck was actually being driven at the day change, then the filtering of speed and elevation data for that file, which relies on forward and backward time calculations, would not provide the correct results. The drive cycle evaluation tool, used for the creation of the synthetic drive cycles, also requires each data file to start at zero speed. Therefore, the files from consecutive days were combined when a file ended with non-zero speed, and the division was made at the next stop. While combining the files, there were several checks of data integrity that were also performed, and information on the file length, maximum speed, average speed, average moving speed and any errors identified in the data for each of the files processed were recorded in a separate file. A sequence of Visual Basic for Applications (VBA) programs were written and run in the Excel environment to perform the file processing, and the files were cleaned and verified in a multi-step process while performing several quality checks of the data. Approximately 1000 lines of VB code were written to perform all of the data processing, filtering and verification functions. Files for which potential errors or corrupt data were identified were reviewed manually to determine what data could be recovered, and data that was clearly corrupt was removed. In some cases, one portion of the file would contain obvious errors, such as gaps in time when the speed was non-zero, speed values out of range or not reasonable based on prior or subsequent data, engine speed or torque data out of range or zero during driving, etc. Data was kept if it would not undermine the quality of the analysis, but in many cases, even large segments of corrupt or questionable data were removed from the files. Fortunately, the overall quality of the data was good, and only a small percentage of the original drive cycle data could not be used. Out of 1711 files, there were 24 files that were entirely or mostly corrupt, and 10 files for which more than 30 minutes of data was corrupt and removed. An additional 64 files contained short segments of data that were corrupt and removed or required cleansing. The primary cause of corrupt data was a lack of GPS data, which contained the elevation data channel (vehicle speed was still normally available from the vehicle CAN bus). Since the road grade, which is calculated from the elevation, is needed for the drive cycle development and the mass calculation procedure, the loss of the GPS signal for extended periods could not be recovered. In cases where one or only a few data points were corrupt in the middle of a long segment of driving, the unknown speed, torque or elevation data points were sometimes filled in by interpolation, or a short portion of the drive cycle data segment would be clipped from the data so that the previous non-corrupt data point matched the next valid speed point with the closest speed. For example, if corrupt data was present when the speed was at 105.5 km/hr., the corrupt data would be removed in addition to valid data until the speed returned to the same value of 105.5 km/hr. (or passed through this speed). Such modifications were only made if the corrupt data segments were relatively short within a long segment of continuous driving, so that the entire segment would not be lost due to a short occurrence of corrupt data. In any event, it is estimated that less than 3% of all of the raw data from the HTDC data set required removal or cleaning. This data processing nonetheless required a considerable amount of time

to complete during the project, due to the quantity of data and the many details involved in performing the processing, but the data quality of the cleansed data is believed to be excellent.

The filtering of the speed data, which was performed prior to re-sampling the data at the 1 Hz frequency used in both the mass estimation and during the synthetic drive cycle analysis, used a discrete first-order low-pass filter applied to a moving median of the raw speed signal. The moving median approach, which used points symmetrically from before and after each time being filtered, eliminates the effect of large deviations in the raw data from the overall trend, so individual data points exhibiting even large errors are rejected. By using a forward-rearward-based signal, the phase shift of the signal is eliminated so that this does not need to be accounted for separately in calculations of the tractive power or for comparisons with other data signals.

The elevation in the HTDC database was obtained from GPS measurements using a RaceLogic VBox II velocity and position measurement system. GPS elevation is known to be less accurate than horizontal positioning measurements (latitude and longitude) [5], and the accuracy of the elevation data recorded was an initial concern for being able to accurately quantify the tractive power requirements from the drive cycle data. The raw data for the GPS elevation was found to exhibit random jumps of up to a meter at any given time, and smaller variations over time in the GPS signal can cause the elevation data to drift somewhat, even when the vehicle is not in motion. Fortunately, roadway elevation does not change rapidly and is very smooth with respect to distance traveled. Engineering standards for road design [6] provide guidelines for how rapidly roadway grade should change, and the maximum grade is also limited based on the type of road traveled. Grades are limited to 7% on interstate highways and 8.75% for the national highway system. This smoothness of road grade allows the time-based GPS elevation signal to be effectively filtered by smoothing the measured changes in elevation that occur as a function of distance traveled. To filter the signal, the sine value of grade (elevation change per unit distance traveled) was calculated using the speed signal in conjunction with the elevation. In a first pass, the grade was set to zero whenever the vehicle was not in motion, and if the calculated grade exceeded 8%, it was assumed that the value was in error and the grade was set to the value of the previous time interval. This set an upper limit of 8% for the roadway grade, which was selected since the roads traveled by the trucks were primarily major highways where the grade should not exceed this value. A moving average of the grade was then calculated using forward and rearward data from the HTDC measurements, as in the case of the velocity filtering, so that there was no shift in the elevation data relative to the other data channels. The moving average provided a second degree of smoothing that gives a very clean set of grade data. The road elevation was then calculated by integrating the grade data using the distance traveled. The starting elevation from each file was used as the initial elevation for the filtered elevation data. It should be noted, however, that the tractive energy calculation does not depend on the absolute elevation, only the elevation changes.

The elevation determined using this filtering approach was compared with land elevation data extracted from the U.S. Geological Survey (USGS) map database (based on a lookup of the measured GPS coordinates) for several segments of travel to have some indication of the accuracy of the raw elevation data, and the grade data was then compared between the raw data and the filtered grade. Figure 10 shows a comparison of the raw GPS elevation data, the filtered data and the USGS survey data along a

route traveled along Interstate 75 between Knoxville and Cleveland, Tennessee, in addition to some secondary roads in the Cleveland area. It is evident that the overall trend of elevation changes is correct for this data. The USGS database includes topological data points on a grid spaced at 30 m spatial resolution horizontally, and the elevation data was interpolated based on the input latitude and longitude values. This is therefore not an accurate representation of the roadway elevation data since the interpolated data does not correspond to the specific positional data in most cases, and the highway elevation will be considerably smoother than the surrounding landscape due to roadway design. The GPS measurement, in spite of its shortcomings, matches the overall elevation change extremely well. It should be noted that the filtered elevation data follows the raw data very closely for most of the segment traveled, to the extent that the two curves cannot generally be distinguished when considering the data over extended time periods. The signals can diverge somewhat at times, however, as in the last 1000 seconds of Fig. 10.

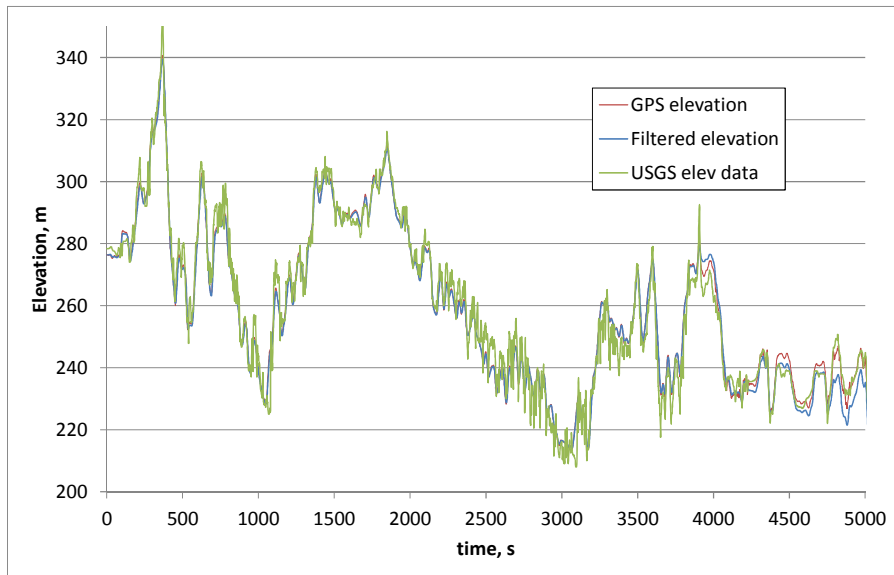
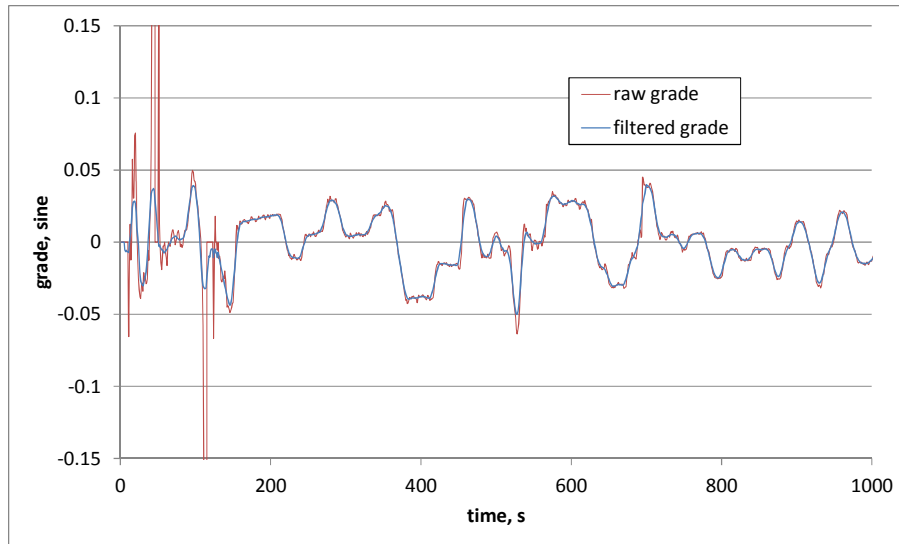
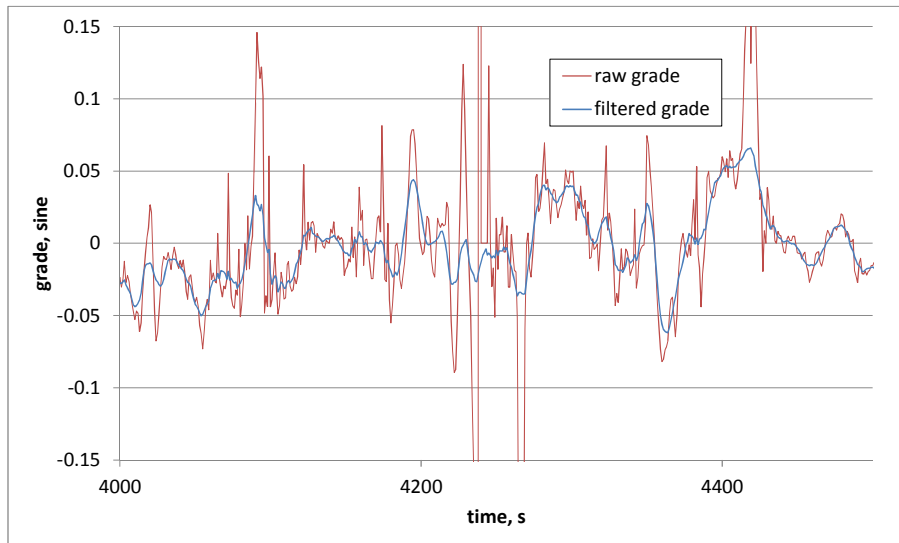


Figure 10 Comparison of the measured elevation and USGS elevation data for the same route (based on a lookup using the measured position).

Figure 11 shows a comparison between the grades calculated using the raw elevation data and the filtered grade. In the first segment, Fig. 11(a), the grade signal smoothing is rather subtle over most of the time traveled, but there are several apparent errors in the signal, with spikes that significantly exceed the 8% (0.08) levels permitted in the selected filtering methodology. For the segment shown in Fig. 11(b), the measured variations in grade are much more pronounced and the filtering is clearly necessary to remove some of the more frequent occurrences of spikes in the grade signal.



(a)



(b)

Figure 11 Comparison of the grade determined from raw elevation data and after filtering, for two time segments.

Although the elevation filtering approach used for the data processing does present the possibility of removing higher grade levels from the data, the measured elevation data includes enough noise that filtering is required. The approach selected provides a reasonable tradeoff that allows the general elevation changes to be captured while eliminating grade signals that, based on the nature of highway design, are unlikely.

3.2. Mass Estimations

Once pre-processing of all of the data files was completed, the project team was nearly ready to perform the drive cycle analysis to generate the synthetic drive cycles. The load carried by the vehicle, however, is also important for the drive cycle characterization and this data is needed for each “micro-trip” in the drive cycle, i.e. each segment of driving between stops. (The term micro-trip is used in the literature for drive cycle evaluations, although we will not use it extensively in our discussion.) In

developing the synthetic drive cycle, it was decided by the project team that separate evaluations should be performed for different ranges of the total vehicle mass so that large differences in acceleration capabilities would not be mixed. Additionally, since the mass plays a primary role in the level of tractive power that is calculated, separating the data based on several ranges of the mass allows more accurate evaluation of the complete range of tractive power variations that occur for the vehicles during actual use.

As mentioned previously in the report, ten trailers were instrumented (for measuring the mass of the trailer using an AirWeigh system), along with the 6 tractors. The fleet owned and operated over 180 trailers total, however, and normal operations did not permit the trailers instrumented for load measurement to always be paired with the instrumented tractors. As a result, in all but a small portion of the test data, the trailer attached to the tractor was not instrumented for load measurements, and the total tractor-trailer load measurement was thus not available for the majority of the data in the HTDC database. An approach was developed to infer the mass based on the other measured data from the vehicle. This section describes the mass estimation calculation and presents the results of the mass distribution for the fleet.

By using the engine torque data, a knowledge of the vehicle speed allows, in principle, a calculation of the mass based on Newton's second law of motion if we know all of the forces acting on the vehicle. Aerodynamic drag force, rolling resistance, and gravitational force can all be estimated using the same assumptions described in section 2 of this report. Even small errors in the measured speed data, however, can lead to large errors for instantaneous calculations of the acceleration, and the mass prediction done in this manner does not lead to consistent results during the driving segment. Averaging of the mass based on this approach is problematic, at least for an automated approach. If the measured engine power data is used to estimate the tractive energy, based on a reasonable assumption for power transmission losses and an average power required from the vehicle accessories, then the measured tractive energy over the drive segment (based on the measured engine power output) can be compared to the cumulative tractive energy that is calculated using only the drive cycle data (along with relevant vehicle parameters). By iteratively adjusting the mass value in the speed-based tractive energy calculation, one can determine the appropriate mass so that the two tractive energy values are matched. This approach integrates the instantaneous values of forces and accelerations so that the data are automatically smoothed and averaged using a physically based metric, the tractive energy, that relates directly and naturally to the vehicle mass.

The mass remains nearly constant during any period of continuous driving, since the only mass change—barring a loss of cargo while in transit—is the fuel consumed during travel, which is a very small fraction of the total vehicle mass. Mass changes due to cargo loading or unloading were only considered to take place at stops and it was assumed that the vehicle load change would not take place for stops less than 20 minutes in duration. These simple criteria allowed potential break points where mass changes might occur in each day's drive cycle to be identified automatically, and the mass estimation could proceed one segment at a time. The approach described in the previous paragraph was programmed using Visual Basic for Applications (VBA) in the Excel environment, and the mass estimation process was performed for each identified driving segment individually. If the mass in two or more sequential

segments was found to remain within a specified tolerance, then the segments are joined and the average mass determined for the combined segments. This process is repeated by the program until the mass for each segment contained in each file is determined. The automated process allowed the mass calculations for all of the files to be performed efficiently. Once the mass calculation is complete for a file, each drive segment with a unique mass from the original drive cycle data file is exported as a separate drive cycle, and the mass, in kilograms, is appended to the filename so that the mass can be read by the tractive energy evaluation tool. The program plots both tractive energy curves along with the speed profile for each file after the mass is calculated and the image is exported to a .png file so that the results can be easily reviewed and verified. In some cases, a segment where a mass change took place was not identified by the tool and the tractive energy curves did not match over the full range. When this occurred, the mass calculation would be incorrect, so the file had to be reprocessed, with user intervention to control the divisions of the driving segments and adjustment of the mass values. Other problems with the mass calculation could occur, but by stopping the calculation process at particular points and manually adjusting the segment breakpoints prior to finalizing the mass recalculations for each segment, the correct segmentation could be achieved and the estimation of the mass was completed so that values for the two tractive energy functions (engine-power based and drive-cycle based) matched over the complete drive cycle.

Figure 12 shows a typical tractive energy plot when the automated mass calculation did not provide the proper segmentation. This type of error was easy to identify when reviewing the results, so it was clear which cases required user intervention to correct problems that occurred during the automated mass calculation. At about 8 hours into the day's drive cycle shown in the figure, it is clear that the mass changed (the predicted and measured tractive energy curves are not aligned) but the software did not identify the stop where the mass change occurred since there were two brief periods of movement that occurred during the time of loading. By rerunning the case with a breakpoint set in the code so that it stops after identifying the stops where mass changes are expected, the user can add the missing stop time to the list and restart the software to continue the calculation. Table 2 shows the data contained in the Excel calculator while the calculation is being performed. The mass program enters formulas into the spreadsheet to find the correct data for the table, and when a new stop point is entered into the main data sheet, the rest of the table is filled in automatically. This permits corrections to be done relatively easily when this type of problem occurs in the mass determination. To correct this particular issue, a manual override to set the end time to 8.0 (hours) for driving segment 7 was entered and the mass value from driving segment 7 was copied to the new driving segment 8, before restarting the program to continue the calculation. With the two simple changes, it automatically recalculated the masses with the selected divisions and identified that mass case 6 and 7 were within tolerance for the same mass. The program combined these two driving segments by setting their masses equal in the spreadsheet before continuing with the calculation (as shown in the table, this was also the case for driving segments 1 through 5). The final result for the day's drive cycle was that three separate driving segments with different masses were identified, and the corresponding files with the drive cycle data were automatically written when the calculation was completed, and the image with the corrected tractive energy plots, as shown in Figure 13, was exported as a .png file.

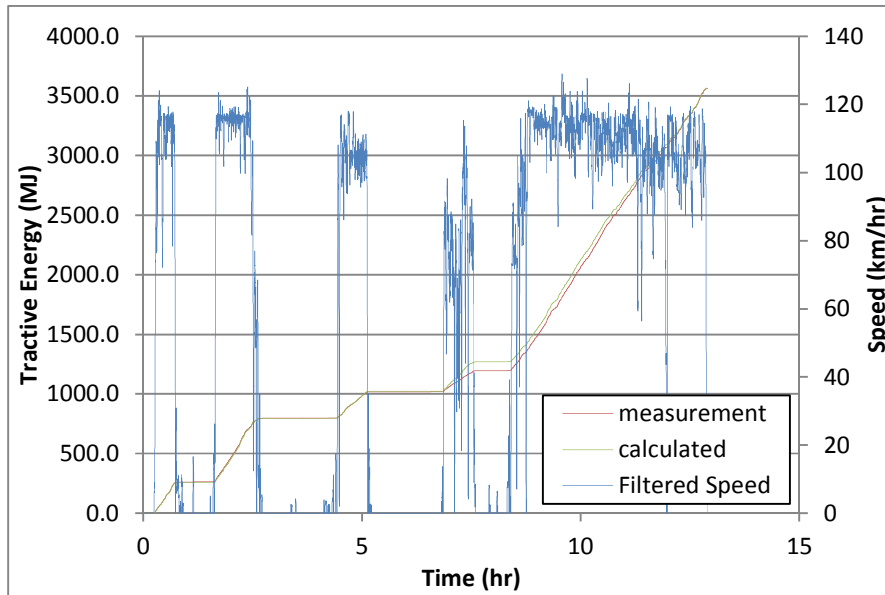


Figure 12 Plot of the tractive energy curves, based on measured engine data and determined from the drive cycle data, as used in the mass estimation. This sample case shows a mass change occurring at about 8 hours that was not properly identified by the automated calculation.

Table 2: Data contained in the Excel spreadsheet during the calculation of the mass for the case shown in Fig. 12.

Driving segment	Mass, kg	End time, hr	calculated tractive power, MJ	measured tractive power, MJ	end row in data sheet
1	27463.0	1.13	257.0	260.4	4077
2	27463.0	1.52	257.7	261.2	5486
3	27463.0	3.38	794.2	795.5	12158
4	27463.0	4.13	794.8	795.5	14860
5	27463.0	4.32	795.5	795.6	15543
6	14720.3	6.82	1021.2	1019.3	24555
7	25297.8	12.91	3566.7	3564.0	46476

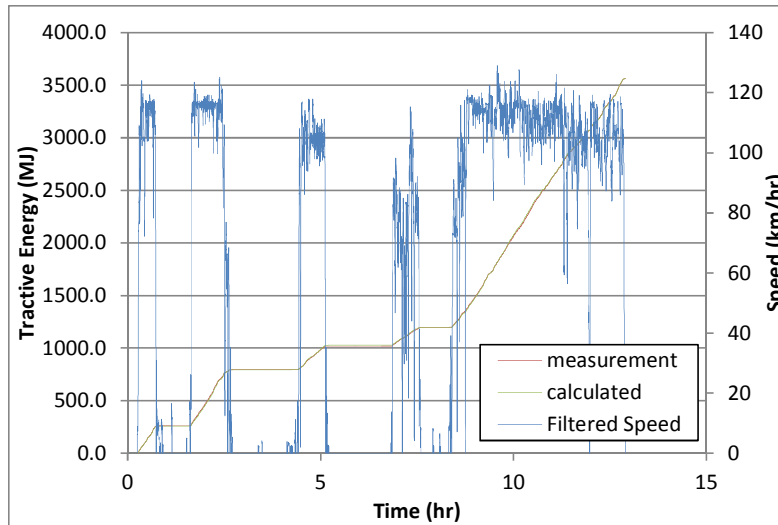


Figure 13 Plot of the tractive energy curves after the corrections were completed in the mass calculation.

The accuracy of the mass estimation was evaluated initially by comparing the calculated mass result with the measured mass for a case in which the trailer was instrumented with the AirWeigh measurement system. The AirWeigh system is designed to provide an accurate measurement when the vehicle is stopped, on level ground, and the parking brake is disengaged. Under these conditions, the measured weight should be within 1% of the actual vehicle weight. While driving, load transfer causes the indicated weight signal to vary about the actual weight. Figure 14 shows a plot of the measured mass value, determined by summing the AirWeigh mass data from the steer axle, drive axles and trailer axles, for one day's travel. Based on the figure, between 0 and 7.5 hours, the mass of the truck is approximately constant. During the stop following the first driving period, at about 2 hours, there is a minor increase in the mass that appears in the measured data. During this time, however, the GPS data shows that the truck was stopped at a rest area along the interstate highway, and it is quite unlikely that fuel was added or that the mass actually changed other than the driver exiting the vehicle. The variation in the signal during this period is likely due to the parking brake being applied and changes to the pressure in the air bags, which is what the system uses for measuring the weight. From the measured mass data from this signal, one sees that there is some uncertainty as to when the data is fully accurate. Nonetheless, the variation observed here is less than 700 kg, and the uncertainty in interpreting the recorded signal is relatively insignificant relative to the mass data precision needed for our purposes. It should be noted that this uncertainty is not associated with any fault of the AirWeigh equipment, but rather is a consequence of the manner that it was used to record a continuous signal that we must interpret without the knowledge of air brake status and the local road grade during stops. In any event, the mass measurement from the AirWeigh system gives a signal that can be interpreted to get a reasonably accurate measurement of the mass during each segment of travel.

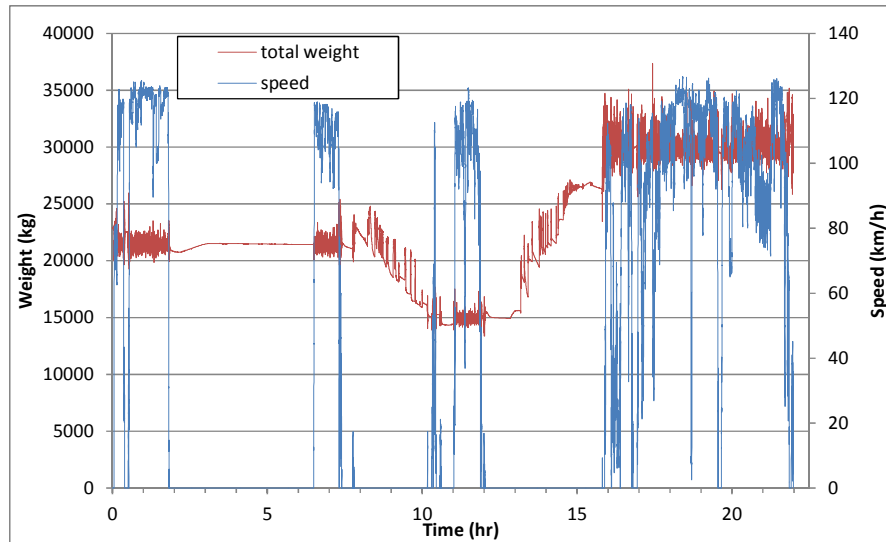


Figure 14 Plot showing the measured weight data during a day with two load changes.

The unloading of the trailer during the period from 8 to 10 hours can be observed in the mass plot, then after a period of travel between 10 and 12 hours, the trailer was reloaded to a third level of mass for the day. The measured values of mass for these three periods of different loads were 21,500 kg, 14,900 kg, and 26,400 kg, based on the mass before or after the load changes were complete. The corresponding masses predicted using the mass estimation algorithm for the three segments of travel were 21,650 kg, 13,900 kg, and 23,300 kg, respectively. For the first two segments, the error between the calculated and measured mass was within 1000 kg, and the error was about 3100 kg for the last segment. This level of accuracy, while not outstanding, was considered acceptable for the project, and the routine for the mass estimation was run to calculate the mass for all of the files.

As was the case for the day considered in the previous figure, it was rather common for the mass to change one or more times during a day's travel in the fleet tested. From the 1711 original files (one per truck for each day it operated), there were a total of 2918 mass-separated travel segments identified. The vehicle mass levels were categorized using three levels—low mass, medium mass and high mass—so that the driving segments from the separate ranges could be evaluated separately using the synthetic drive cycle tool. The low mass range was defined to correspond to a total vehicle mass below 20,000 kg (44,000 lbs.); medium mass was defined by a vehicle mass greater than or equal to 20,000 kg, but less than 28,180 kg (62,000 lbs.); and high mass was defined to include all masses greater than or equal to 28,180 kg. The distance traveled during each mass segment was calculated and the mass distribution as a function of distance traveled was determined. Figure 15 shows the mass histogram, and the separation points between the low, medium and high mass categories are shown with black dashed lines.

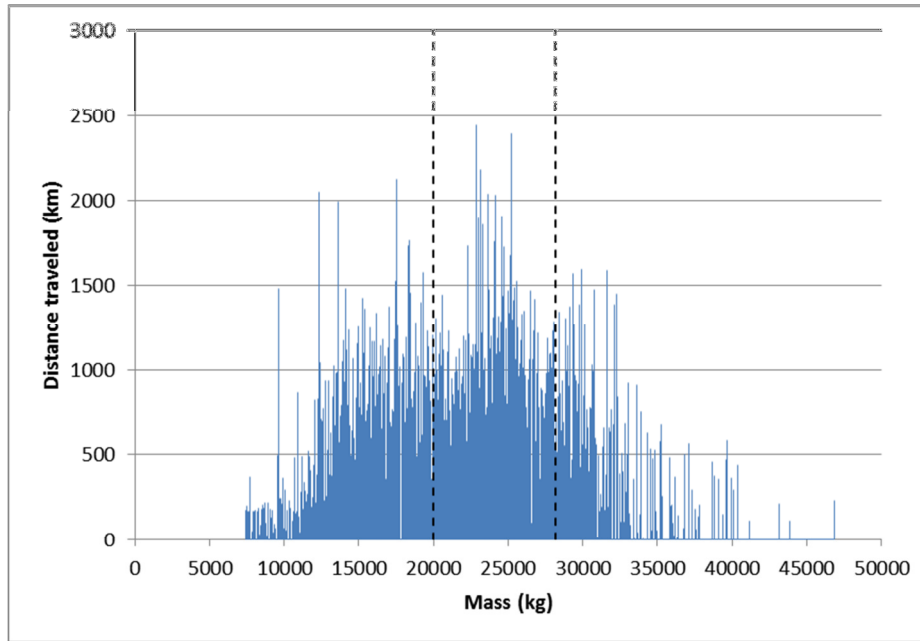


Figure 15 Distribution of masses for all segments of travel in the HTDC project.

The mass segments include cases where the trucks ran without the trailer attached (referred to as running “bobtail”), and this is represented by the lowest range of mass in the figure, around the empty tractor-only weight of about 8200 kg (based on specifications for the 2005 Volvo VNL tractor). The range of data shown in the figure around this mass level represents different volumes of fuel carried as well as the inaccuracy of the mass estimation method. The mass of an empty empty box trailer is about 7000 kg, so the mass levels under about 15,000-16,000 kg (including fuel) represent the loaded cases. Again, there is some dispersion in the data due to the inaccuracy of the mass estimation used, so the delineation between empty and loaded cases is not as clear as the analysis suggests, but it does provide an estimate of the overall distribution.

The mass data determined above was used to analyze all of the drive cycle data for the project, and the mass distributions and tractive power values were calculated based on this data. The mass estimates were later questioned since the miles traveled with vehicle mass near the maximum gross vehicle weight limit of 80,000 lbs. (36,300 kg) were fairly limited, even though fleets generally attempt to operate with trucks as full as possible. Additional comparisons of measured vs. estimated mass were made to validate the mass levels. Unfortunately, it was found that the comparison done in the initial case discussed above was not representative of the overall mass level accuracy, and errors of up to 8500 kg were found in the mass estimates. This was discovered only after most of the other analyses were complete, and there was not enough time remaining in the project to re-evaluate the masses and rerun all of the analysis. Nonetheless, the project team wanted to understand the mass distribution as well as possible and estimate the probable error in the mass estimates. It was observed that the greatest difference between the estimated and measured mass occurred at the higher mass values, and the estimated mass almost always under-predicted the measured value. It is logical, therefore, to consider multiplying the estimated mass values by a constant value to see if a better match is obtained with the measured data. Six days of results for which the measured mass was available were considered, and

there were 14 separate mass levels among these files. A constant multiple was applied to all of the data to adjust the original mass estimates, and the multiplier was optimized so that the error in the adjusted mass estimate is minimized on a root mean square (RMS) basis. The multiplier that minimizes the error was found to be 1.1265, meaning that a roughly 13% increase in the estimated mass yields the best match to the measured data. The average absolute error after applying this correction is 2548 kg. This value provides a measure of the uncertainty of the modified mass values. The data used to determine the mass multiplier are shown in Table 3, and the histogram of the masses using this modified value is shown in Fig. 16. With the mass adjustment factor applied to the data, we observe a cluster of cases in the histogram that are near the 36,000 kg level, i.e. close to the maximum gross load limit. This does not validate that the mass adjustment is correct, but the results do better agree with what one would expect than did the original estimate.

Table 3: Data used for the mass adjustment.

Truck # and date	measured mass	estimated mass	adjusted mass estimate
1_20061102	29800	24577	27687
	14900	17503	19718
	30600	27729	31238
1_20061103	29400	26688	30065
	15000	16625	18729
2_20070207	32500	26750	30135
	16600	14600	16448
3_20061222	21500	21650	24390
	14800	13942	15706
	30300	23336	26289
3_20061224	30100	30241	34068
3_20070103	21700	19372	21824
	15400	10369	11681
	31800	23278	26224

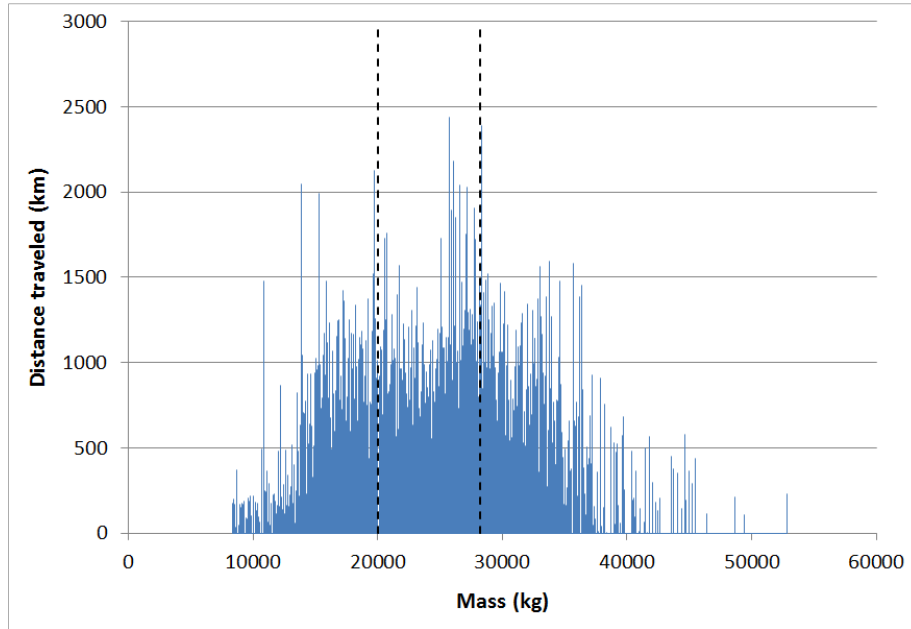


Figure 16 Adjusted mass distribution, based on a 12.65% increase compared to the original mass estimate.

It is evident that there were a fairly substantial number of miles driven either empty or with low loads being hauled. By considering the cumulative miles traveled as a function of load for the adjusted mass distribution, we found that about 6% of all miles traveled were driven with the estimated mass at or below 15,000 kg, which is the approximate mass of the empty tractor-trailer. Before adjusting the mass estimates, roughly 13% of the cumulative mileage was at or below 15,000 kg. The adjusted mass estimate yields an average overall mass of 24,774 kg (54,618 lbs.). Before applying the adjustment factor, the original distribution of masses gave an average value of 21,991 kg (48,482 lbs). This was calculated by weighting each estimated mass data point with the distance traveled along the segment at that mass to calculate a weighted mean.

4. Synthetic Drive Cycle Creation

The driving data measured in the HTDC project included 1,152,483 kilometers of travel while the six trucks ran for a total of 24,231 hours during a full year of measurements (these values represents the cleansed data, after removing corrupt data and incomplete drive segments, and is the total engine run time for the measurements, including idling). It would be extremely time consuming to analyze this quantity of data directly for any type of energy efficiency evaluation. As an alternative to completing a direct analysis of all the drive cycle data, a primary objective for this project was to reduce the driving data to create a set of synthetic drive cycles, of one hour or less in duration, that are representative of all of the data so that analysis can be performed using the more manageable length drive cycle(s). This section first explains what is meant by a “synthetic” drive cycle and the methodology used to develop one, and it describes the software ORNL has developed for this purpose.

4.1. The concept of a synthetic drive cycle

As presented in section 2, the tractive energy is a primary factor in determining fuel consumption, and the tractive power required to move a vehicle forward at each instant in time is determined by the particular operating conditions experienced. As demonstrated by the equations developed in that section, the combination of speed, acceleration and grade, along with the parameters that characterize the vehicle configuration, uniquely determine the tractive power required at each instant in time. As a direct consequence of this correspondence between the vehicle operating condition and the tractive power, the fuel consumption is uniquely determined by the distribution of operating conditions that comprise the vehicle's usage history, i.e. its drive cycle. In reality, driving the same drive cycle multiple times with the same vehicle can result in somewhat different levels of fuel consumption since the driver may not shift at the same points in time, etc., so that even the same vehicle operating conditions can result in different engine operating conditions, which may result in small differences in the fuel consumption. This type of variation is secondary, however, to the tractive energy contributions, and we only address the tractive energy impact on fuel efficiency.

Since a vehicle's fuel efficiency is determined by the ratio of fuel consumed to the distance traveled, the vehicle usage can be scaled without changing the fuel efficiency. If we drive for two hours on flat ground at a steady speed of 80 km/hr. and then for two hours at 100 km/hr., we would consume twice as much fuel as if we drove only one hour at each speed (all other factors remaining equal). The fuel efficiency (or its reciprocal, the fuel economy) will be the same for either the one-hour or two-hour trip, however, since both the fuel consumption and the distance traveled will change by the same factor. If the same accelerations and decelerations occur during transitions from one speed to another in both cases, or if the fuel consumed in the speed transitions is negligible compared to the steady speed periods, it also would not matter if the higher speed operation occurs first or last. Similarly, the same tractive energy would be required if several segments of different lengths for the two speeds occurred in different orders during the trip (for example 15 minutes of driving at 100 km/h, followed by 20 minutes at 80 km/h, then 45 minutes at 100 km/h, and finally 40 minutes at 80 km/h), as long as the total ratio of time spent at each of the two speeds remained the same. Generalizing this idea, it can be shown, under the assumptions used in developing the tractive energy model, that two drive cycles will require the same tractive energy (for any given vehicle configuration) if the same set of operating conditions are experienced in both cycles and the fraction of time spent at each operating condition to the total cycle duration is the same in both cycles. This result is the basis for a characterization of drive cycles based on the distribution of all operating conditions experienced. This simple theorem also enables us to develop a drive cycle of a relatively short duration that will give the same fuel efficiency result as would be achieved from a much longer drive cycle (for example, during days or months of travel) simply by matching the distribution of operating conditions from the original drive cycle. This is the fundamental premise for the development of a drive cycle that accurately represents a given set of driving data, and we refer to the shortened cycle as a "synthetic drive cycle" since it represents a synthesis of all of the data contained in the larger set of driving data.

We note, in passing, that emissions from a vehicle are more complicated than fuel consumption since temperature plays a strong role in the chemistry governing engine emissions rates. When the engine

and exhaust temperature are sufficiently high, however, the emissions, like fuel consumption, tend to be largely governed by the engine speed and torque. This allows “hot start” emissions to be determined in a manner similar to the fuel consumption, and a drive cycle that is representative for fuel efficiency purposes will also be representative with respect to hot start emissions.

4.2. The Drive Cycle Generation (DCGen) Tool for developing a synthetic drive cycle

ORNL has developed a set of tools for the analysis of measured drive cycles and the creation of synthetic drive cycles whose characteristics will be similar to an input set of driving data. These tools have been developed and refined during several projects including the Heavy Truck Duty Cycle (HTDC) project, the Medium Truck Duty Cycle (MTDC) project, and the current Truck Technology Efficiency Assessment (TTEA) project. The initial version of the Drive Cycle Generation (DCGen) tool used random sampling of microtrips (driving periods between two adjacent stops) from a single file of drive cycle data to generate a substitute drive cycle that was intended to be representative of the original. Various metrics such as average speed and acceleration, maximum speed, and number of stops per mile were used to characterize the relevance of the drive cycle generated. Convergence criteria based on these metrics could be set and the tool would repeat the process of its random selection of microtrips until the criteria were satisfied (when possible). It was found that this did not always provide drive cycles that led to consistent fuel economy estimates, even when the metrics of the reduced drive cycle were similar to the original cycle, and depending on the characteristics of the original drive cycle, the tool often did not find a converged result at the desired level of convergence. In subsequent versions of the software, different algorithms were developed to divide the input drive cycle into shorter segments and piece these together to better match the characteristics of the original drive cycle, and better means to characterize drive cycles based on the specific vehicle operating condition have been developed.

As discussed previously, matching the distribution of operating conditions from the original driving data is the primary goal in creating a synthetic cycle that will result in the same fuel efficiency, and the new drive cycle tools focus heavily on matching the distribution of vehicle operating conditions. For the tractive energy model, the operating condition at each point of time is comprised of the speed, acceleration, and the grade. It is challenging to visualize and identically match a distribution of three variables, but by considering the bivariate distribution of the speed and acceleration, and using real grade conditions occurring simultaneously to the speed and acceleration points, the overall distribution should be very well approximated. This is the approach that has been followed for the synthetic drive cycle creation. An example of a speed vs. acceleration bivariate histogram from a single day of driving is presented in Fig. 17. The bivariate histogram shows the cumulative duration of time that the vehicle was driven at each operating condition. Each bin represents a range of speeds and accelerations, and is defined by discretizing the full range of the speeds and accelerations from the drive cycle. The color of each bin corresponds to the number of times during the drive cycle that the speed and acceleration were within the range represented by that bin. The scale at the right of the figure indicates the total time duration experienced at each operating condition in the drive cycle. By representing a drive cycle in this manner using the speed-acceleration distribution, the time order of the operating conditions is eliminated. The distribution can also be scaled so that the overall duration is not a factor.

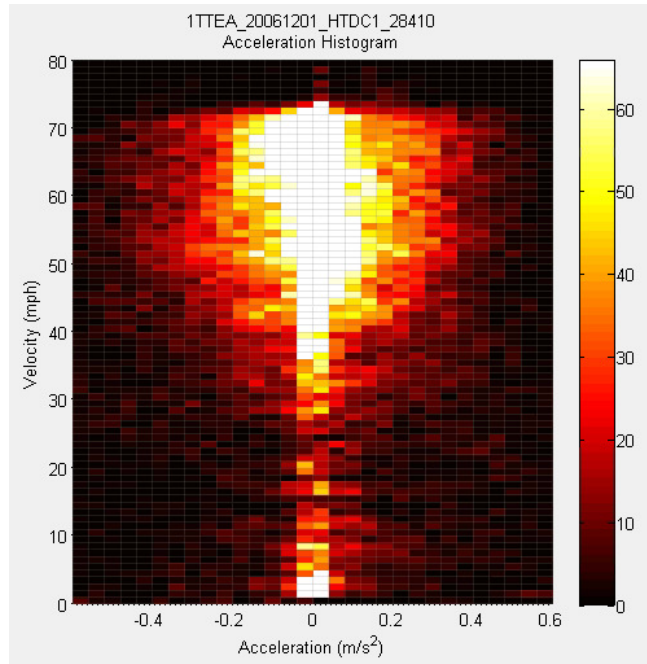


Figure 17 Bivariate histogram of the velocity and acceleration for a day of driving.

The drive cycle analysis for this project required a high degree of accuracy for matching the acceleration-speed distribution of the synthetic drive cycle to that of the complete measured data sets. A new version of the DCGen tool was developed in which the user manually selects drive cycle segments using a target speed-acceleration distribution generated from the complete set of driving data. This version of the tool consists of three separate Matlab-based programs, which use many of the same functions incorporated in earlier versions of the automated DCGen tool, but relies on the user's judgment to create the synthetic cycle as opposed to having it generated using a purely algorithmic approach. The following describes the function and use of each program module in the DCGen tool.

The first program module provides an interface that allows the user to load any number of drive cycle files, and the distributions from each file are combined into a "total" bivariate histogram that represents the concatenation of all of the input files. The individual drive cycle files can be reviewed and processed for further use in the subsequent modules of the software, as needed. Reduction of the data that is stored from each file is necessary when using large data sets, and the user must select the individual histograms or files he will use in the other modules of the DCGen tool. For subsequent analysis in creating the synthetic drive cycle, it is necessary to break the file into discrete drive cycle segments, and the user must launch the segmentation function for any files that will be used as basis functions in the synthetic cycle creation. Typically, histograms that are similar to that of the entire data set are selected in order to make the matching of the histograms more efficient, but the user has full control of the selection process. The software allows the user to segment additional files at any time in the synthetic cycle creation if it is found that portions of the total histogram are not represented by segments that were initially selected. The user interface for the first software module of the DCGen tool is shown in Fig. 18.

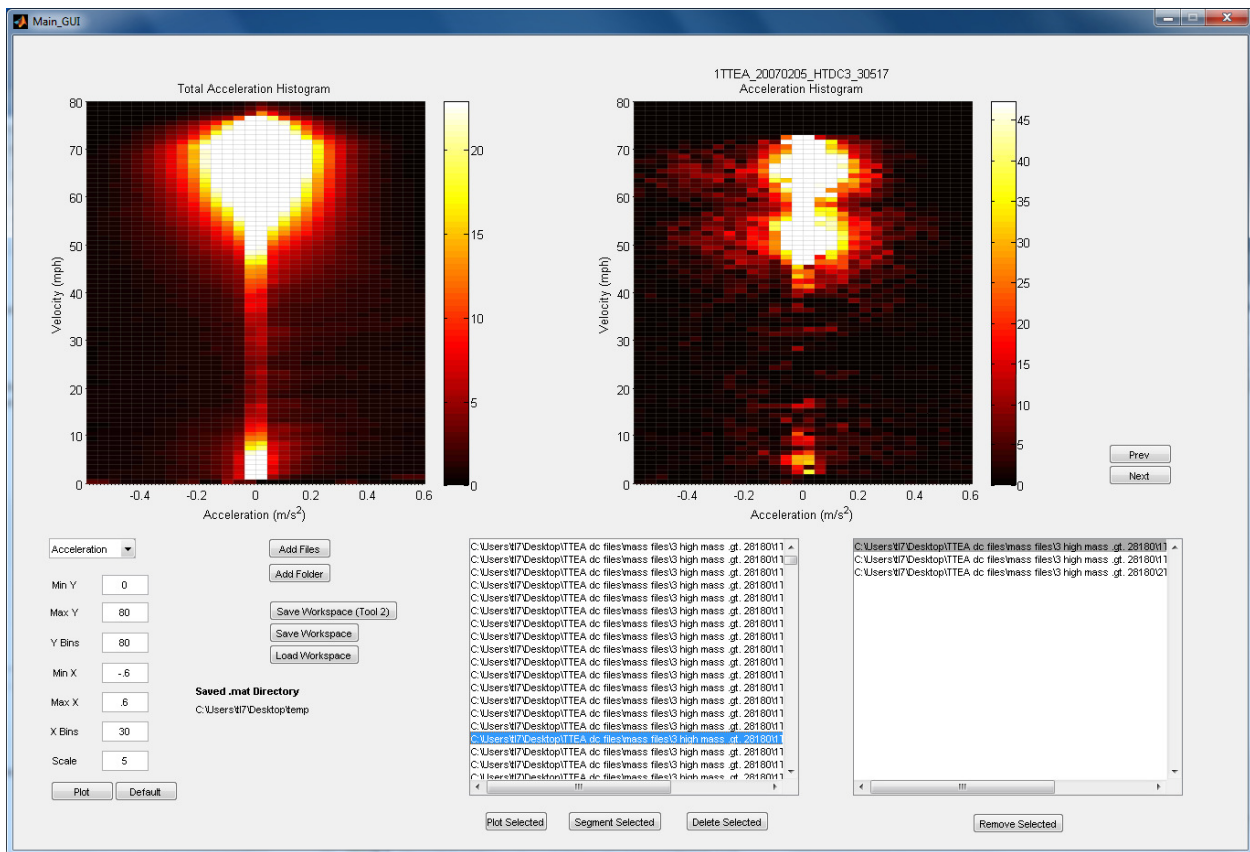


Figure 18 The DCGen tool module 1 interface.

Once the user has selected the desired set of files and created the total histogram representing all of the driving data to be analyzed, the data is processed to create individual drive cycle segments that will be used in subsequent steps of the synthetic cycle creation. These segments are loaded into the second program module, which allows for specific segments to be selected from each file for inclusion in the synthetic cycle. The user must select segments one at a time in order to generate a tentative synthetic histogram (which is simply an accumulation of the individual segments' histograms) that matches that of the complete data set. The tool manages the accounting of the synthetic histogram as segments are selected and presents a histogram representing the difference between the total histogram, scaled to a user-selected target cycle length, and the segments selected for inclusion in the synthetic drive cycle. The user's objective when creating the synthetic drive cycle, therefore, is to achieve a difference histogram that approaches zero. The difference histogram and data for an individual segment, as they are presented in the second software module during the selection process, are shown in Fig. 19, and the corresponding segment speed and elevation are shown in Fig. 20. The software has been developed to automate the search for segments meeting specific criteria of speed and accelerations, and the portions of the histogram for which additional data points are required can be quickly identified and matched with the available segments. The interface for the search function is shown in Fig. 21. Functions to automate the process of identifying appropriate drive cycle segments for inclusion in the synthetic cycle were implemented in the software to improve the efficiency of the synthetic cycle creation.

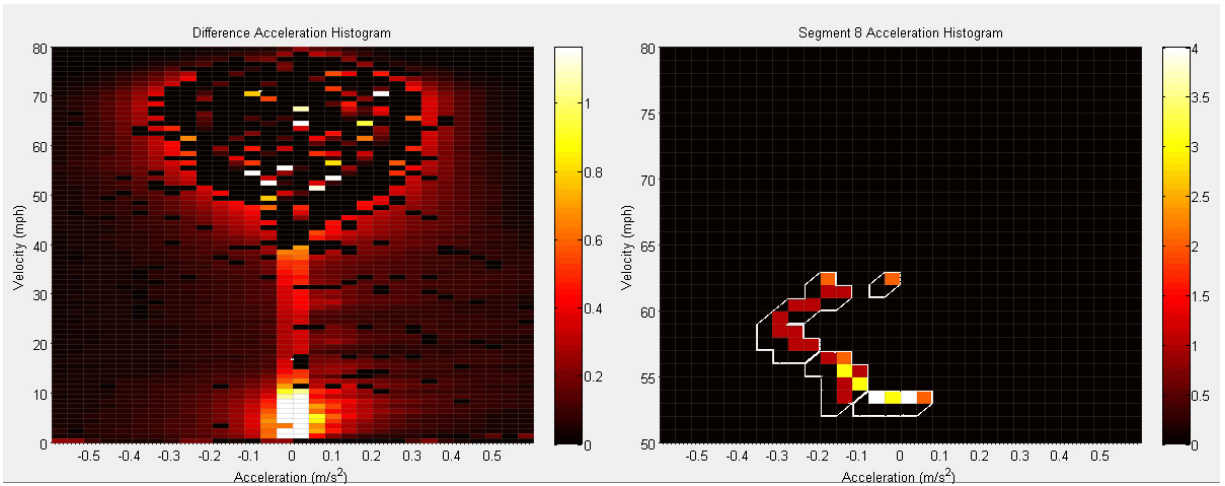


Figure 19 Difference and segment histograms during the creation of a synthetic drive cycle.

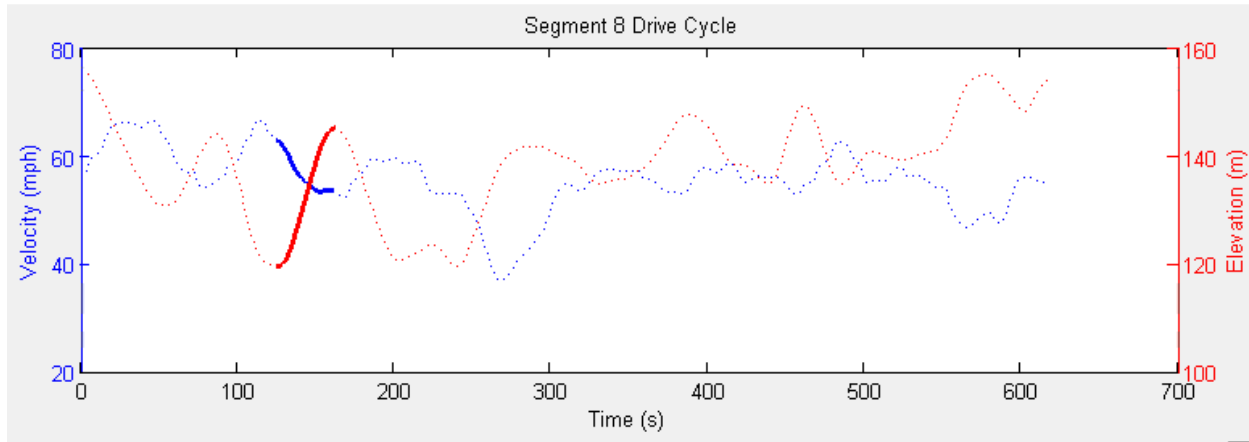


Figure 20 Plot of a single drive segment in DCGen tool program module two, showing the speed and elevation changes.

	Min	Max	
Velocity (mph)	55	56	<input checked="" type="checkbox"/>
Acceleration (m/s ²)	-0.04	0	<input checked="" type="checkbox"/>
Auto Search?	<input checked="" type="checkbox"/>		<input type="button" value="Search"/>
Segment ID	Segment Sub Segments		
122	601	616	31.25
202	421	437	17.65
161	485	504	10.00
89	504	524	9.52
8	524	576	7.55
231	330	388	6.78
188			
194			
158			
66			

Figure 21 DCGen tool, second module segment search interface.

After selecting drive cycle segments so that the tentative synthetic histogram is as similar as possible to the original histogram, the third program module is run for the final creation of the synthetic drive cycle. The main goal of this module is to arrange the drive segments selected in the second program module to create the final synthetic duty cycle and to ensure that the speed and elevation profiles comprising the synthetic cycle are continuous and smooth. This is done by matching the starting and ending speeds between subsequent segments and inserting or removing points as needed. Final refinements of the synthetic cycle histogram are also made using this module so that the synthetic histogram matches the total histogram as closely as possible. The program incorporates the elevation data corresponding to each selected segment (if it was present in the original data files) and integrates this data into the final synthetic drive cycle. A completed synthetic drive cycle is shown in Fig. 22. The individual segments included in the cycle can be seen in alternating colors in the velocity and elevation profiles.

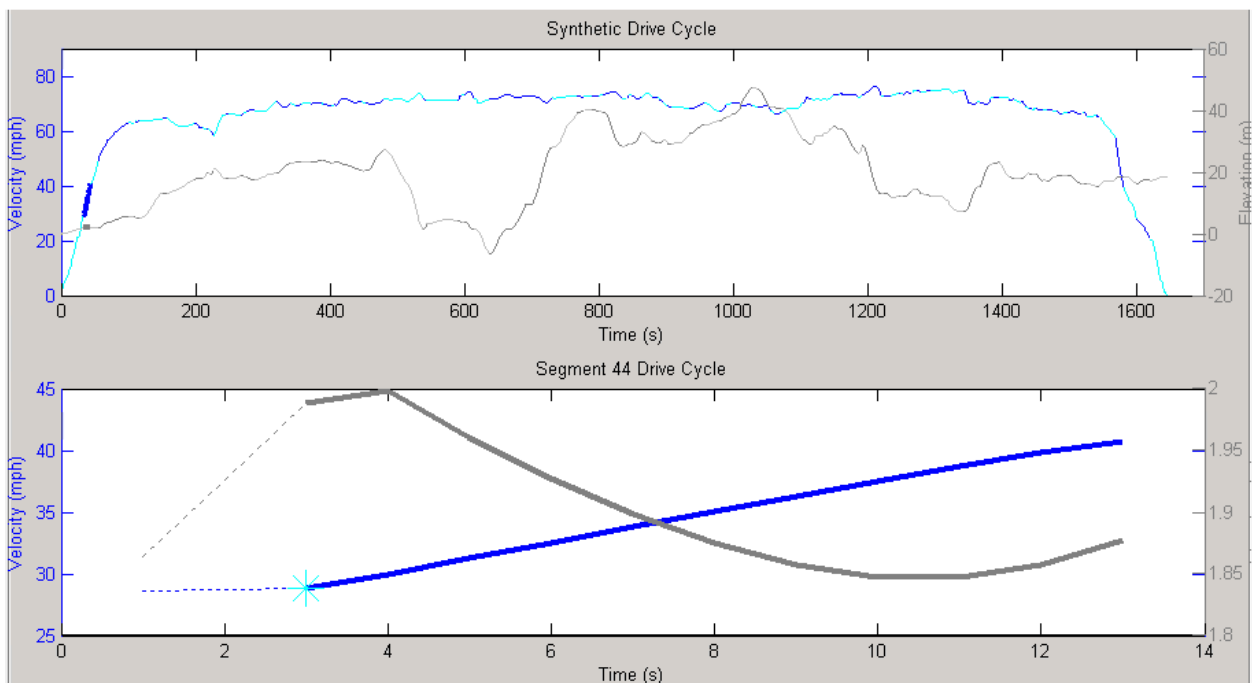


Figure 22 Manually-generated DCGenT synthetic plot.

When the segments from module two are initially arranged, the speed data inevitably contains some gaps between segments so that the speed profile is not continuous. To remedy this problem, the user can rearrange segments for a better match of endpoints, and he may add or modify points at the beginning or end of any segment in order to create the desired continuous cycle. The interface used to edit data for a segment is shown in Fig. 23.

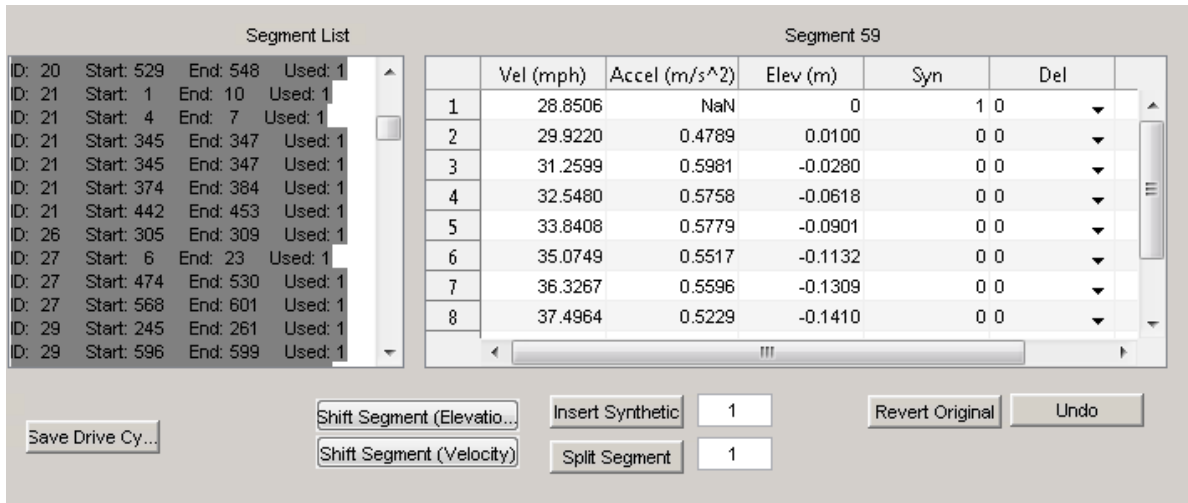


Figure 23 Manual DCGenT segment data.

Once all of the segments have been combined for the synthetic cycle and gaps between segments are corrected, the synthetic histogram is created and compared to the original data set using the total histogram. The user must make any final adjustments to the synthetic drive cycle to correct errors in the synthetic histogram that develop during the creation process. Figure 24 shows a comparison of the original (total) histogram and the synthetic histogram for a completed synthetic drive cycle. (The speed range presented is truncated for clarity.)

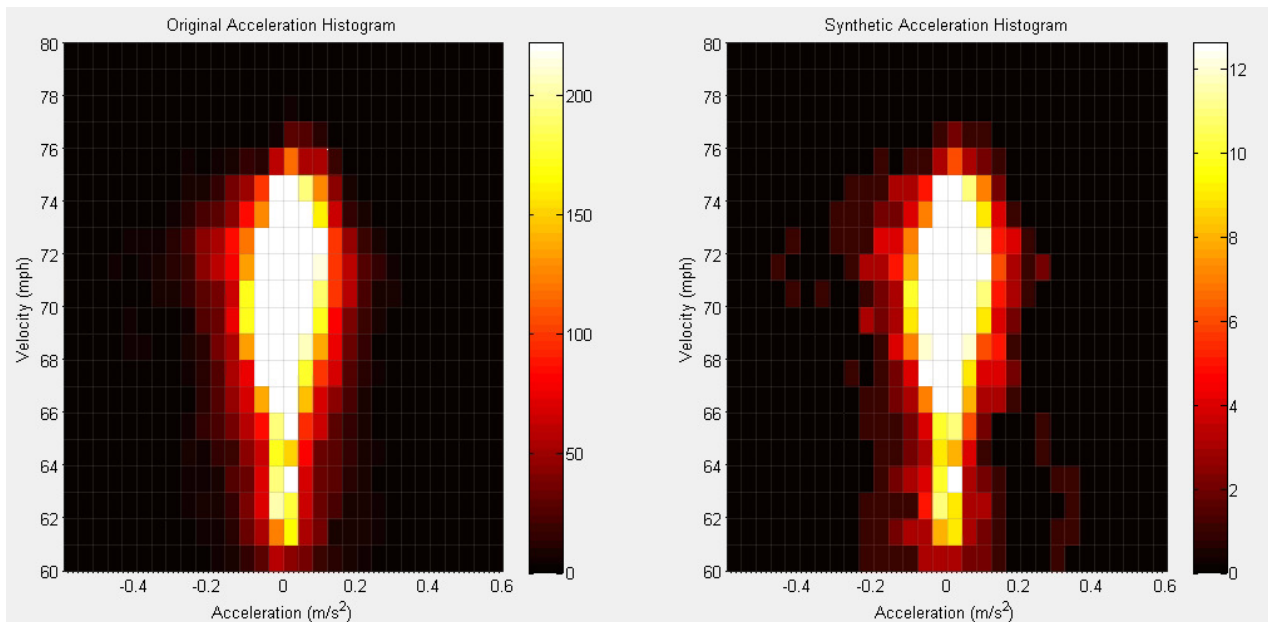


Figure 24 Manual DCGenT synthetic histogram.

This implementation of the DCGen tool was developed to create synthetic drive cycles that very closely represent any set of driving data. The synthetic cycle can be generated to have a length that is appropriate for use in tools such as PSAT and Autonomie for modeling vehicle systems, or for testing purposes. While an original data set of even a full day's worth of data would require an excessive

amount of time to process with some vehicle models, the DCGenT can be used to create synthetic duty cycles and these cycles can be run significantly faster and will yield the same fuel economy result. Since building hardware can be expensive, the modeling approach using real data is beneficial to not only researchers for testing aerodynamic and other fuel saving technologies without physically instrumenting a vehicle, but also to truck manufacturers and truck fleets for selecting vehicles tuned to their fleet's specific duty cycle.

4.3. Validating the Use of a Synthetic Drive Cycle and the Tractive Energy Model for Predicting the Fuel Efficiency Benefits from Advanced Vehicle Technologies

The synthetic drive cycle development methodology and software have been described and a basic theory was presented to explain why a synthetic cycle used with the tractive energy method will yield the same results as would be attained using the complete set of drive cycle data. In this section, the ability of the synthetic drive cycle to represent a larger data set is validated by comparing results from approximately 8 hours of driving to those from a synthetic drive cycle developed to represent the full data. A comparison of the energy savings estimates was made with the tractive energy model as well as by comparing the predicted fuel economy using Autonomie vehicle performance software.

Figure 25 shows measured driving data from a complete day of driving during which 858.9 km were traveled over 28,787 seconds of vehicle operation. This data was used to generate a synthetic drive cycle with the DCGen tool, as described in the previous section. The original drive cycle was reduced to a synthetic cycle with a duration of 1645-seconds. The synthetic cycle representing the original cycle is shown in Figure 26.

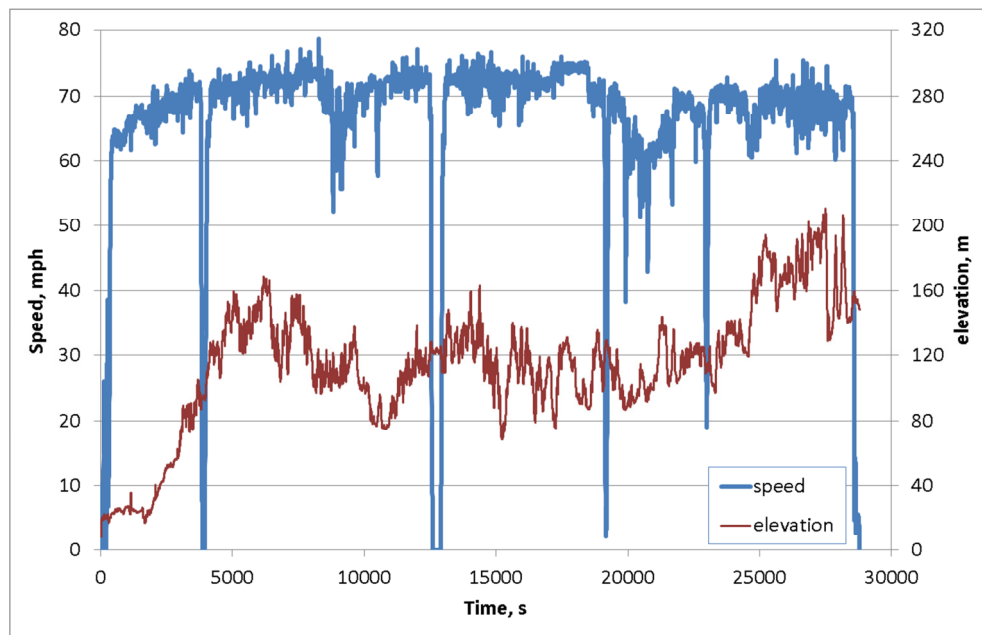


Figure 25 Driving data used to develop the validation synthetic drive cycle.

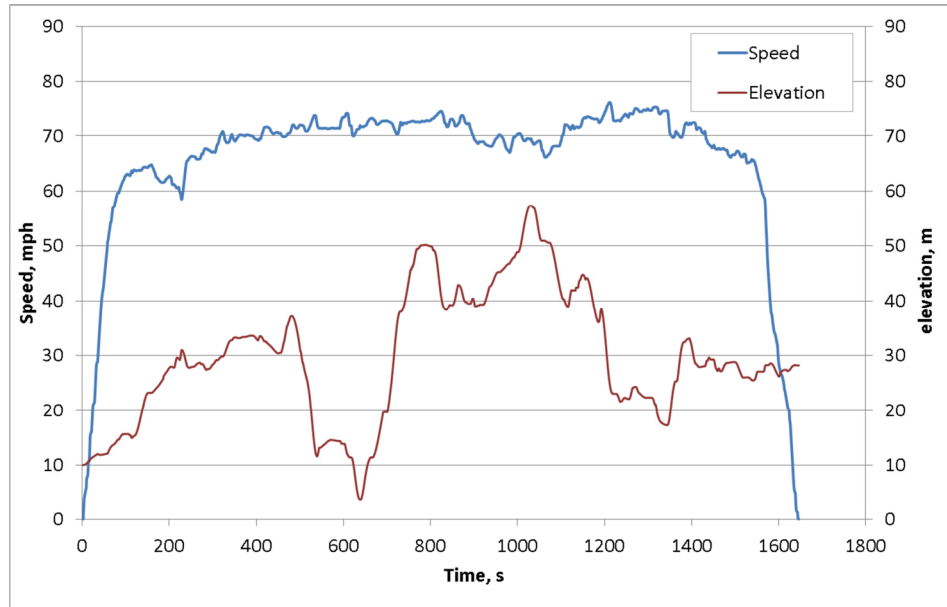


Figure 26 Synthetic drive cycle developed from the driving data presented in Fig. 25.

Figure 27 compares the bivariate velocity vs. acceleration distributions for the original and synthetic drive cycles. Due to the short duration of the accelerations to and decelerations from highway speeds relative to the length of the rest of the drive cycle, the number of occurrences for each bin in the histograms corresponding to the low-speed accelerations/decelerations is very low. The bins do not even appear in the histograms when using a normal range of scales, and the low speed range was omitted in Fig. 27. This low incidence of the low speed bins indicates that the corresponding operating conditions are rather insignificant in characterizing the drive cycle.

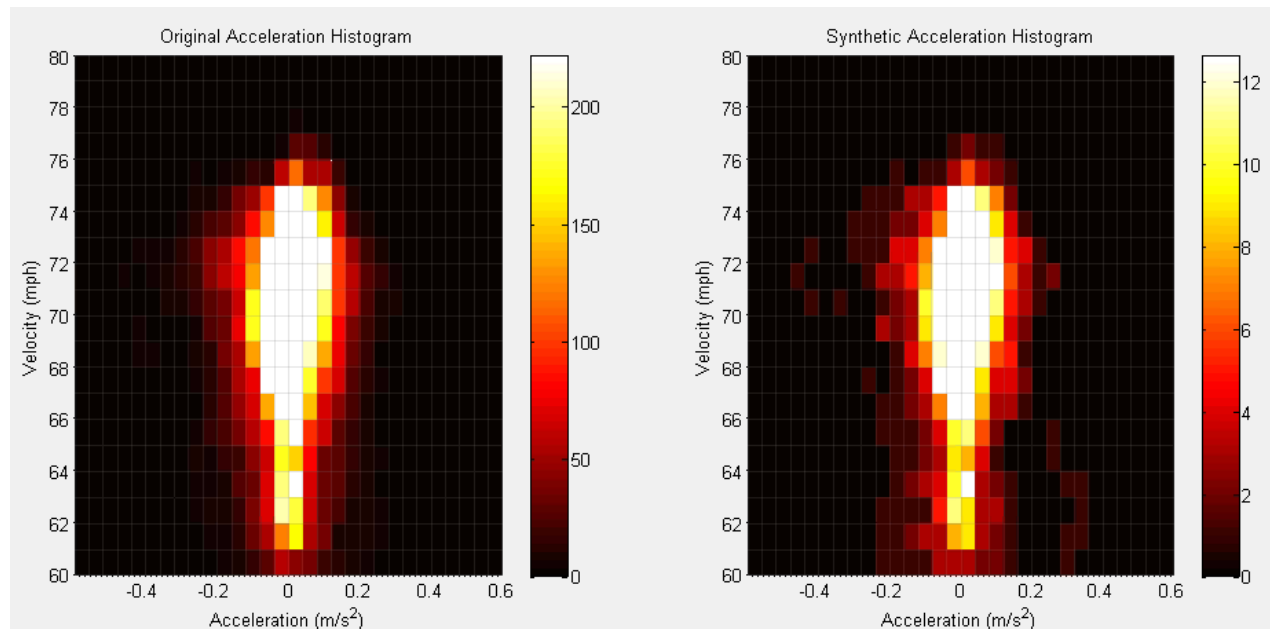


Figure 27 Bivariate histogram of the original driving data and of the synthetic drive cycle developed for the validation.

Figure 27 shows that the histogram for the validation synthetic drive cycle matches the original cycle extremely well for the dominant operating conditions experienced. There are a few bins that differ slightly in magnitude from the original histogram. Since scaling the original cycle's bivariate histogram for the reduced length of the synthetic drive cycle results in bins in the target bivariate histogram that contain non-integer time durations, while the synthetic drive cycle was developed using one-second time intervals, it is not possible to have an identical match between the two cycles. Furthermore, even in cases where a better match may be numerically possible, the process of creating the synthetic cycle using the DCGen tool does not always lead to an ideal solution. In spite of the differences, the overall agreement between the original and synthetic histograms is considered to be excellent.

To compare the low-speed operating conditions for this cycle, the scale was adjusted so that most of the bins are visible in the histogram plots, as shown in Fig. 28. It is evident that many conditions in the synthetic cycle with low speeds show a higher occurrence than the corresponding points in the original drive cycle. This is again a result of the fact that only integer time durations are included in the drive cycles, and bins with low frequencies of occurrence cannot be reproduced very accurately by the scaling process used in the synthetic drive cycle creation. Since the lower speed region must be traversed by accelerating and decelerating at finite rates, some points in the synthetic cycle must be present in these ranges. It can be seen that a fairly broad range of accelerations were covered at each speed in the original drive cycle, although each operating condition only has a low frequency of occurrence. The distribution of accelerations can be represented in a coarse manner in the synthetic cycle by ensuring that a similar range of accelerations occurs in the synthetic cycle, at least on average across several speed intervals. In creating the synthetic cycle, an attempt was made to do this by including accelerations that occurred in clusters in the original cycle into the final synthetic cycle. For example, if there are 5-10 points over a 10 mph range of speeds for which the individual occurrence in the original cycle is 0.1-0.25, then including a single point in the synthetic drive cycle at one speed within this range provides a means to represent the original accelerations in a general sense, within the limitations of the 1-second intervals used for the synthetic drive cycle. In any event, the low speed operating conditions for this cycle represent only a small portion of the overall distribution, and the effect on the fuel consumption of these variations relative to the original drive cycle are relatively small. We note that the same approach of including data to represent, in an average sense, operating conditions that occurred at low levels of occurrence over multiple speed levels or across several acceleration bins was used not only for the low speed range, but also for the highway operations at the higher acceleration level. This is why some bins for the synthetic cycle histogram in Fig. 27 are populated even though the corresponding bins in the original histogram appear to have no occurrences for the same operating condition.

With the synthetic cycle completed, a validation to demonstrate the accuracy of fuel economy results based on the synthetic cycle development was completed by performing simulations of fuel economy using Autonomie vehicle performance software with the two drive cycles shown above, original and synthetic. Autonomie is a plug-and-play vehicle model architecture designed to simulate vehicle performance and evaluate powertrain technologies for improving fuel economy [7]. It estimates fuel consumption by applying a detailed physical representation of all of the major powertrain components

on the vehicle, and links the forces required to propel the vehicle with an engine map, which characterizes the fuel consumption of the engine as a function of engine speed and torque. An Autonomie vehicle model has been developed at ORNL to represent the vehicles used in the HTDC study. A heavy duty diesel engine map available in Autonomie was used in the model, but the engine parameters were tuned to be representative of the 15-liter, 6-cylinder Cummins ISX 475 diesel engine that was present on the HTDC test vehicles. The transmission in the model is a 10-speed manual transmission, which is also representative of the tractors with a manual transmission used in the study. The mass simulated in the Autonomie evaluation was 22,000 kg, which was the mass estimated for the measured driving segment. Other parameters in the model were selected to be consistent with those used in the tractive energy analysis. Specifically, the truck’s aerodynamic drag coefficient was taken to be 0.62, while a constant value of 0.007 was used for the coefficient of rolling resistance in the analysis. The same vehicle model configuration has been used in prior evaluations to represent the same HTDC test vehicles, and this model has been validated against measured fuel consumption results at ORNL.

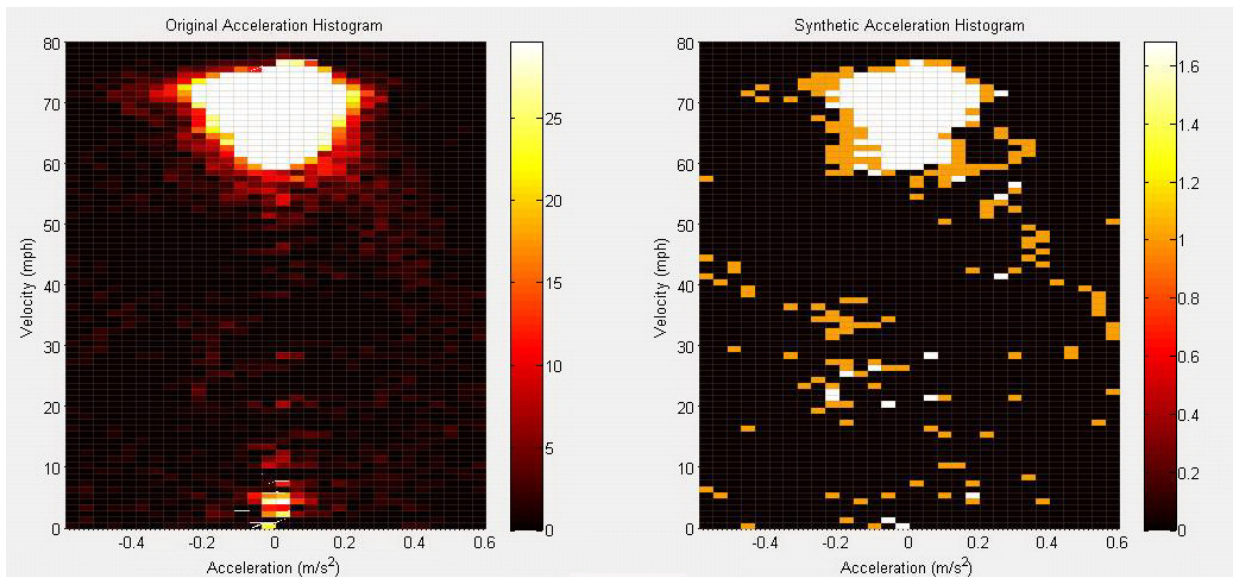


Figure 28 Original and synthetic histograms shown with the scale modified to highlight the low speed operating conditions.

The model was run for both the original drive cycle and the synthetic cycle, which is intended to closely represent the original cycle. The fuel economy values predicted using the two drive cycles were 5.62 and 5.57 mpg, respectively. This level of consistency in the predicted fuel consumption (within 1%) gives a high level of confidence that the synthetic drive cycle is highly representative of the original cycle and that the fuel economy estimate using a carefully constructed synthetic drive cycle can yield results that are very close to those from the full set of driving data that the synthetic cycle represents.

In addition to performing the fuel economy analysis with Autonomie, the tractive energy model was run using both drive cycles to determine the relative contributions from each energy loss factor to the total tractive energy, in addition to evaluating the fuel savings expected with various combinations of technologies based on the tractive energy method. The contributions of each energy loss factor to the driving tractive energy, given by Eqs. (4), (5) and (7), are expressed as a percentage of the driving

tractive energy (see Eq. (8)). The relative contribution from each energy loss term is strongly dependent on the drive cycle, so this comparison is an excellent test of how well the synthetic cycle matches the original driving data. These terms are also the basis for the energy saving estimates using the tractive energy model, so their accuracy is critical to that of the tractive energy predictions. Table 4 shows the results obtained for the energy loss factors based on the tractive energy model.

Table 4: Comparison of results for the energy loss factors in the tractive energy model, for the original and synthetic drive cycles from the validation case.

Energy Loss Factors (Expressed as a Percentage of the Total Driving Tractive Energy)	Original Drive Cycle	Synthetic Drive Cycle
Brakes (corresponding to regenerative braking potential)	3.0%	4.0%
Aerodynamic drag, driving	55.7%	54.8%
Aerodynamic drag, braking	3.3%	2.5%
Rolling Resistance, driving	35.1%	34.8%
Rolling Resistance, braking	2.1%	1.9%

It is found that all of the factors calculated using the synthetic drive cycle are within 1% of those from the original drive cycle, which indicates that the prediction of the fuel saving potential of each advanced efficiency technology (and their combinations) when using the synthetic drive cycle will be very consistent with the result based on the original driving data. Since the elevation changes were not forced to be proportional when creating the synthetic drive cycle, there is a slightly greater increase in the potential energy in the synthetic drive cycle than occurred in the original drive cycle. The fact that the potential energy is non-zero in both cases (it represents 0.8% of the driving tractive energy for the original drive cycle and 2.0% for the synthetic cycle) is the reason that the relative energy contributions of the other terms do not sum to 100%. The impact of this small difference in the potential energy change is minimal on the overall results, although it is responsible for some of the differences occurring in Table 4.

The tractive energy analysis was run for both cycles to quantify the fuel savings potential associated with reductions in mass, rolling resistance and/or aerodynamic drag. The fuel savings estimates are presented in Fig. 29. Note that according to the assumptions of the tractive energy model, the estimated energy savings from combinations of the technologies are additive when considering either of the two cases independently, i.e. with regenerative braking or without regenerative braking. Due to the effect of the braking tractive energy contributions, however, the energy savings associated with each energy loss factor are different depending on whether regenerative braking is used or not. The only noticeable difference in the results between the predictions made with the tractive energy model for the two drive cycles is the energy savings associated with regenerative braking for this case.

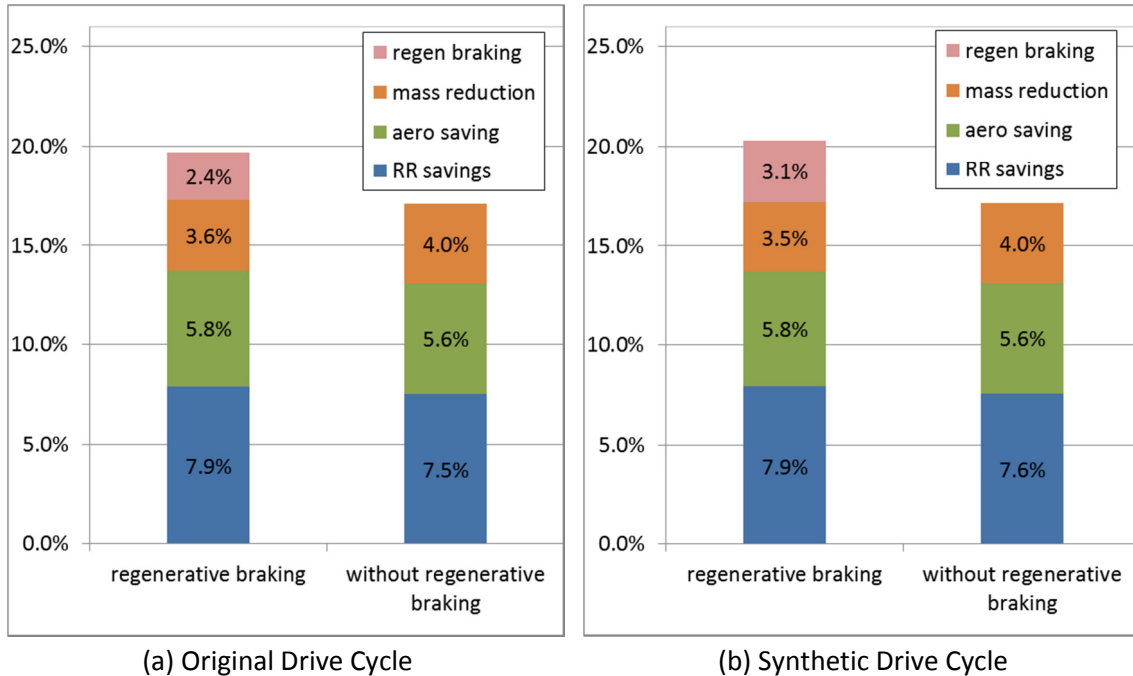


Figure 29 Relative Fuel Savings estimates based on the tractive energy model for (a) the original drive cycle and (b) the synthetic drive cycle. The variations evaluated were for a mass reduction of 2000 kg, a reduction in C_{RR} by 0.0015 and a 10% reduction in C_d . The efficiency of the regenerative braking system is assumed to be 80%.

Table 5 shows the default values used in the tractive energy analysis for all of the primary parameters in the model. The same assumptions are used in all of the tractive energy evaluations presented in this report. These values were selected to be representative of typical class 8 tractor-trailers. The variations considered were selected to correspond to the level of reduction that could be achieved when advanced efficiency technologies are employed on an initially non-optimized vehicle configuration. A mass reduction (corresponding to vehicle lightweighting) of 2000 kg is assumed in the reduced mass scenario. The energy savings result is based only on the fuel efficiency improvement resulting from the decreased mass, and it is assumed that the payload does not increase as a result of the mass reduction. The rolling resistance coefficient reduction employed in the analysis is 0.0015 (also referred to as 1.5 kg/ton), which is a typical level of reduction that can be realized when converting from conventional dual tires to New Generation Wide Base Single (NGWBS) tires. The reduction in the coefficient of aerodynamic drag assumed in the analysis is 10%, which is a level of reduction that could be achieved in tractor-trailers if implementing aerodynamic drag reduction devices such as trailer skirts, etc. The same levels of reduction will also be used in all of the tractive energy analysis cases.

Table 5: Default values for parameters used in the tractive energy analysis.

	C_d	C_{RR}	η_{eng}	η_{trans}	LHV, MJ/L	P_{access} , kW	η_{regen}
Default values	0.62	0.007	0.42	0.9	35.8	14.9	0.80

5. Tractive Energy Analysis Results Based on the Synthetic Drive Cycle

5.1. The synthetic drive cycle corresponding to the overall fleet usage

For the analysis of the complete driving data from the HTDC project, the data files were processed as described in Section 3 of this report. We began to process the data corresponding to the low, medium and high mass levels separately using the DCGen tool, but the results from the first module analysis showed that there was very little difference in the speeds and accelerations experienced for the three mass levels. It was expected that there would be a non-negligible decrease in accelerations with increasing mass since the power-to-weight ratio decreases with greater load. The data indicated very little difference between the three cases, however, so the drive cycle developed for the medium mass case was used to analyze all three mass levels. The tractive energy analysis was still repeated for each case separately, however, to account for impact that the difference in mass has on the fuel efficiency evaluations. Figure 30 shows the comparison of the distributions of speed vs. velocity, based on the bivariate histogram, for the three mass levels considered. Careful comparison of the three cases does reveal some differences between them, but the overall profile is surprisingly similar. It is hypothesized that highway conditions, for which most of the range of accelerations are experienced, cause the accelerations to be limited by aerodynamic drag to a point that the mass differences play a relatively minor role. Accelerations also tend to be limited by traffic conditions, so that in many conditions it may not be possible to accelerate at the maximum level that the engine is capable of. Another possible mitigating factor is driver training. Since drivers are trained to only accelerate gradually so that the best efficiency can be achieved, this will tend to reduce the higher accelerations that could be achieved when a lower vehicle loading is present. The fact that the class 8 tractor-trailer application operates primarily on the freeway with quite limited low speed operations very likely influenced this effect significantly, since accelerations at lower speeds probably do show greater acceleration variations with load.

It is interesting to observe that the dominant accelerations for the low speed operations are still at very low levels. This effect was examined in some detail to understand the cause and verify that there was not a problem with the software. Since the distribution shown is scaled to only show the operating conditions that are most frequent in the drive cycle, many of the operating points at higher accelerations, while still present, are overwhelmed by the lower acceleration conditions. For a segment of driving such as that analyzed for the validation synthetic cycle from the previous section of the report, the low speed-high acceleration operating conditions are still apparent, even though their contribution to the overall drive cycle is rather limited. When all driving data is included together, however, the periods of driving at relatively steady, low to medium speeds end up being much more significant than the higher acceleration conditions at the same speed. If a truck drives for just 30 minutes at a speed range of 30-40 mph and maintains a fairly stable speed, this will generate over 1500 seconds of low acceleration conditions for this speed range. This compares to only a few seconds at a time of data within any given speed range that is generated when the truck accelerates from a stop to highway speeds or decelerates rapidly after exiting the highway. There are enough operating conditions on secondary roadways in this application when the trucks drive at steady speeds that this is much more dominant than the high acceleration operations that take place. In the full distribution, as contained in the speed-acceleration histograms, there are thousands of data points for accelerations up to and

beyond the 0.2 m/s^2 level, but these thousands of points do not register significantly in comparison to the millions of data points contained in the overall distribution. One can see an “aura” of low density operating points surrounding the main portions of the drive cycle, but these account for a rather small percentage of the total vehicle usage. Using the statistics of the very large data sets from the HTDC project, the analysis identifies the portions of the drive cycle that are most representative of the overall usage, and it is precisely this information that this drive cycle analysis and synthetic cycle development aims to capture.

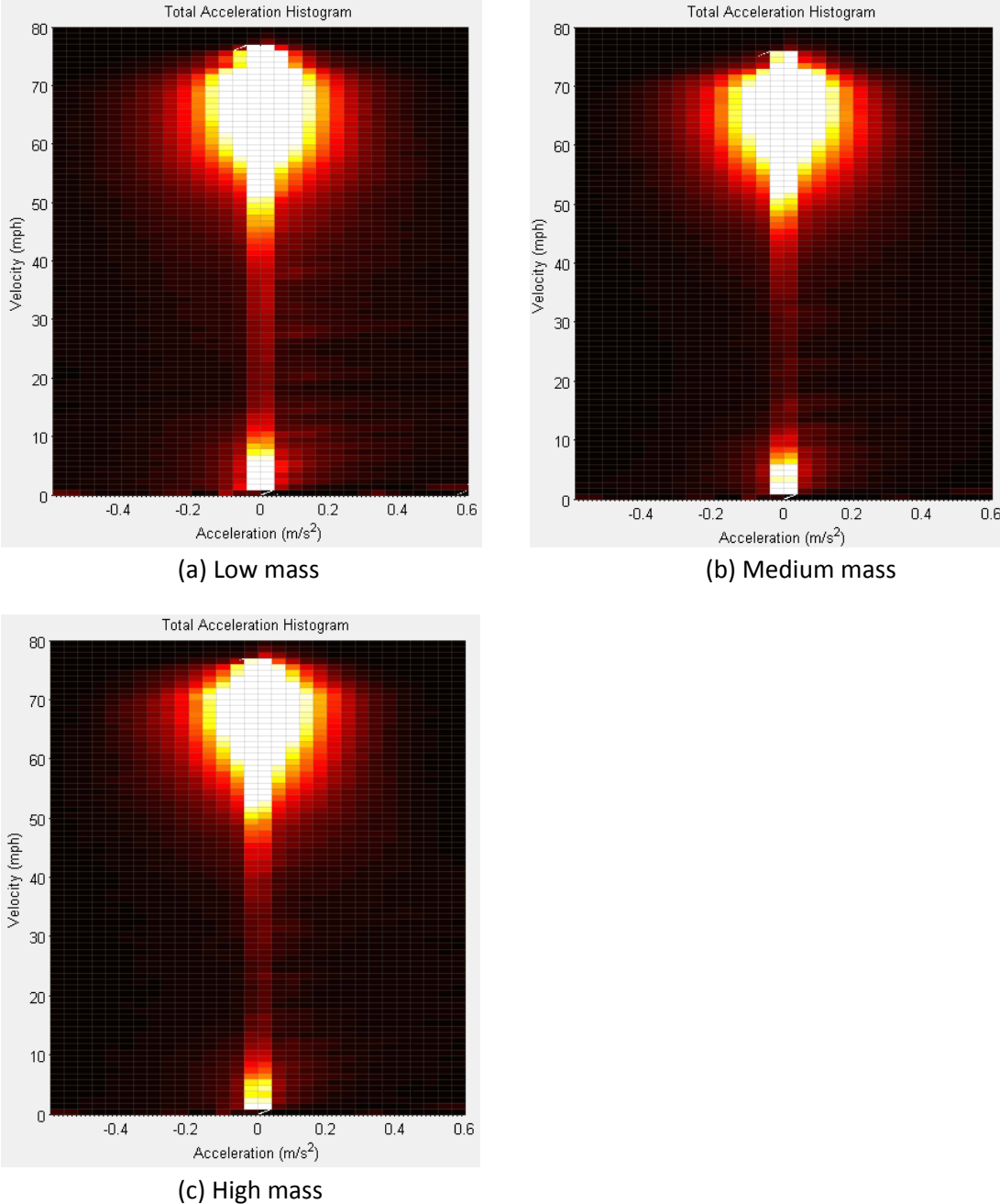


Figure 30 Comparison of the speed vs. acceleration distributions for the low, medium and high mass operating conditions.

The procedure described in section 4.2 was again applied to generate a synthetic drive cycle that represents the overall usage for this trucking fleet’s operation. The medium mass case, which was the largest data set, was used to develop the synthetic drive cycle. The synthetic drive cycle generation using the medium mass case was started before the comparisons were made for the low and high mass cases, and it would have required significant changes to the data to start over using the complete data set for the synthetic cycle creation. Since resources for the project were limited, it was decided to proceed with the medium mass distribution, since it is so similar to the total usage and included over half of the total driving time.

The base synthetic drive cycle created for the project is shown in Fig. 31. The second by second data for this drive cycle is included in a table in the Appendix. This was generated using the non-zero speed data initially, although some brief stops were added at the beginning and end of the cycle and after the short micro-trip in the first 100 seconds. The total length of this drive cycle is 1997 seconds.

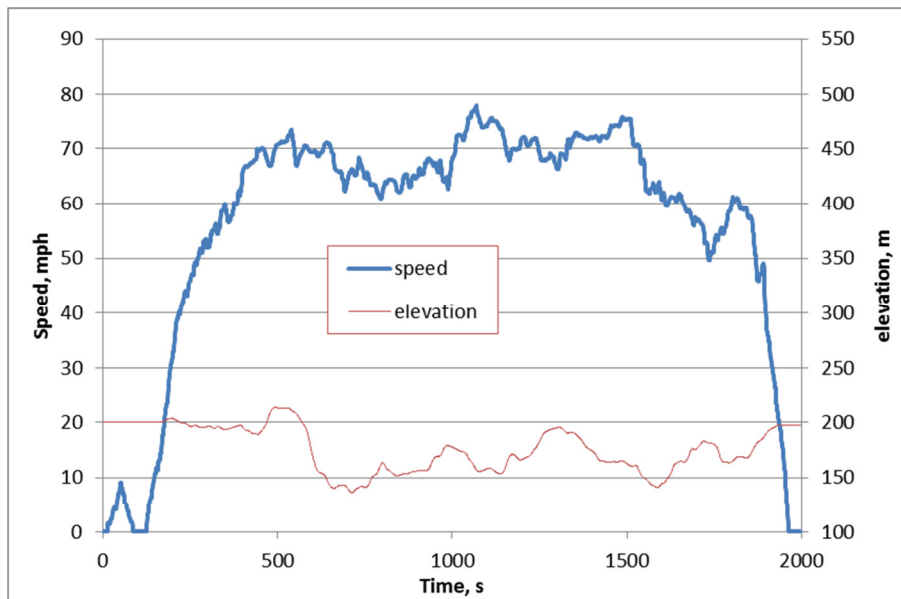


Figure 31 The main synthetic drive cycle developed for the TTEA project, representing the overall usage of the HTDC fleet.

The bivariate speed-acceleration histogram is shown for the HTDC synthetic drive cycle in Fig. 32, along with the total histogram that includes all of the driving data corresponding to the medium mass case. As in the case of the synthetic drive cycle development for the validation case, there are a number of bins in the synthetic cycle histogram representing operating conditions that are not evident in the total histogram representing the original data. These points are a result of using 1-second time intervals when creating the synthetic cycle, as discussed in the previous section. The number of such points in the synthetic histogram for this case is a bit higher than in the case of the validation synthetic drive cycle since the complete set of driving data, with the much larger duration of time represented in the original histogram, contains a more broad set of data in all bins of the histogram. Nonetheless, the overall match to the total histogram is excellent: the error between the synthetic cycle and the original drive cycle distribution, based on a sum of squares metric (L2 norm) is less than 2%.

The accelerations and decelerations for the initial speed ramp-up to and final deceleration from highway speeds occur at a significantly lower rate than a truck would normally follow, but this provides the lower level accelerations that are representative of the lower speed range, as discussed previously.

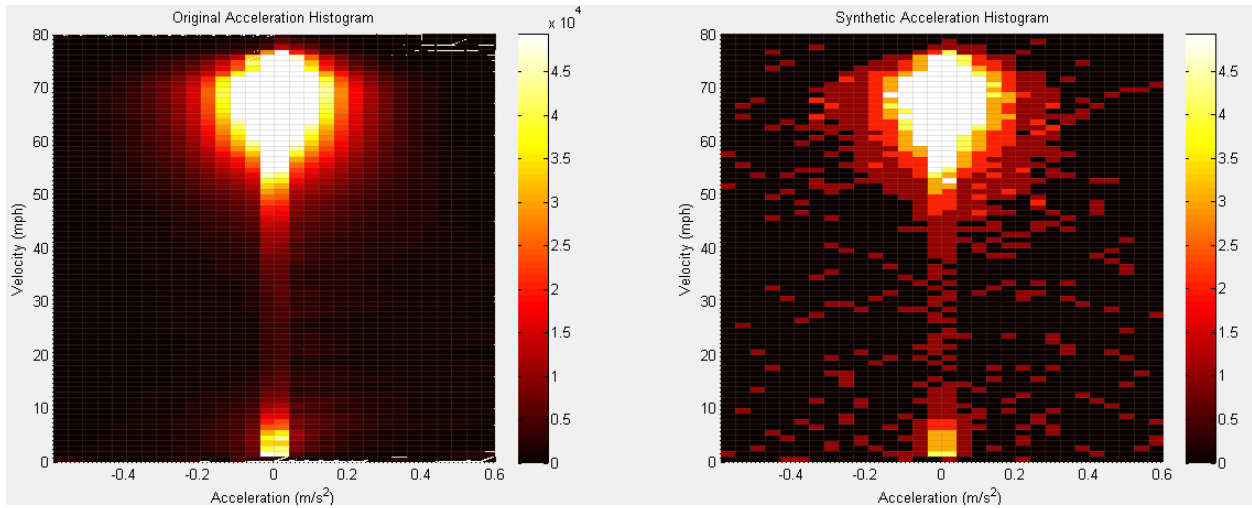


Figure 32 Comparison of the distribution of the synthetic drive cycle and the original histogram containing all of the data from the medium mass operation.

The base synthetic cycle was modified to include the same fraction of idling data as was present in the complete data set. This is handled implicitly (the fraction of idle time is used as an input) in the tractive energy model when evaluating idling energy losses, but for the purpose of presenting a drive cycle with the proper level of idling, representative of the full usage, adding the idling explicitly to the drive cycle is appropriate. A summary of the idling and driving data statistics from all of the measured data is presented in Table 6, and Figure 33 shows the modified synthetic drive cycle with idling present at the average level from all three mass levels. The idling was divided into two types, depending on the duration of each stop. Short idling was defined as having a duration of less than 5 minutes. This would include stops at traffic signals and stop signs, operations in moderate congestion, and short-term stops such as may occur for a rest stop. Long idling was defined to be anything over 5 minutes in duration. This would include stops to pick up or drop off a load, significant traffic congestion or incidents on the highway, and long-term stops (for example, overnight) when the engine is permitted to run to maintain “hoteling” functions. A stop is only considered to be idling if the engine speed is non-zero, and these data only include times when the engine continues to operate. The majority of the long idling periods consisted of multiple hours of continuous stopped operations. It is evident from the table data that this fleet consumed rather significant quantities of fuel due to idling, since the overall fraction of idling time to the total operation time was very nearly 50%. The short idling was only responsible for about 2.6% of this total, while long idling was responsible for 46.3% of all engine operation time.

Table 6: Summary of idling, separated by mass case.

	Low mass	Medium mass	High mass
Total driving time duration, not including stops, sec	15,493,295	22,745,343	4,834,513
Short idle durations (<5 minute stops), sec	1,083,571	1,042,229	215,590
Long idle durations (>5 minutes), sec	15,968,788	19,107,477	5,527,152
% time short idling:	3.33%	2.43%	2.04%
% time long idling:	49.07%	44.54%	52.26%
Total % idle time:	52.40%	46.97%	54.29%
Estimated fuel consumption due to idling, L	8763	10,355	2951
Avg consumption per distance traveled due to idling, L/100 km	2.14	1.73	2.19
Long-idle only avg consumption, L/100 km	2.01	1.64	2.11

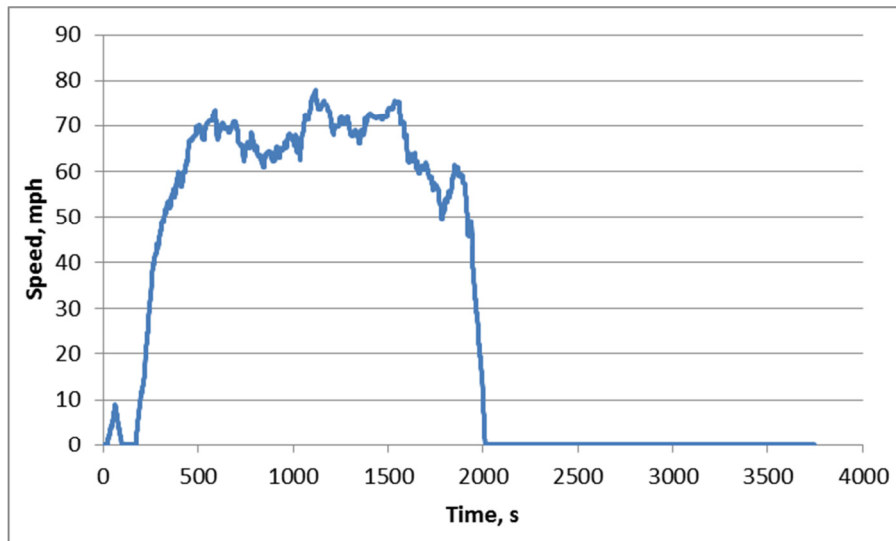


Figure 33 Modified synthetic drive cycle, with the proper ratio of idle time for the overall average. The cycle duration is 3448 seconds.

The total duration of idling for the six trucks was responsible for the consumption of approximately 22,000 liters (5830 gallons) of diesel fuel, or nearly 1000 gallons for each truck. This corresponds to about 4.5% of the total fuel consumed by the trucks during the year. If auxiliary power units (APUs) were used in the fleet, the fuel savings, assuming a 1.4 L/hour reduction in idling fuel consumption, would have been 15,790 L (4172 gallons). This quantity of idling fuel consumption clearly justifies the use of APUs for fleets with such high levels of idling. The short duration idling only corresponded to about 2.7% of the engine operation time. The fuel savings possible with engine start-stop technology would have been no greater than 1200 liters of fuel for this fleet for the year. While it is a worthwhile goal to minimize idling to the greatest extent possible, this level of fuel savings probably cannot justify the purchase of start-stop engine technology by itself. Nonetheless, this technology could become quite

common even in heavy duty vehicles in the future, and would reduce fuel consumption by about 0.2% for this class 8 tractor-trailer application.

5.2. Tractive energy reductions and fuel savings associated with vehicle efficiency technologies

We now present the energy savings results calculated with the tractive energy model based on the synthetic drive cycle representing the fleet’s overall usage. The results for each of the low, medium and high mass cases are first presented, then these results are combined based on a distance-based weighting of each mass case. The tractive energy model was first run using a mass of 17,755 kg, which is the average mass for the low mass grouping of driving data determined from the analysis presented in section 3.2 (after adjustment). The total driving tractive energy and the contributions from each energy loss factor used in the analysis are show in Table 7. The tractive energy for a reduction in mass is also shown, since this result is used in calculating the mass sensitivity in the tractive energy analysis [2]. The fuel savings estimated for a 2000 kg mass reduction, a rolling resistance coefficient reduction by 0.0015 (1.5 kg/ton), and a reduction in aerodynamic drag by 10%, both with and without regenerative braking, are shown in Fig. 34. These changes in the parameters, used in the tractive energy model are believed to be representative of reductions achievable through vehicle lightweighting, improvements in tire rolling resistance corresponding to a replacement of traditional dual tires with New Generation Wide Base Single (NGWBS) tires, and the use of aerodynamic reduction devices that are available for tractor trailers. The energy reductions achievable with regenerative braking are modeled by considering the total energy consumed by braking during decelerations, and we have assumed an overall efficiency of 80% for the regenerative braking system. The average predicted fuel economy for the low mass case is 7.32 mpg for the baseline vehicle configuration.

Table 7: Intermediate results of the tractive energy analysis for the low mass case, using the synthetic drive cycle. The results are based on the default model parameters shown in Table 5.

Tractive Energy Contributions	Total Energy (MJ)	Percent of $E_{\text{trac,drive}}$
$E_{\text{trac,drive}}$	181.24	--
$E_{\text{trac,drive}}$ (mass reduced 2000kg)	171.73	94.8%
$E_{\text{RR,drive}}$	55.16	30.4%
$E_{\text{RR,brake}}$	6.34	3.5%
$E_{\text{aero,drive}}$	96.20	53.1%
$E_{\text{aero,brake}}$	10.21	5.6%
E_{brakes}	13.71	7.6%

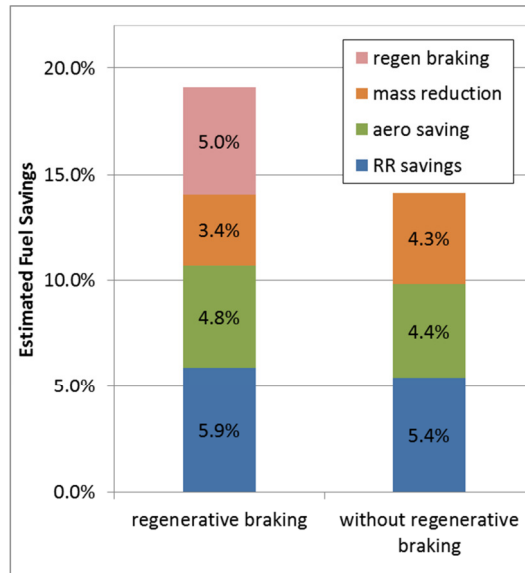


Figure 34 Fuel savings estimate for combinations of advanced efficiency technologies for the low mass case.

The results for the tractive energy contributions and the fuel savings corresponding to vehicle lightweighting, the use of low rolling resistance tires, aerodynamic drag reduction devices, and regenerative braking for the medium mass case are shown in Table 8 and Fig. 35. This is based on a mass of 27,248 kg used in the tractive energy model, which is the average mass determined in section 3.2 (after adjustment) for the medium mass grouping of driving data. The average predicted fuel economy for this mass case is 6.04 mpg in the baseline vehicle configuration.

Table 8: Predicted driving tractive energy and contributions from energy loss factors for the medium mass case, using the synthetic drive cycle.

Tractive Energy Contributions	Total Energy (MJ)	Percent of $E_{trac,drive}$
$E_{trac,drive}$	227.52	--
$E_{trac,drive}$ (mass reduced 2000kg)	217.64	95.7%
$E_{RR,drive}$	81.62	35.9%
$E_{RR,brake}$	12.77	5.6%
$E_{aero,drive}$	92.68	40.7%
$E_{aero,brake}$	13.73	6.0%
E_{brakes}	27.31	12.0%

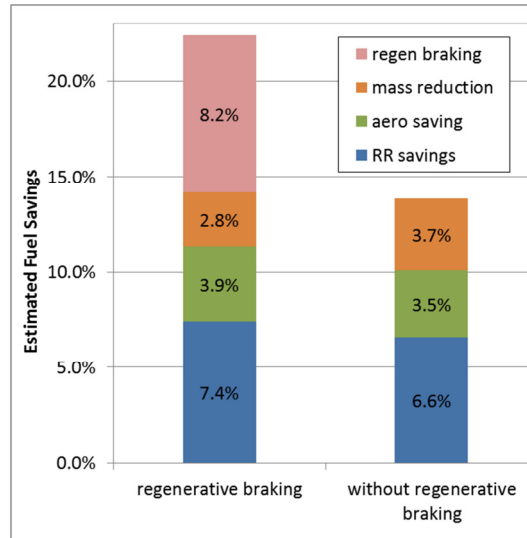


Figure 35 Fuel savings estimate for combinations of advanced efficiency technologies for the medium mass case.

For the high mass case, the results from the tractive energy analysis are presented in Table 9 and Fig. 36. The analysis used a mass of 34,741 kg, corresponding to the average mass determined in section 3.2 (after adjustment) for the high mass grouping of driving data. The baseline configuration had a predicted fuel economy of 5.30 mpg for this mass case.

Table 9: Driving tractive energy and contributions from the different energy loss factors for the high mass case, based on the synthetic drive cycle.

Tractive Energy Contributions	Total Energy (MJ)	Percent of $E_{trac,drive}$
$E_{trac,drive}$	264.96	--
$E_{trac,drive}$ (mass reduced 2000kg)	254.91	96.2%
$E_{RR,drive}$	101.64	38.4%
$E_{RR,brake}$	18.70	7.1%
$E_{aero,drive}$	90.32	34.1%
$E_{aero,brake}$	16.09	6.1%
E_{brakes}	38.96	14.7%

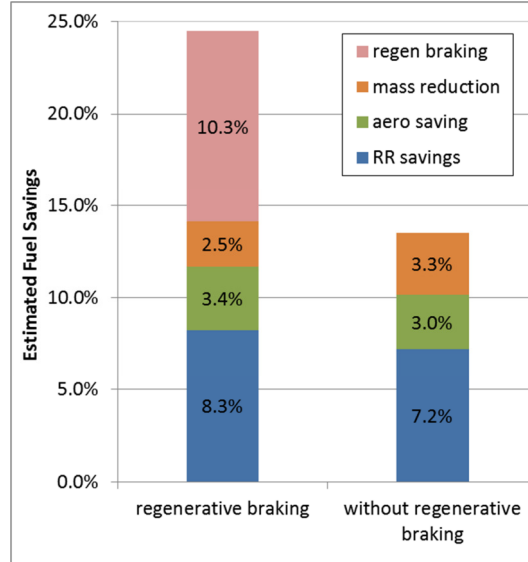


Figure 36 Fuel savings estimate for combinations of advanced efficiency technologies for the high mass case.

These results show that as the mass increases, the contribution to the driving tractive energy from both the tire rolling resistance and braking increase, while the other factors contribute approximately the same to the tractive energy. As a result, the fuel savings from rolling resistance and regenerative braking increase for the higher load conditions, while the relative fuel savings generated by the same aerodynamic improvement or mass reduction are somewhat lower as the mass increases, although the net fuel savings due to these factors will remain very similar at different mass levels. The savings predicted from regenerative braking becomes relatively significant at the higher mass levels, which is somewhat surprising for the predominantly freeway operations that this application experiences.

5.3. Average fuel savings for the overall fleet usage

To use the above results from each mass case to quantify the energy savings potential from different vehicle efficiency technologies and combinations of technologies for the overall operation of the fleet, we must appropriately weight the results based on the fraction of distance traveled at each mass level. The following analysis provides a means to use the same analysis methodology used in the tractive energy model for a single run to combine the mass cases in a consistent and appropriate manner.

It is clear that the tractive energy contribution from a given mass case (or another vehicle configuration, to generalize) is proportional to the distance traveled for that configuration, and we can define an average tractive energy per unit distance traveled, which we denote as E'_{trac} . This distance-normalized tractive energy factor corresponds to the overall usage (i.e. the drive cycle) corresponding to each given vehicle configuration. For each configuration, j , we can therefore express the tractive energy on a per-distance-traveled basis as

$$E_{trac,j} = E'_{trac,j} L_j, \quad (11)$$

where L_j is the distance traveled in configuration j . The overall tractive energy requirement due to the combination of all vehicle configurations (i.e. for the full fleet usage) is given by

$$E_{trac,overall} = E'_{trac,overall} \sum_{j=1}^N L_j = \sum_{j=1}^N E'_{trac}(m_j) L_j. \quad (12)$$

where N is the number of configurations and the first sum on the left hand side represents the distance traveled in all of the configurations. We should be cognizant that, by combining tractive energy terms across the different vehicle configurations, we have implicitly assumed that the vehicle parameters used in the tractive energy model that do not influence each $E'_{trac,j}$ term remain constant. For example, this assumes that a single average engine thermal efficiency is appropriate for all of the configurations considered. While the thermal efficiency, in reality, will vary with the engine load, the effect is not expected to be dramatic with the drive cycle not differing for the three mass cases we are considering. This analysis, is therefore reasonable for our particular scenario, but if very different configurations are evaluated using this approach, one should realize that the assumptions of the model may become less realistic than for a single configuration.

Continuing with our line of reasoning, based on Eq. (8) and Eq. (12), we expect that the distance-normalized tractive energy relationship must hold true both for the total driving tractive energy and for the individual contributions to the driving tractive energy corresponding to each energy loss factor (driving and braking contributions from rolling resistance and aerodynamic drag, as well as the contribution from the braking tractive energy). Combining the two equations, we can therefore decompose the contributions associated with the various technologies using the following relationship:

$$E'_{trac,i} = \frac{\sum_{j=1}^N E'_{trac,i}(m_j) L_j}{\sum_{j=1}^N L_j} = \sum_{j=1}^N E'_{trac,i}(m_j) w_j, \quad (13)$$

where i represents each energy loss factor and w_j , the mass weighting factor, is given by the ratio of the distance traveled at each mass to the total distance traveled. Using Eq. (13), the results for each energy loss factor calculated for each configuration can be converted to obtain the average tractive energy loss factors associated with the overall fleet operation. Table 10 shows the set of distance-normalized loss factors (and the mass sensitivity) for the different mass cases and that determined using Eq. (13) for the combined vehicle usage. The values for $\Delta E'_{trac,drive,mass}$ and $\Delta E'_{trac,braking,mass}$ represent the change in the driving and braking tractive energies, respectively, associated with a mass reduction of 2000 kg. For the calculation, the distance traveled in each mass case is shown in Table 11.

Table 10: Distance-normalized tractive energy factors from the tractive energy analysis for each mass case, and the combined result for the full fleet.

	$E'_{trac,drive}$	$E'_{RR,drive}$	$E'_{RR,brake}$	$E'_{aero,drive}$	$E'_{aero,brake}$	$E'_{braking}$	$\Delta E'_{trac,drive,mass}$	$\Delta E'_{trac,braking,mass}$
Low mass	3.601	1.094	0.126	1.907	0.202	0.272	-0.189	-0.052
Medium mass	4.522	1.618	0.253	1.837	0.272	0.541	-0.197	-0.059
High mass	5.268	2.015	0.371	1.791	0.319	0.772	-0.200	-0.063
Combined	4.284	1.479	0.222	1.857	0.253	0.473	-0.194	-0.057

Table 11: Distance traveled in each mass case.

	distance traveled (km)	average mass (kg)
Low mass	389,240	17,755
Medium mass	594,307	27,248
High mass	126,636	34,741
Combined	1,110,182	24,774

With the combined tractive energy terms, the sensitivity factors for the tractive energy model were calculated for the overall vehicle usage and the final fuel savings estimates associated with the vehicle efficiency technologies considered were determined. The contribution from each energy loss factor for the overall combined vehicle usage is shown in Table 12, and the fuel savings estimates corresponding to our standard parameter variations were determined for the complete fleet usage. These fuel savings estimates are shown in Fig. 37.

Table 12: The contributions to the driving tractive energy from each energy loss factor for the overall, combined fleet usage, based on the synthetic drive cycle.

Tractive Energy Contributions	Total Energy (MJ)	Percent of $E_{trac,drive}$
$E_{trac,drive}$	216.10	--
$E_{trac,drive}$ (mass reduced 2000kg)	206.29	95.5%
$E_{RR,drive}$	74.63	34.5%
$E_{RR,brake}$	11.19	5.2%
$E_{aero,drive}$	93.65	43.3%
$E_{aero,brake}$	12.77	5.9%
E_{brakes}	23.87	11.0%

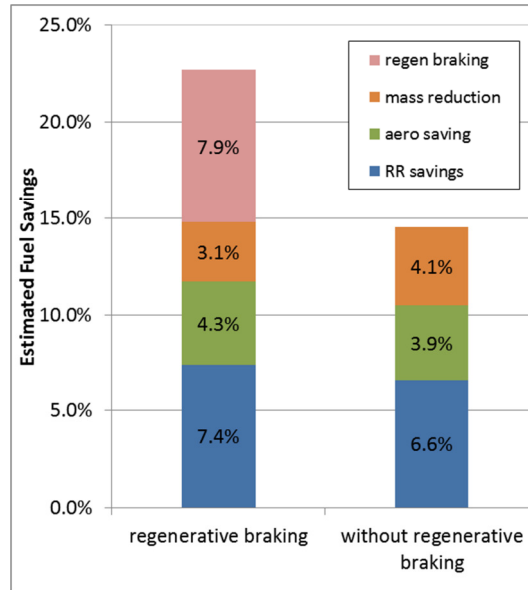


Figure 37 Fuel savings estimate for combinations of advanced efficiency technologies for the combined usage in the HTDC fleet.

5.4. Summary of the tractive energy model results for the class 8 tractor-trailer application evaluated

The savings in fuel consumption predicted by the tractive energy model for this class 8 tractor-trailer fleet are rather impressive for the technologies considered. By implementing the rolling resistance and aerodynamic drag technologies, which can be done as retrofits to existing vehicles, over a 10% improvement in fuel economy can be achieved, based on the assumptions for the vehicle parameter changes. The reduction in the rolling resistance coefficient by 0.0015, or 1.5 kg/ton, used in this analysis depends on the initial and final set of tires used on the vehicle, but this level of reduction is very typical, if not on the conservative side, when replacing typical dual tires with NGWBS tires. Similarly, the 10% reduction in aerodynamic drag coefficient used in the analysis seems to be rather typical based on results that have been reported in the literature for fuel efficiency gains with aerodynamic drag reduction devices. Vehicle lightweighting, while it represents a change in vehicle design that must be implemented for new vehicles, can also yield quite significant fuel savings, and research and development of lighter materials and manufacturing methods that can reduce truck mass should be pursued by vehicle manufacturers and the transportation research community. The predicted benefits of the use of a regenerative braking system in this tractor-trailer application are quite impressive. For the overall usage of this fleet, regenerative braking is predicted to reduce fuel consumption by nearly 8%, and if low rolling resistance tires and aerodynamic drag reductions are used at the same time, the regenerative braking increases the benefits by an additional 1.2%. As shown in Fig. 36, if a fleet operates at higher average mass levels, the hybrid savings can exceed 10%. This fuel savings potential suggests that further study of hybridization of class 8 tractor-trailers should be pursued.

5.5. Consideration of the accuracy of using a substitute drive cycle as opposed to the synthetic drive cycle

The synthetic drive cycle approach was developed to accurately characterize the usage of the fleet, and the validation of this method shows that the fuel savings estimates are very representative of what can be achieved in the fleet when implementing advanced vehicle efficiency technologies. As an alternative approach, we selected a single drive cycle for which the vehicle mass was constant that had a usage as similar as possible to the overall usage of the fleet. Histograms of individual drive cycles were compared to the total histogram representing the complete fleet usage, and a measured drive cycle that visually similar to the total histogram was selected. The tractive energy analysis was then run using this “substitute” measured drive cycle. Since many drive cycles used for fuel efficiency evaluations are selected based on short-term driving measurements without careful evaluation of the overall usage, it seems reasonable to consider the errors in following such an approach. This comparison is intended to shed some light on how accurate one might expect fuel efficiency predictions to be when arbitrarily selected drive cycles are used to represent a particular usage.

The drive cycle selected for this evaluation was from the medium mass set of data. A comparison of the acceleration-velocity bivariate histogram is compared to that of the total histogram for the medium mass case in Fig. 38.

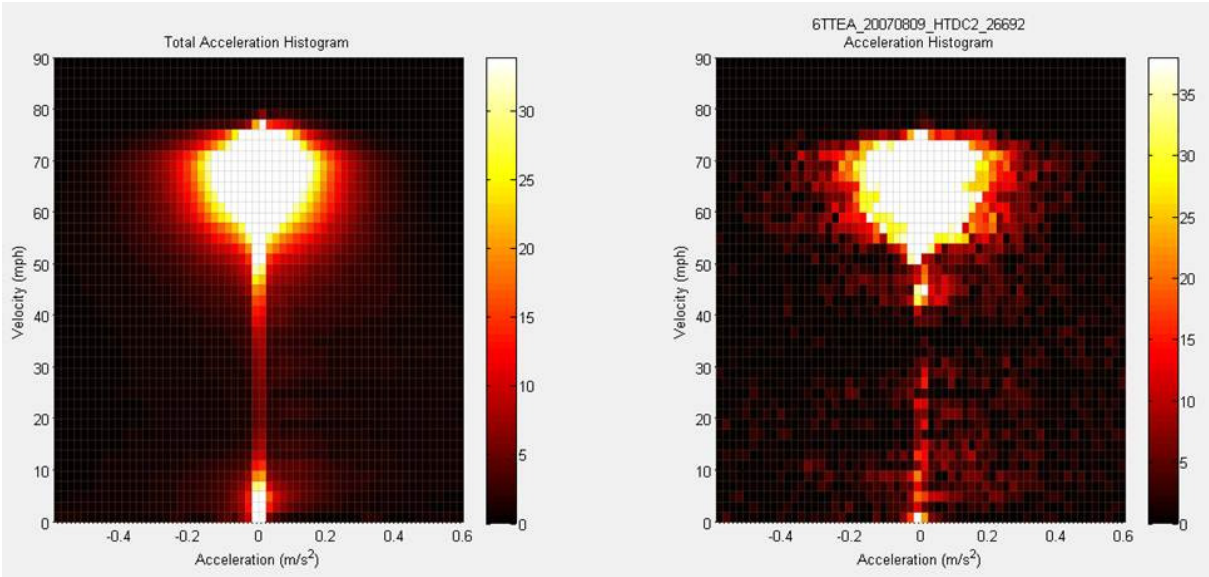


Figure 38 Comparison of the histogram for substitute measured drive cycle to that of the overall usage for the HTDC fleet.

The substitute cycle matched the shape and highway speeds and accelerations quite well. When comparing individual days of driving, it is fairly common to have portions of travel that are not characteristic of the overall usage, for example extended driving at a lower speed or missing some range of accelerations in the highway operation so that the individual day’s histogram does not appear to be similar to the total histogram. The single-day drive cycle was processed in the same way as all other driving data used in this study prior to running the tractive energy model. The same cycle was also used

in the MOVES model emissions analysis (see section 6 of this report), and the idling duration was adjusted to have the same percentage of idling as the overall usage. The same mass value and all other input parameters used in the medium synthetic cycle analysis were also used in the tractive energy analysis for the substitute synthetic cycle so that the comparisons would be on the same basis.

Table 13 and Fig. 39 show the results of the tractive energy analysis. Comparing the percent contributions to the driving tractive energy in Table 13 to those for the medium mass synthetic cycle result (Table 8, result is repeated in the last column of Table 13) shows clearly that there are large differences between the characteristics of the synthetic cycle and the substitute drive cycle.

Table 13: The contributions to the driving tractive energy from each energy loss factor for the overall, combined fleet usage, based on the synthetic drive cycle.

Tractive Energy Contributions	Total Energy (MJ)	Percent of $E_{\text{trac,drive}}$ substitute measured cycle	Percent of $E_{\text{trac,drive}}$ medium mass synthetic cycle
$E_{\text{trac,drive}}$	2566.32	--	--
$E_{\text{trac,drive}}$ (mass reduced 2000kg)	2436.66	94.9%	95.5%
$E_{\text{RR,drive}}$	726.29	28.3%	34.5%
$E_{\text{RR,brake}}$	238.92	9.3%	5.2%
$E_{\text{aero,drive}}$	793.85	30.9%	43.3%
$E_{\text{aero,brake}}$	276.67	10.8%	5.9%
E_{brakes}	506.68	19.7%	11.0%

The percentage contribution to the driving tractive energy due to vehicle braking is nearly twice as great for the substitute cycle, while the driving tractive energy contributions from both rolling resistance and aerodynamic drag are considerably lower. Comparing the fuel savings estimate with Fig. 35 shows that there is a sizable difference in this result, also. In particular, the predicted savings from regenerative braking is considerably greater for the substitute drive cycle, but differences of 0.7 to 1.3% for each of the no regenerative braking results also exist.

This comparison shows that large errors in the predicted fuel savings can occur if the usage is not well represented by the drive cycle used for fuel efficiency evaluations. Even when the usage, as evidenced by the acceleration-velocity histogram, appears to match fairly well, relatively large differences can occur. To ensure that a selected drive cycle is representative of the actual usage of a particular application, it is rather important that a statistical evaluation of the usage be conducted.

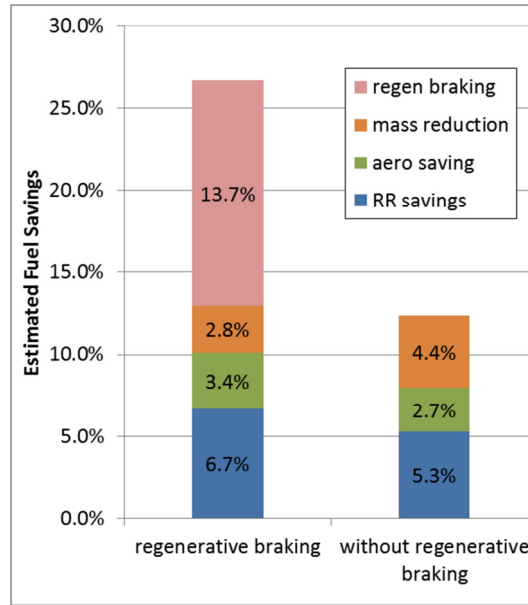


Figure 39 Fuel savings estimate using the substitute measured drive cycle.

6. EPA MOVES (Motor Vehicle Emission Simulator) Model Analysis

The Motor Vehicle Emissions Simulator (MOVES) is the U.S. Environmental Protection Agency's (EPA) current regulatory computer model used for estimating on-road emissions from cars, trucks, motorcycles, and buses. It incorporates the latest emission measurement data and more sophisticated calculation algorithms than MOBILE, the previous vehicle emissions regulatory model. Transient driving conditions that influence the instantaneous engine load, such as vehicle acceleration, cruising and coasting, road grade, and aerodynamic and rolling resistances have been shown to influence emissions [8-10], and for that reason, these vehicle activities or parameters have been integrated into MOVES using the vehicle specific power (VSP) approach [11].

The official release of MOVES2010 occurred on March 2, 2010. (The numbers next to the acronym refer to the version number of the model.) At the present, the two latest versions are MOVES2010a released in September 2010, and MOVES2010b released in April 2012 which includes a number of improvements over the former. However, the net impact of the changes on emissions between versions 2010a and 2010b is very small at both the County and Project level scales. The MOVES web site [12] is the source for the software, technical and user manuals, and other guidance documents.

In MOVES, emission rates are calculated using operating mode distributions. Operating mode is defined in terms of classes or ranges of VSP and vehicle road speed that have distinct emission rates associated with them. For heavy duty (HD) vehicles, scaled tractive power (STP), which will be defined later in the report, is used instead of VSP. The operating mode distribution is the fraction of time the vehicle operates (or carries out its behavior) within a definite range of VSP (or STP) and vehicle speeds, which are referred to as bins. A bin is similar to the location in an array or matrix that will be treated later as an algebraic entity for further calculations. The operating modes of most concern for HD vehicles are

shown in Table 14. For example, operating mode bin no. 14 is defined as Cruise/Acceleration, 6 kW ≤ STP < 9 kW; 1 mph ≤ Speed < 25 mph.

Table 14: MOVES operating modes

opModeID	opModeName
0	Braking
1	Idling
11	Low Speed Coasting; STP < 0; 1 ≤ Speed < 25
12	Cruise/Acceleration; 0 ≤ STP < 3; 1 ≤ Speed < 25
13	Cruise/Acceleration; 3 ≤ STP < 6; 1 ≤ Speed < 25
14	Cruise/Acceleration; 6 ≤ STP < 9; 1 ≤ Speed < 25
15	Cruise/Acceleration; 9 ≤ STP < 12; 1 ≤ Speed < 25
16	Cruise/Acceleration; 12 ≤ STP; 1 ≤ Speed < 25
21	Moderate Speed Coasting; STP < 0; 25 ≤ Speed < 50
22	Cruise/Acceleration; 0 ≤ STP < 3; 25 ≤ Speed < 50
23	Cruise/Acceleration; 3 ≤ STP < 6; 25 ≤ Speed < 50
24	Cruise/Acceleration; 6 ≤ STP < 9; 25 ≤ Speed < 50
25	Cruise/Acceleration; 9 ≤ STP < 12; 25 ≤ Speed < 50
26	Cruise/Acceleration; 12 ≤ STP; 25 ≤ Speed < 50
27	Cruise/Acceleration; 12 ≤ STP < 18; 25 ≤ Speed < 50
28	Cruise/Acceleration; 18 ≤ STP < 24; 25 ≤ Speed < 50
29	Cruise/Acceleration; 24 ≤ STP < 30; 25 ≤ Speed < 50
30	Cruise/Acceleration; 30 ≤ STP; 25 ≤ Speed < 50
33	Cruise/Acceleration; STP < 6; 50 ≤ Speed
35	Cruise/Acceleration; 6 ≤ STP < 12; 50 ≤ Speed
36	Cruise/Acceleration; 12 ≤ STP; 50 ≤ Speed
37	Cruise/Acceleration; 12 ≤ STP < 18; 50 ≤ Speed
38	Cruise/Acceleration; 18 ≤ STP < 24; 50 ≤ Speed
39	Cruise/Acceleration; 24 ≤ STP < 30; 50 ≤ Speed
40	Cruise/Acceleration; 30 ≤ STP; 50 ≤ Speed

Note: this table was extracted from the MySQL "operatingMode" table and was edited for clarity

A priority hierarchy is used by the model to estimate emissions at the Project level scale. It can utilize (1) the default drive schedules built into MOVES, (2) a user-supplied drive cycle, or (3) a user supplied operating mode distribution. First preference is given to a user-supplied operating mode distribution, followed by a user-supplied drive cycle, and lastly to applying built-in default schedules that require user-supplied average speed information. In the end, to estimate emissions MOVES always relies on the operating mode distribution; however, if the user only supplied average speed information, the model will apply this in conjunction with the default driving schedules to create a generalized operating mode distribution.

Only 12 default driving schedules currently exist in MOVES for HD vehicles; each has an average speed associated with it [13]. A description of these driving schedules is shown in Table 15. For representing a

real world driving condition, this approach is incomplete. On the other hand, a user-supplied drive cycle that contains second-by-second speed and road grade information from which the model can then generate a more realistic operating mode distribution is a significant improvement over the average speed approach.

Table 15: MOVES default driving schedules for HD vehicles

driveScheduleID	averageSpeed (mph)	driveScheduleName
301	5.8	HD 5mph Non-Freeway
302	11.2	HD 10mph Non-Freeway
303	15.6	HD 15mph Non-Freeway
304	19.4	HD 20mph Non-Freeway
305	25.6	HD 25mph Non-Freeway
306	32.5	HD 30mph Non-Freeway
351	34.3	HD 30mph Freeway
352	47.1	HD 40mph Freeway
353	54.2	HD 50mph Freeway
354	59.4	HD 60mph Freeway
355	71.7	HD High Speed Freeway
399	25.3	HD Freeway Ramp

Note: this table was extracted from the MySQL "driveschedule" table and was edited for simplicity

MOVES is capable of quantifying the reduction of some exhaust emissions by the use of certain technologies available for diesel buses and trucks that have been retrofitted with emission control equipment. However, this is generally used for state implementation plans (STP) and/or transportation conformity analyses at the local county level in non-attainment area. (This is an area considered to have air quality worse than the EPA's National Ambient Air Quality Standards, and the local or state governing agency for the area must devise a plan to meet the standard or risk losing some forms of federal financial assistance.) A retrofit is defined broadly to include any technology that when applied to an existing diesel engine will achieve emission reductions beyond that currently required by EPA regulations at the time the engine was certified [14]. Trailer aerodynamic kits and low rolling resistance tires can be considered examples of aftermarket retrofits [15]. But for SIPs in non-attainment areas, correction factors are simply applied to vehicle fleet populations to show reduction in emissions due to the percentage effectiveness of the retrofit. Thus, advanced efficiency technologies to improve fuel economy, such as aerodynamic drag reduction devices, low rolling resistance tires, and lightweight materials are not easily represented directly in MOVES. However, the default parameters that the model uses for STP calculations can be edited or altered in the MySQL database. For the most part these default parameters in MOVES are based on overall fleet averages derived from historic data, but they are defined in terms of road load coefficients, tire rolling resistance, aerodynamic drag, and friction losses in the drivetrain. MOVES is written in Java™ and uses the MySQL relational database management system. The principal user inputs and outputs, and the internal working storage locations necessary for MOVES to run are located in the MySQL database.

The MOVES2010a model, hereafter referred to simply as MOVES, was used to estimate exhaust emissions using the drive cycles of class 8 tractor-trailers based on real-world usage. The emissions evaluated with these simulations were carbon monoxide (CO), nitrogen oxides (NO_x), gaseous hydrocarbons (HC), primary PM₁₀ and PM_{2.5}. The summation of nitrogen oxide (NO) and nitrogen dioxide (NO₂) is NO_x. Particulate matter less than 10 microns or less than 2.5-microns in aerodynamic diameter are PM₁₀ or PM_{2.5}, respectively which denote the size of the particles. Total PM here refers to the summation of organic carbon (OC) and elemental carbon (EC) derived from running exhaust only. Sulfate particulates from the exhaust, brake and tire wear were not modeled. MOVES was also used to estimate energy consumption which is a surrogate measure for fuel usage and/or carbon dioxide (CO₂) emissions.

6.1. Objective

The University of Tennessee, Knoxville (UTK) performed all of the MOVES modeling and analysis for this project. This phase of the study focused on truck drive cycle impacts on running exhaust emissions. Real world (measured) drive cycles and synthetic (i.e., condensed or abbreviated) drive cycles were compared to understand the drive cycle effects on emissions and to validate the use of the synthetic cycle as a replacement for the original driving data in emissions calculations.

The following analyses using MOVES were performed in the study: (1) second-by-second emission estimates were compared with measured emissions from a dynamometer test performed using a measured drive cycle; (2) MOVES model emission estimates based on measured drive cycles from Oak Ridge National Laboratory's (ORNL) heavy truck duty cycle (HTDC) data set were compared with emission estimates from representative synthetic drive cycles; (3) emissions benefits of advanced efficiency technologies such as aerodynamic drag reduction devices, low rolling resistance tires, and lightweight materials for class 8 long-haul trucks were assessed using MOVES; and (4) results obtained using the default drive cycles in MOVES were compared with model results from simulations using a measured, representative truck drive cycle for this application as well as with the synthetic drive cycle developed for the project.

6.2. MOVES Modeling Analysis/Discussion

6.2.1. MOVES mean base rates for running exhaust emissions

The MOVES mean base rates are average emission rates for pollutants in each combination of regulatory class, model year group, fuel type, pollutant process, and operating mode bin combination. The mean base rates are adjusted by ambient temperature and humidity and by air conditioning (AC) correction factors. The mean base running exhaust emissions are stored in the "emissionRateByAge" table in the MOVES input MySQL database file. All simulations using the MOVES model in this study were performed using mean base rates for a model year of 2005 and an age of 0-3 years of HD trucks to compare with the tested emission results on the ORNL test cycle. These are the inputs that are relevant for the trucks tested in the Heavy Truck Duty Cycle (HTDC) project at the time that all measurements

were performed. It should be noted that the same vehicle model year and age were applied to all vehicle drive cycle data used in the MOVES phase of this study.

6.2.2. Emissions calculation procedure using the MOVES method

In MOVES, the scaled tractive power (STP) parameter is used for estimating HD vehicle emissions. STP was designed to fit into the existing operating mode framework which was developed originally for light-duty vehicles [16]. Road load coefficients, including tire rolling resistance, aerodynamic drag, and friction losses in the drivetrain are incorporated into the STP term using these default placeholder coefficients (the rolling A term, the rotating B term and the drag C term) which will be defined later, and are located in the "sourceUseType" table in the MySQL database. The default source mass for the vehicle category is 31.4038 tonne (69,234 lb); this is based on other historic data that were collected for this vehicle category and represents an average vehicle mass for the category.

The general steps to determine running exhaust emissions for HD diesel trucks in MOVES are the following:

1. The scaled tractive power (STP) in units of kW is calculated for each second using the general equation

$$STP_t = \frac{Av_t + Bv_t^2 + Cv_t^3 + mv_t(a_t + g \sin \theta)}{f_{scale}} \quad (14)$$

where

v = velocity (m/s)

a = acceleration, (m/s²)

m = mass, (tonne)

t = time, (s)

g = acceleration due to gravity, (9.8 m/s²)

θ = road grade, (radians)

A = rolling resistance, (kW-s/m)

B = rotating resistance, (kW-[s/m]²)

C = aerodynamic drag, (kW-[s/m]³)

f_{scale} = scaling or fixed mass factor (default value = 17.1)

The velocity is the actual second-by-second speed data. Acceleration is calculated from velocity as $(v_t - v_{(t+1)})/(1 \text{ s})$. (All data used in the analysis used 1-second time intervals.)

For Combination long-haul trucks (i.e., heavy duty diesel vehicles see default values):

Rolling A term = $\mu_0 \cdot g \cdot m$, with default value = 2.08126 kW-s/m

Rotating B term = $\mu_1 \cdot g \cdot m$, default value = 0 kW-s²/m²

Drag C term = $(C_d \cdot \rho_{air} \cdot R)/2 + \mu_2 \cdot g \cdot m$, default value = 0.0041884 kW-s³/m³

where

$\mu_0 = (C_{RR})$ zero-order tire rolling-resistance coefficient, (unitless)

μ_1 = first-order tire rolling-resistance coefficient, (s/m)

μ_2 = second-order tire rolling-resistance coefficient, (s²/m²)

C_d = aerodynamic drag coefficient of the vehicle, (unitless)

R = cross-sectional frontal area of the vehicle, (m²)

ρ_{air} = density of air, (1.202 kg/m³)

2. The operating mode for each second is then determined using the STP_t value.
3. Finally, using the operating mode and the source type/vehicle model year-age, the mean base running exhaust emissions are selected from the “emissionratebyage” table in the MOVES input database file for the regulatory class, the model year, and the age group using diesel fuel.
4. Temperature and humidity were not adjusted in this study.

6.2.3. **Comparison of MOVES predictions with measured emissions data from one of the HTDC test trucks**

Data from the West Virginia University (WVU) test sequence no. 5271 using the test drive cycle ORNL4LS (presented in a previous section of this report) were processed to create second-by-second emissions estimates using the MOVES mean base rates, vehicle speed, and road grade profiles. The ORNL4LS drive cycle is shown in Fig. 40. The WVU data were derived from chassis dynamometer measurements and exhaust emission sampling. Three repeated emission tests were conducted for this cycle during December 2007. The tests were performed on one of the test vehicles from the HTDC project, a Volvo tractor that had a model year 2005 Cummins ISX 475 hp diesel engine. It had a standard exhaust system that was not fitted with a particulate trap or a catalytic converter.

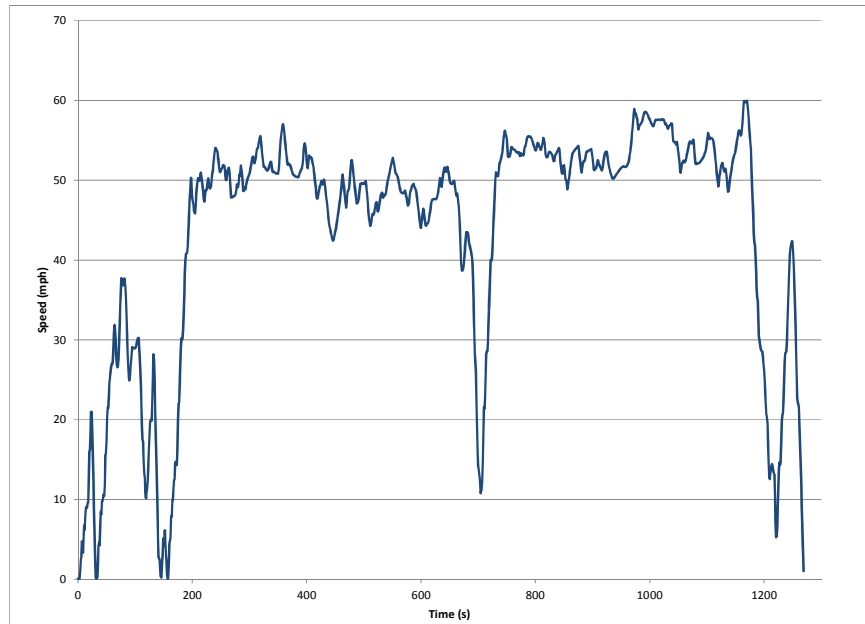


Figure 40 Measured dynamometer hub speed data from the WVU dynamometer testing with the ORNL4LS drive cycle.

Figure 41 is a 10-minute segment showing second-by-second NO_x emissions as measured during the dynamometer testing conducted at West Virginia University and this is compared with the NO_x emissions predicted by MOVES for the same drive cycle. Predictions for CO and HC emissions, and the fuel rate using the ECU data are shown in Figures 42 through 44, respectively.

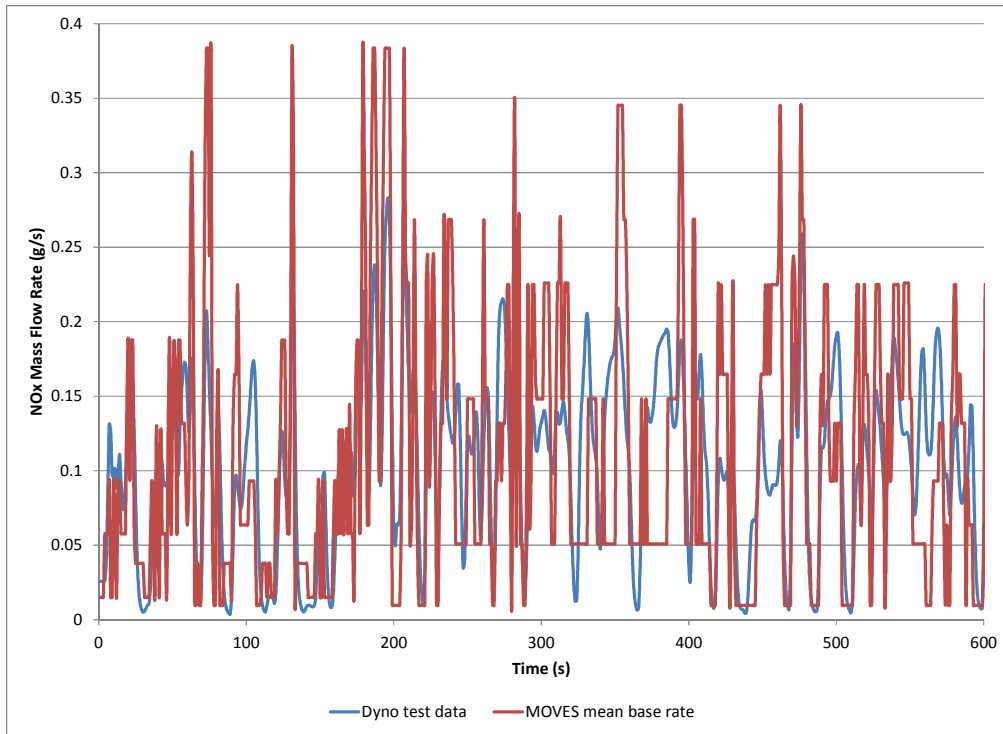


Figure 41 Nitrogen oxide emissions measured during the dynamometer test and the mean base rates predicted by MOVES using speed data from the ECU.

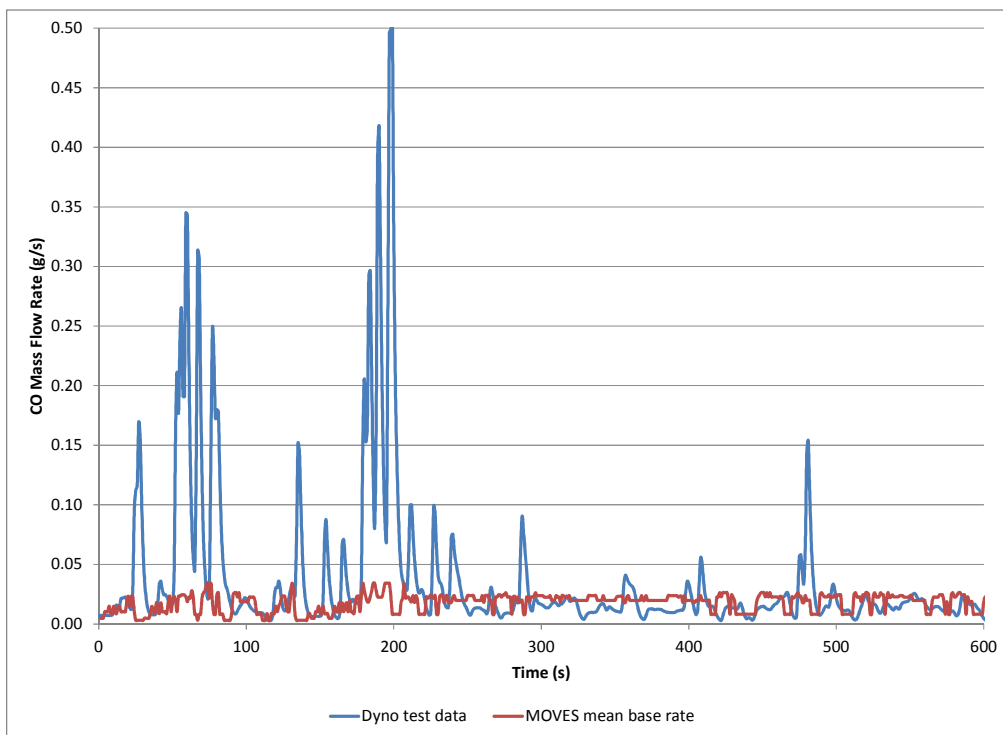


Figure 42 Carbon monoxide emissions measured during the dynamometer test and the mean base rates predicted by MOVES using speed data from the ECU.

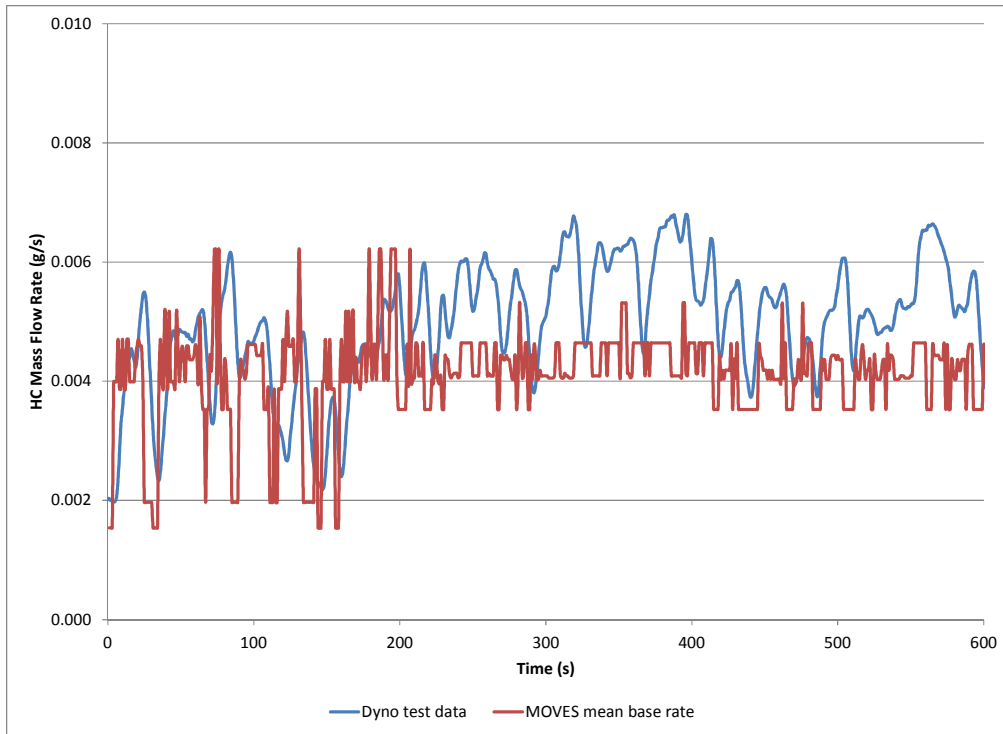


Figure 43 Gaseous hydrocarbon emissions measured during the dynamometer test and the mean base rates predicted by MOVES using speed data from the ECU.

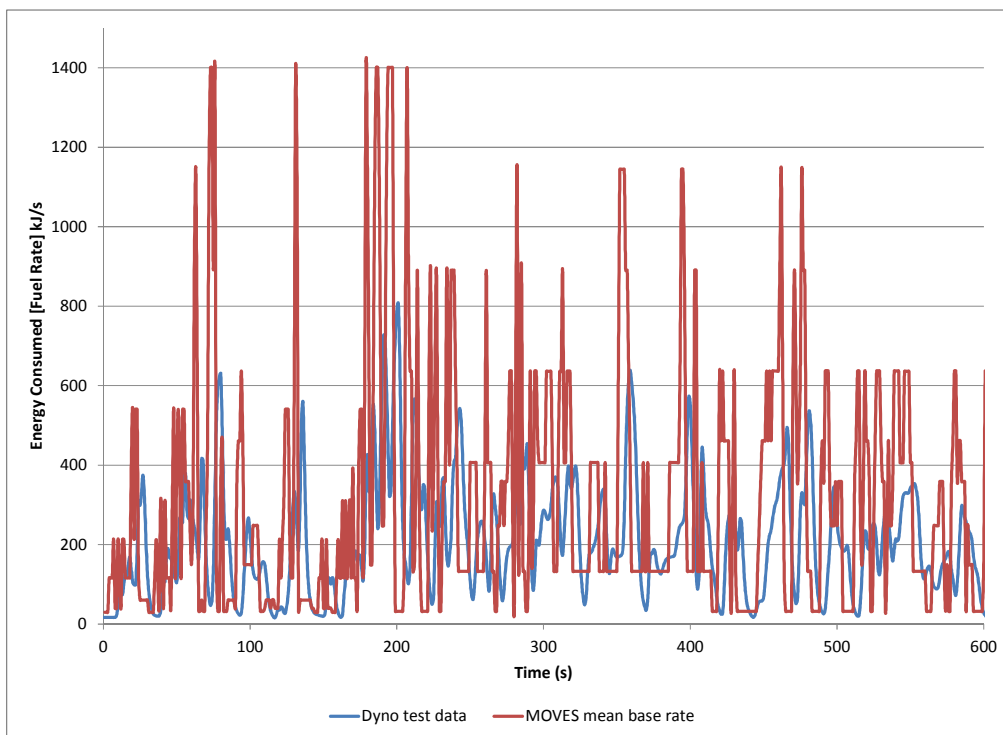


Figure 44 Energy consumption measured during the dynamometer test and the mean base rates predicted by MOVES using speed data from the ECU.

It is evident from the CO and HC predictions that the MOVES model still under-estimated the emissions during some parts of the drive cycle. The CO prediction, during periods of heavy acceleration (for example, from around 175-200 s), does not match the magnitude of the measured CO emission. Although the MOVES model does significantly under-predict the CO emissions that were measured for this vehicle, the absolute level of these emissions are extremely low, and the levels during relatively steady speeds are reasonably well-predicted. Since MOVES uses an emissions map derived from steady state emissions data for its predictions, some transient operating conditions are not well predicted. Also, the data used in the emissions maps for the model are based on measurements from multiple vehicles and are not representative of any single truck. The periods where higher spikes in the CO were measured took place when the vehicle was accelerating at near-maximum levels, which for vehicles with exhaust gas recirculation (EGR) generally leads to less lean conditions that tend to generate high CO levels. This is a known weakness of the MOVES model (and other map-based emission prediction models), and a more detailed analysis tool capable of modeling the transient engine operating conditions would be needed to accurately predict such transient emission variations. Emission maps are research and development tools that allow characterization of fuel consumption and emissions at a given time on the basis of vehicle operating parameters, including engine speed and torque, etc. Given the very low level of CO emissions, this is not felt to be a cause for concern. Similarly, for the HC emissions, the errors between the measured and predicted emissions, while large on a relative basis for this particular vehicle, are relatively small in consideration of the absolute emission levels.

The discrepancies observed between the model and test results were communicated to the MOVES team at EPA for their comment. The consensus was that the model had been developed for the purpose of estimating overall fleet emissions and should not be expected to match the second-by-second emissions of a single truck. That is, the MOVES emission rates reflect a fleet average, and the modal emission rates are meant to model aggregate emissions over different driving patterns. As a result, the modeling team at EPA was not surprised by the emission rate differences between a single truck and MOVES. Nonetheless, the EPA did note that they were re-evaluating the HD emission rates in this model year range based on their evaluation of new data recently collected from several trucks in the field.

Total emissions were compared between dynamometer measurements and MOVES data. However, instead of using the default MOVES vehicle parameters described above, the following values were applied: coefficient of drag ($C_d = 0.58$), frontal area ($R = 10 \text{ m}^2$), rolling resistance coefficients ($\mu_0 [= C_{RR}] = 0.007$, $\mu_1 = 0$ and $\mu_2 = 0.0$), and gross vehicle weight ($m = 18.71$ tonne or 41,248 lb). These were used because they are more representative of the actual test vehicle's configuration. Thus, the rolling, rotating, and drag terms for the STP equation were $A = 1.28351 \text{ kW-s/m}$, $B = 0$, and $C = 0.00427162 \text{ kW-s}^3/\text{m}^3$, respectively.

Table 16 summarizes energy consumption and total emissions from the dynamometer test and MOVES. These results revealed that MOVES tended to under-predict NO_x , CO, and HC emissions and over-predict energy consumption relative to the dynamometer test. However, since the aggregated emission values for the dynamometer test and MOVES are comparable, it adds support to the previous comment from EPA that MOVES can model fleet averages but it cannot match the second-by-second emissions of a single truck.

Table 16: Comparison of total emissions and energy consumption results from dynamometer measurements and MOVES predictions.

Emission/Energy Results	dynamometer test result	MOVES	% Difference (Dyno-MOVES)/Dyno
NO _x (g)	139	111	20.2%
CO (g)	43	23	45.1%
HC (g)	6.9	5.3	24.0%
Energy consumption (kJ)	282,502	300,565	- 6.4%

6.2.4. Validation of the synthetic cycle methodology for MOVES simulations: comparison of results using a synthetic drive cycle that represents a full day of measured drive cycle data

To evaluate the accuracy of using a synthetic drive cycle to represent large sets of driving data, a comparison was made between MOVES predictions using a single day’s drive cycle data and a much shorter synthetic drive cycle developed to represent the day of driving. This was done to first validate the procedure used to generate the synthetic drive cycle. The original drive cycle was from a typical 8 hour freight hauling episode. The synthetic drive cycle was developed by ORNL using the DCGen tool (see section 4 of this report for more details). The vehicle speed and road grade profiles for the measured drive cycle, as well as the synthetic drive cycle were used in MOVES. These two cycles were provided by ORNL also for comparative study to test technologies associated with aerodynamic drag reduction, low rolling resistance tires, and lightweight materials for trucks.

The original drive cycle, which was measured in August 2007, included a total travel distance for the route of approximately 860 km (535 miles). It included about 2% engine idling time where vehicle speed was less than 1.6 km/h (i.e., below ~ 1 mph), which is based on the MOVES idling definition. The synthetic cycle is 1646 second in duration with approximately 48.5 km (30.1 mi) of travel distance and about 0.3% of idling time. For both cycles, instead of using the default MOVES vehicle parameter values, the parameters corresponding to the vehicle configuration and actual load during the measured drive cycle were used. These parameters are coefficient of drag ($C_d = 0.58$), frontal area ($R = 10 \text{ m}^2$), rolling resistance coefficients ($\mu_0 [= C_{RR}] = 0.007$, $\mu_1 = 0$ & $\mu_2 = \sim 0.0$), and gross vehicle weight ($m = 18.71$ tonne or 41,250 lb). Thus, the rolling, rotating and drag terms in the STP equation were $A = 1.28351 \text{ kW-s/m}$, $B = 0$, and $C = 0.00427162 \text{ kW-s}^3/\text{m}^3$, respectively.

Emissions were modeled using (1) the default vehicle parameters listed above, (2) a mass reduction of 2,000 kg with the remaining default parameters, (3) a rolling resistance reduction ($C_{RR} = 0.0055$) with the remaining default parameters, (4) an aerodynamic drag reduction ($C_d = 0.52$) with the remaining default parameters, (5) both rolling resistance and aerodynamic drag reductions with the default parameter of mass only, and (6) all three vehicle parameters are reduced (i.e., mass, rolling resistance and

aerodynamic drag). The purpose of these comparisons was to quantify the emissions benefit associated with the use of advanced efficiency technologies on the truck, and to quantify the accuracy of using the synthetic drive cycle approach in the calculation.

The comparisons between the original drive cycle and the synthetic drive cycle validation case are shown in Table 17. The first column in the table shows the metrics evaluated (the various predicted emissions and the energy consumption). The comparisons are made between all of the runs evaluated for each metric. The second column shows the parameter variations that were used for each run. These are either the default parameters (defined above) to represent the baseline vehicle configuration, or variations relative to the baseline case corresponding to a change in mass, rolling resistance, and/or aerodynamic drag coefficients. These parameter changes were applied one at a time and then in combination to evaluate how the parameter changes (corresponding to different efficiency technologies) affected the emissions rates. All of the cases with the parameter variations were compared to the default parameter case, which is highlighted in the table for each metric considered. The third column contains the emission rates or fuel energy consumption predicted by the model for the full day's drive cycle, and the corresponding rates using the synthetic cycle are listed in the fifth column. For each of the parameter variation cases considered, the percent difference in the emission rates and fuel energy consumption, relative to those calculated for the default parameter run, are listed in the fourth column for the original drive cycle. These data correspond to the emissions reduction (or increase, in the case of a positive percentage change) that the model predicts when the vehicle parameters are reduced (e.g. by implementing appropriate technology modifications to the vehicle). The corresponding difference, relative to the default parameter case, calculated by using the synthetic drive cycle is shown in the sixth column of the table. The last column shows the difference between the percent reduction calculated using the synthetic drive cycle and the reduction calculated with the original drive cycle. This provides an indication of how similar the emissions/energy savings prediction is when using the original drive cycle vs. the synthetic cycle.

Table 17: Summary of MOVES predicted emissions for the validation synthetic cycle case, with a comparison of the original and synthetic drive cycle results.

Metric	Description	MOVES result with the original drive cycle	% Difference due to parameter variation(s) (original cycle)	MOVES result with the synthetic validation drive cycle	% Difference due to parameter variation(s) (synthetic cycle)	Difference between %original & %synthetic [syn-original]
NO _x (g/mi)	Default parameters (baseline vehicle configuration)	7.461		7.561		
	Change in mass (2,000 kg reduction)	7.446	-0.2%	7.569	0.1%	0.3%
	Change in C _{RR} = 0.0055	7.127	-4.5%	7.226	-4.4%	0.1%
	Change in C _d = 0.52	7.069	-5.3%	7.194	-4.9%	0.4%
	Change in C _{RR} = 0.0055 & C _d = 0.52	6.713	-10.0%	6.908	-8.6%	1.4%
	Change in mass (2,000 kg reduction) & C _{RR} = 0.0055 & C _d = 0.52	6.671	-10.6%	6.869	-9.2%	1.4%
CO (g/mi)	Default parameters (baseline vehicle configuration)	1.181		1.197		
	Change in mass (2,000 kg reduction)	1.188	0.6%	1.203	0.5%	-0.1%
	Change in C _{RR} = 0.0055	1.176	-0.4%	1.189	-0.7%	-0.3%
	Change in C _d = 0.52	1.176	-0.4%	1.188	-0.8%	-0.4%
	Change in C _{RR} = 0.0055 & C _d = 0.52	1.169	-1.0%	1.183	-1.2%	-0.2%
	Change in mass (2,000 kg reduction) & C _{RR} = 0.0055 & C _d = 0.52	1.174	-0.6%	1.187	-0.8%	-0.2%
HC (g/mi)	Default parameters (baseline vehicle configuration)	0.224		0.227		
	Change in mass (2,000 kg reduction)	0.224	0.0%	0.227	0.0%	0.0%
	Change in C _{RR} = 0.0055	0.225	0.4%	0.229	0.9%	0.5%
	Change in C _d = 0.52	0.226	0.9%	0.229	0.9%	0.0%
	Change in C _{RR} =0.0055 & C _d =0.52	0.227	1.3%	0.230	1.3%	0.0%
	Change in mass (2,000 kg reduction) & C _{RR} = 0.0055 & C _d = 0.52	0.227	1.3%	0.230	1.3%	0.0%
PM _{2.5} (OC + EC) (g/mi)	Default parameters (baseline vehicle configuration)	0.303		0.311		
	Change in mass (2,000 kg reduction)	0.301	-0.7%	0.309	-0.6%	0.1%
	Change in C _{RR} = 0.0055	0.292	-3.6%	0.300	-3.5%	0.1%
	Change in C _d = 0.52	0.290	-4.3%	0.299	-3.9%	0.4%
	Change in C _{RR} =0.0055 & C _d =0.52	0.279	-7.9%	0.290	-6.8%	1.1%
	Change in mass (2,000 kg reduction) & C _{RR} = 0.0055 & C _d = 0.52	0.277	-8.6%	0.288	-7.4%	1.2%
Total energy consumed (kJ/mi)	Default parameters (baseline vehicle configuration)	20,587		20,840		
	Change in mass (2,000 kg reduction)	20,488	-0.5%	20,821	-0.1%	0.4%
	Change in C _{RR} = 0.0055	19,598	-4.8%	19,870	-4.7%	0.1%
	Change in C _d = 0.52	19,427	-5.6%	19,777	-5.1%	0.5%
	Change in C _{RR} = 0.0055 & C _d = 0.52	18,396	-10.6%	18,952	-9.1%	1.5%
	Change in mass (2,000 kg reduction) & C _{RR} = 0.0055 & C _d = 0.52	18,253	-11.3%	18,808	-9.8%	1.5%

Notes: Emissions are based on mean base rate (w/out temperature & humidity adjustments); default parameters: m = 18,710 kg; C_{RR} = 0.007; C_d = 0.58; frontal area 10 m².
 chg = changed parameter; def = default parameter; syn = synthetic cycle

Using NO_x as an example, the emission rate for the original drive cycle modeled with the default parameters was 7.46 g/mile, while the corresponding result for the synthetic validation drive cycle is 7.56 g/mile. The results obtained with the original drive cycle and using the synthetic drive cycle are within just a few percent, and this level of consistency between the two drive cycles for the overall prediction is observed for all of the metrics evaluated. This shows excellent agreement between the results from the two drive cycles and validates that the synthetic cycle is highly representative of the original drive cycle. It is the change in emissions that occur when the vehicle configuration is modified that is most critical for our purposes, however, and we consider these differences in detail. When the mass is reduced by 2,000 kg, the NO_x emission rate was 7.45 g/mile for the original drive cycle, and it was 7.57 g/mile for the synthetic drive cycle. The percent difference between the changed parameter case and the default parameter results is -0.2% for the original drive cycle and 0.1% for the synthetic cycle. A negative difference means that a reduction in emissions occurred for the change from the default to the changed parameter case, while a positive percentage indicates that an increase occurred as a result of the change in parameters. In this case, the difference is extremely small, and even though the direction of change predicted by the two drive cycles are opposite in sign for this case, both cycles result in a predicted change that is near zero and the difference between the two predictions for the emission reduction associated with a 2000 kg mass reduction is only 0.3%. As seen in the table, the results when using the original drive cycle and those from the synthetic drive cycle are all very close to one another. The difference in the emissions/fuel consumption variation calculated using the synthetic vs. the original drive cycle for any of the metrics is within 1.5%, and in most cases this difference is only a fraction of a percent. The greatest differences appearing in the last column occur when the predicted reductions are the greatest, so the relative error in the predicted emissions reduction for these cases does not become extremely large. Results from both drive cycles show the general trends for the emissions reductions to be quite similar, although some of the predicted emission reductions due to the combinations of technologies are estimated to be lower when using the synthetic drive cycle. Based on these results, we conclude that the synthetic drive cycle provides results that are in excellent agreement with those obtained from the original drive data. This close agreement between the emissions reductions predicted with the original and the synthetic drive cycle indicates that we can reliably use a synthetic drive cycle in the EPA MOVES model to predict the emissions benefits achievable when specific changes in vehicle configuration are applied for a given vehicle usage. These results validate the methodology of using a synthetic drive cycle representing a larger set of drive cycle data to estimate the benefits that can be achieved with particular vehicle configuration changes using MOVES.

6.2.5. Evaluation of the emissions reductions from advanced efficiency technologies for the overall HTDC fleet usage using MOVES

As described in section 4 of this report, a synthetic drive cycle that is representative of the overall usage for the HTDC test fleet was developed based on a detailed statistical evaluation of all of the measured drive cycle data from the HTDC project. This synthetic drive cycle was initially developed to represent the medium mass case, but it was found that this usage was very similar to that for all of the mass cases considered, and the same synthetic drive cycle was used to evaluate the fleet's overall usage. As opposed to the synthetic validation cycle considered in the previous section for a single day's worth of driving, the overall usage synthetic drive cycle represents over one million kilometers of travel during

more than 20,000 hours of operation, and it would not be possible to perform the MOVES analysis using the complete data set in a reasonable period of time. However, we validated that the results obtained by running MOVES using a carefully constructed synthetic drive cycle having a similar statistical distribution of speeds, accelerations and elevation variations yields the same result as would be obtained using the complete data set. The synthetic drive cycle representing the full fleet usage is 3610 seconds in duration with approximately 50.4 km (31.3 mi) of travel distance; it also includes about 47% of idling time, which is the same percentage experienced in the actual fleet for the medium mass case.

For the MOVES analysis using the overall usage synthetic drive cycle, the baseline vehicle parameters for the mass, rolling resistance, and aerodynamic drag were selected to correspond as closely as possible to the configuration of the real vehicles tested. As in the previous section, these will be denoted as the default parameters: coefficient of drag ($C_d = 0.62$), frontal area ($R = 6.5 \text{ m}^2$), rolling resistance coefficients ($\mu_0 [= C_{RR}] = 0.007$, $\mu_1 = 0$ & $\mu_2 = 0.0$), and gross vehicle weight ($m = 24.187$ tonne or 53,323 lb). Thus, the rolling, rotating, and drag terms in the STP equation for the baseline vehicle configuration were $A = 1.6592 \text{ kW-s/m}$, $B = 0$, and $C = 0.00343788 \text{ kW-s}^3/\text{m}^3$, respectively. A primary objective of this study was to conduct an assessment of the emissions reductions that could be realized in the fleet if combinations of various vehicle efficiency technologies are employed. As in the previous analyses, we evaluated the emissions benefits based on implementation of the following technologies: (1) vehicle light-weighting as represented by a vehicle mass reduction of 2,000 kg, (2) the use of low rolling resistance tires, based on a change in the coefficient of rolling resistance, C_{RR} , from a value of 0.007 to 0.0055, and (3) aerodynamic drag reduction, as could be achieved through the use of trailer skirts, more streamlined tractor and trailer designs or other aerodynamic reduction devices. Our evaluation uses drag improvements corresponding to a reduction in the coefficient of aerodynamic drag, C_d , from a value of 0.62 to 0.52. In addition to the individual technology evaluations, the emissions benefits corresponding to combinations of these technologies are evaluated by running MOVES with the various combinations of the modified parameter values.

Table 18 shows the MOVES predictions for the expected emissions reductions associated with these advanced efficiency technologies. It should be noted that the emissions analysis does not lend itself to an evaluation of the benefits of regenerative braking, so this is not included as it was for the analysis in previous sections of the report using the tractive energy analysis. The results indicate that emissions of CO and HC are rather insensitive to the variations evaluated. The change in emissions for these criteria emissions are less than 1% for all of the variations evaluated. For NOx emissions, the rolling resistance reduction and the aerodynamic drag reduction cases are similar, with each modification yielding a NOx emission reduction that is slightly over 4%. The mass reduction considered, however, is predicted to be less effective, with a 1.4% reduction predicted. It is interesting to observe that for all of the technology combination cases considered, the combined NOx emission reduction is greater than the sum of the reductions provided by each individual technology case. The trends for the PM emission and fuel energy consumption results (which is also proportional to CO₂ emissions) are similar to the NOx result, although the magnitudes of the predicted reductions differ somewhat. The MOVES model predicts a reduction in emissions for all of the technology implementation cases, except for the case of the HC emissions, which increase slightly while the other emissions are decreased. The CO emission for the reduced mass case is

also slightly higher than the baseline case, but the level of the increase is only 0.7%. The predictions do show that relatively significant emissions reductions can be achieved with the implementation of these technologies. By implementing all three of the technologies together, the model predicts that NO_x, PM and CO₂ emissions can be reduced by 11.0%, 8.3% and 12.4%, respectively.

Table 18: Emissions reductions associated with different advanced efficiency technologies as predicted by MOVES using the synthetic drive cycle representing the HTDC driving data.

Metric	Description	MOVES result	% Difference relative to baseline case
NO _x (g/mi)	Baseline vehicle configuration*	7.721	
	Vehicle light-weighting (calculated assuming a 2,000 kg mass reduction)	7.613	-1.4%
	Low rolling resistance tires (C _{RR} = 0.0055)	7.399	-4.2%
	Aerodynamic drag reduction (C _d = 0.52)	7.403	-4.1%
	Low rolling resistance and aero drag reduction	6.994	-9.4%
	Change in mass (2,000 kg reduction) & C _{RR} = 0.0055 & C _d = 0.52	6.875	-11.0%
CO (g/mi)	Baseline vehicle configuration*	1.512	
	Vehicle light-weighting (calculated assuming a 2,000 kg mass reduction)	1.517	0.3%
	Low rolling resistance tires (C _{RR} = 0.0055)	1.508	-0.3%
	Aerodynamic drag reduction (C _d = 0.52)	1.509	-0.2%
	Low rolling resistance and aero drag reduction	1.498	-0.9%
	Change in mass (2,000 kg reduction) & C _{RR} = 0.0055 & C _d = 0.52	1.500	-0.8%
HC (g/mi)	Baseline vehicle configuration*	0.345	
	Vehicle light-weighting (calculated assuming a 2,000 kg mass reduction)	0.345	0.0%
	Low rolling resistance tires (C _{RR} = 0.0055)	0.346	0.3%
	Aerodynamic drag reduction (C _d = 0.52)	0.346	0.3%
	Low rolling resistance and aero drag reduction	0.347	0.6%
	Change in mass (2,000 kg reduction) & C _{RR} = 0.0055 & C _d = 0.52	0.348	0.9%
PM _{2.5} (OC + EC) (g/mi)	Baseline vehicle configuration*	0.373	
	Vehicle light-weighting (calculated assuming a 2,000 kg mass reduction)	0.366	-1.9%
	Low rolling resistance tires (C _{RR} = 0.0055)	0.361	-3.2%
	Aerodynamic drag reduction (C _d = 0.52)	0.362	-2.9%
	Low rolling resistance and aero drag reduction	0.348	-6.7%
	Change in mass (2,000 kg reduction) & C _{RR} = 0.0055 & C _d = 0.52	0.342	-8.3%
Total energy consumed (kJ/mi)	Baseline vehicle configuration*	20,574	
	Vehicle light-weighting (calculated assuming a 2,000 kg mass reduction)	20,158	-2.0%
	Low rolling resistance tires (C _{RR} = 0.0055)	19,594	-4.8%
	Aerodynamic drag reduction (C _d = 0.52)	19,615	-4.7%
	Low rolling resistance and aero drag reduction	18,406	-10.5%
	Change in mass (2,000 kg reduction) & C _{RR} = 0.0055 & C _d = 0.52	18,019	-12.4%

Notes:

Emissions are based on mean base rate (w/out temperature & humidity adjustments);

* Parameters for the baseline vehicle configuration: m = 24,187 kg; C_{RR} = 0.007; C_d = 0.62; frontal area 6.5 m².

6.2.6. Comparison of results using an alternative drive cycle with those from the synthetic cycle

In addition to presenting the results of the MOVES analysis based on the overall usage synthetic cycle, we also provide a comparison of these results to those corresponding to a different type of drive cycle. One approach that could be taken to select an appropriate drive cycle is to compare the characteristics of a large set of data and find a single measured drive cycle for which the characteristics are similar to the larger set, without doing the detailed matching of velocity and acceleration distributions that was done for the synthetic drive cycle. As a means to compare results for a measured drive cycle that is somewhat similar to those obtained using the overall usage synthetic drive cycle, a full day's measurement whose bivariate speed-acceleration histogram was visually similar to that of the complete HTDC data set was selected using the drive cycle tools (see section 4 for more details). This substitute measured drive cycle was evaluated with the MOVES model to determine how accurately the results compare with the synthetic cycle results.

Results of the comparison between the substitute measured drive cycle and the synthetic drive cycle are shown in Table 19, using the same format as in Table 17 except that the synthetic cycle, which is most representative of the complete set of driving data, is used as the reference case here. We observe that the absolute level of predicted emissions is certainly not as accurate as was the case in Table 17, but we wish to evaluate whether the predicted reductions (on a relative percentage basis) in the emissions can still be well estimated using the substitute measured drive cycle. In the present comparison, we see that the greatest difference between the predicted emissions reductions for the two drive cycles (column 6) is 3.4%, where it was only 1.5% for the previous comparison. While the general trends for the MOVES-predicted emissions reductions are still correct using the substitute cycle, the magnitudes of the reductions are not as consistent with the synthetic cycle as one would like and relatively large errors in the magnitude of emissions reductions occur with the substitute drive cycle. For example, the model predicts a 9.4% reduction in NO_x emission relative to the baseline configuration for the combination of reduced rolling resistance and reduced aerodynamic drag when using the synthetic drive cycle, but for the same case using the substitute measured drive cycle, the predicted NO_x reduction is only 6.2%. The 3.2% difference here represents about 1/3 of the predicted benefit. This magnitude of error resulting from the use of the less representative drive cycle occurs in several of the comparisons in Table 19. Based on these results, it appears that using a drive cycle selected based on a general agreement with the application considered is not unreasonable for the prediction of general trends in emissions reductions, but errors in the magnitude of the predicted savings are expected to be greater using this approach than when a highly representative cycle can be used in the MOVES analysis.

Table 19: Comparison of MOVES-predicted emissions using the synthetic drive cycle with those calculated using a substitute measured drive cycle.

Metric	Description	Synthetic drive cycle	% Difference (synthetic) [(chg-def)/def]	Substitute measured drive cycle	% Difference (substitute) [(chg-def)/def]	Difference between %subst & %synthetic [syn-full]
NO _x (g/mi)	Default parameters (baseline vehicle configuration)	7.721		8.313		
	Change in mass (2,000 kg reduction)	7.613	-1.4%	8.171	-1.7%	0.3%
	Change in C _{RR} = 0.0055	7.399	-4.2%	8.033	-3.4%	-0.8%
	Change in C _d = 0.52	7.403	-4.1%	8.058	-3.1%	-1.0%
	Change in C _{RR} = 0.0055 & C _d = 0.52	6.994	-9.4%	7.798	-6.2%	-3.2%
	Change in mass (2,000 kg reduction) & C _{RR} = 0.0055 & C _d = 0.52	6.875	-11.0%	7.606	-8.5%	-2.5%
CO (g/mi)	Default parameters (baseline vehicle configuration)	1.512		1.512		
	Change in mass (2,000 kg reduction)	1.517	0.3%	1.517	0.3%	0.0%
	Change in C _{RR} = 0.0055	1.508	-0.3%	1.510	-0.1%	-0.2%
	Change in C _d = 0.52	1.509	-0.2%	1.511	-0.1%	-0.1%
	Change in C _{RR} = 0.0055 & C _d = 0.52	1.498	-0.9%	1.508	-0.3%	-0.6%
	Change in mass (2,000 kg reduction) & C _{RR} = 0.0055 & C _d = 0.52	1.500	-0.8%	1.512	0.0%	-0.8%
HC (g/mi)	Default parameters (baseline vehicle configuration)	0.345		0.345		
	Change in mass (2,000 kg reduction)	0.345	0.0%	0.345	0.0%	0.0%
	Change in C _{RR} = 0.0055	0.346	0.3%	0.345	0.0%	0.3%
	Change in C _d = 0.52	0.346	0.3%	0.345	0.0%	0.3%
	Change in C _{RR} = 0.0055 & C _d = 0.52	0.347	0.6%	0.346	0.3%	0.3%
	Change in mass (2,000 kg reduction) & C _{RR} = 0.0055 & C _d = 0.52	0.348	0.9%	0.346	0.3%	0.6%
PM _{2.5} (OC + EC) (g/mi)	Default parameters (baseline vehicle configuration)	0.373		0.399		
	Change in mass (2,000 kg reduction)	0.366	-1.9%	0.392	-1.8%	-0.1%
	Change in C _{RR} = 0.0055	0.361	-3.2%	0.389	-2.5%	-0.7%
	Change in C _d = 0.52	0.362	-2.9%	0.390	-2.3%	-0.6%
	Change in C _{RR} = 0.0055 & C _d = 0.52	0.348	-6.7%	0.381	-4.5%	-2.2%
	Change in mass (2,000 kg reduction) & C _{RR} = 0.0055 & C _d = 0.52	0.342	-8.3%	0.372	-6.8%	-1.5%
Total energy consumed (kj/mi)	Default parameters (baseline vehicle configuration)	20574		22,291		
	Change in mass (2,000 kg reduction)	20158	-2.0%	21,773	-2.3%	0.3%
	Change in C _{RR} = 0.0055	19594	-4.8%	21,426	-3.9%	-0.9%
	Change in C _d = 0.52	19615	-4.7%	21,502	-3.5%	-1.2%
	Change in C _{RR} = 0.0055 & C _d = 0.52	18406	-10.5%	20,714	-7.1%	-3.4%
	Change in mass (2,000 kg reduction) & C _{RR} = 0.0055 & C _d = 0.52	18019	-12.4%	20,101	-9.8%	-2.6%

Notes: Emissions are based on mean base rate (w/out temperature & humidity adjustments); default parameters: m = 24,187 kg; C_{RR} = 0.007; C_d = 0.62; frontal area 6.5 m².
chg = changed parameter case; def = default parameter case; syn = synthetic cycle; subst = substitute measured drive cycle

6.2.7. Comparison of emissions estimates for synthetic and real drive cycles versus the default MOVES drive cycles

As a final comparison, default drive cycles that are included in the MOVES model were evaluated to determine how well emissions can be estimated without the availability of specific drive cycle data representing the actual usage of a fleet or trucking application. For this evaluation, we also compare the operating mode distributions, as they are defined in the MOVES model, among all three drive cycles compared in sections 6.3.4 and 6.3.4: the overall usage synthetic drive cycle, the substitute measured drive cycle and the MOVES default drive cycle.

In MOVES, a basic emissions evaluation can be performed by selecting an average driving speed for the application considered. MOVES will identify relevant default drive cycles that are included in the software and weight the results between two of these cycles so that the corresponding weighted average speed matches that input into the model. To run MOVES using the model's default drive cycles, both an average vehicle speed and average road grade (in percent grade) are required as inputs. A difficulty in using this average speed method is in defining the average vehicle speed. The usage for the fleet evaluated contained nearly 50% idling, so it is unreasonable to use the entire drive cycle to calculate average vehicle speed since the vehicle spent almost half of its time at zero speed. In addition, road grade varied between positive and negative values, and the average road grade is typically closer to zero when the positive and negative grades are averaged together. To work around these problems, average vehicle speed was determined by removing all idling greater than 1 minute in duration from the synthetic drive cycle and the average grade was determined separately for positive and negative values. Using this method, total idling, based on the MOVES definition, was reduced to 7% for the synthetic cycle. Separate average positive and average negative road grades were then determined using the condensed vehicle speed data. With the long idling data removed from the synthetic drive cycle, the modified average speed was 88.8 km/h (55.2 mph), while the average positive road grade was 0.9%, and average negative road grade was -1.0%. Using these results, MOVES was run separately for the positive and negative road grade, each at the average speed calculated for the synthetic drive cycle, and the results from the two MOVES runs were averaged together and compared to the synthetic drive cycle.

The results of the MOVES default drive cycle evaluation following this method are shown in Table 20 and are compared with the results using the synthetic drive cycle. The synthetic cycle results are the same as were shown in Table 18, and the format of the table is the same as was used in the previous cycle-to-cycle comparisons. The results for the predicted emissions reductions corresponding to the efficiency technology simulations are somewhat mixed. As in the case of the substitute drive cycle comparison (Table 19), the predicted trends for emissions reductions are generally consistent between the MOVES default drive cycle and the synthetic drive cycle. However, the magnitudes of the predicted emissions reductions again show some discrepancies that are noteworthy. The reduced mass parameter case showed only a moderate emissions reduction ($\leq 2\%$ for each of the metrics evaluated) when using the synthetic drive cycle, but the predicted emissions reductions using the default MOVES drive cycle is considerably higher for some cases. The predicted NO_x emission reduction associated with a 2000 kg mass reduction using the MOVES default drive cycle is 3.8%, which is more than 2.5 times the value of 1.4% predicted with the synthetic drive cycle. Also, similar to the evaluation with the substitute drive

cycle, the predicted NO_x and total energy consumption reductions due to a combination of rolling resistance and aerodynamic drag reductions was about 1/3 less than the estimate using the synthetic drive cycle. The differences between results using different drive cycles are significant relative to the benefits achieved, which highlights the need to use drive cycles that are as representative of the actual application as possible. These results using the MOVES default drive cycle suggest that the cycles could be improved for freeway-dominant usage cases such as the HTDC fleet usage.

When the average speed is input into MOVES to use its default drive cycles for estimating emissions, it selects two cycles, with lower and higher average speeds, and weights them to achieve the same average speed as input. The operating mode distribution is then generated based on this weighting of the two default drive cycles. For the case analyzed above, the two drive cycles selected (out of the available 12 default drive cycles for HD trucks [See Table 15]) had average speeds of 87.2 km/h (54.2 mph) and 95.6 km/h (59.4 mph), as compared to the average speed of 88.8 km/h (55.2 mph) from the synthetic drive cycles. The speed-time plots for these two default cycles are shown in Fig. 45.

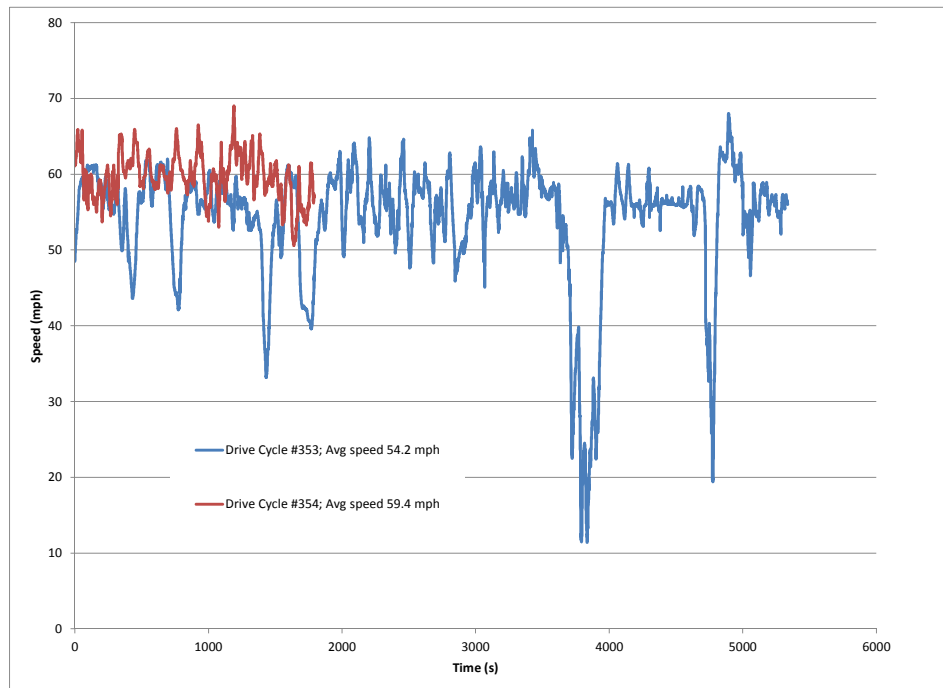


Figure 45 MOVES default cycles for average speeds 87.2 km/h (54.2 mph) and 95.6 km/h (59.4 mph)

Table 20: Comparison of the overall usage synthetic drive cycle and the MOVES default drive cycle based on the average speed of the synthetic cycle.

Metric	Description	Synthetic drive cycle	% Difference (synthetic) [(chg-def)/def]	MOVES default drive cycle	% Difference (MOVES default) [(chg-def)/def]	Difference between %syn & %MOVES [syn- MOVES]
NO _x (g/mi)	Default parameters (baseline vehicle configuration)	7.721		7.252		
	Change in mass (2,000 kg reduction)	7.613	-1.4%	6.978	-3.8%	2.4%
	Change in C _{RR} = 0.0055	7.399	-4.2%	7.000	-3.5%	-0.7%
	Change in C _d = 0.52	7.403	-4.1%	7.070	-2.5%	-1.6%
	Change in C _{RR} = 0.0055 & C _d = 0.52	6.994	-9.4%	6.817	-6.0%	-3.4%
	Change in mass (2,000 kg reduction) & C _{RR} = 0.0055 & C _d = 0.52	6.875	-11.0%	6.524	-10.0%	-1.0%
CO (g/mi)	Default parameters (baseline vehicle configuration)	1.512		1.364		
	Change in mass (2,000 kg reduction)	1.517	0.3%	1.363	-0.1%	0.4%
	Change in C _{RR} = 0.0055	1.508	-0.3%	1.359	-0.4%	0.1%
	Change in C _d = 0.52	1.509	-0.2%	1.360	-0.3%	0.1%
	Change in C _{RR} = 0.0055 & C _d = 0.52	1.498	-0.9%	1.354	-0.7%	-0.2%
	Change in mass (2,000 kg reduction) & C _{RR} = 0.0055 & C _d = 0.52	1.500	-0.8%	1.352	-0.9%	0.1%
HC (g/mi)	Default parameters (baseline vehicle configuration)	0.345		0.284		
	Change in mass (2,000 kg reduction)	0.345	0.0%	0.284	0.0%	0.0%
	Change in C _{RR} = 0.0055	0.346	0.3%	0.284	0.0%	0.3%
	Change in C _d = 0.52	0.346	0.3%	0.284	0.0%	0.3%
	Change in C _{RR} = 0.0055 & C _d = 0.52	0.347	0.6%	0.285	0.4%	0.2%
	Change in mass (2,000 kg reduction) & C _{RR} = 0.0055 & C _d = 0.52	0.348	0.9%	0.285	0.4%	0.5%
PM _{2.5} (OC + EC) (g/mi)	Default parameters (baseline vehicle configuration)	0.373		0.338		
	Change in mass (2,000 kg reduction)	0.366	-1.9%	0.326	-3.6%	1.7%
	Change in C _{RR} = 0.0055	0.361	-3.2%	0.329	-2.7%	-0.5%
	Change in C _d = 0.52	0.362	-2.9%	0.332	-1.8%	-1.1%
	Change in C _{RR} = 0.0055 & C _d = 0.52	0.348	-6.7%	0.322	-4.7%	-2.0%
	Change in mass (2,000 kg reduction) & C _{RR} = 0.0055 & C _d = 0.52	0.342	-8.3%	0.310	-8.3%	0.0%
Total energy consumed (kj/mi)	Default parameters (baseline vehicle configuration)	20574		21178		
	Change in mass (2,000 kg reduction)	20158	-2.0%	20249	-4.4%	2.4%
	Change in C _{RR} = 0.0055	19594	-4.8%	20378	-3.8%	-1.0%
	Change in C _d = 0.52	19615	-4.7%	20605	-2.7%	-2.0%
	Change in C _{RR} = 0.0055 & C _d = 0.52	18406	-10.5%	19808	-6.5%	-4.0%
	Change in mass (2,000 kg reduction) & C _{RR} = 0.0055 & C _d = 0.52	18019	-12.4%	18844	-11.0%	-1.4%

Notes: Emissions are based on mean base rate (w/out temperature & humidity adjustments); default parameters: m = 24,187 kg; C_{RR} = 0.007; C_d = 0.62; frontal area 6.5 m².
chg = changed parameter case; def = default parameter case; syn = synthetic cycle; MOVES = MOVES default drive cycle

It can be seen that these cycles only represent the on-freeway portion of usage since they do not contain any low speed driving or engine idle operation. As a consequence, the driving segments included in the default MOVES drive cycle lacks a range of the operating conditions experienced in the real drive cycle, even if the overall contribution from the low speed conditions is relatively small. Figure 46 shows a comparison of the operating mode distributions for the simulations considered above, using (1) the MOVES default cycle based on the average speed of the synthetic drive cycle, (2) the synthetic drive cycle, and (3) the substitute measured drive cycle. (Note: Table 14 contains a list of the vehicle speed and STP conditions for the operating mode bins.) As revealed in the figure, the operating mode distributions for these cycles include similar proportions of the high-speed conditions; however, the relative magnitudes of the distributions are different for the MOVES default cycle case since it does not include any of the low speed or idle operation conditions. More than twice as much time was spent in bin 33 for the MOVES average speed cycles relative to the full and synthetic cycles, and similarly but at a smaller scale for bin 35, as well. Both of these bins belong to the speed range of 80 km/h (50 mph) and above. It is clear that this difference in the operating mode fraction is responsible for the differences in predicted emissions for the analysis case in which the MOVES default cycles were used to correspond to the average speed of the synthetic drive cycle.

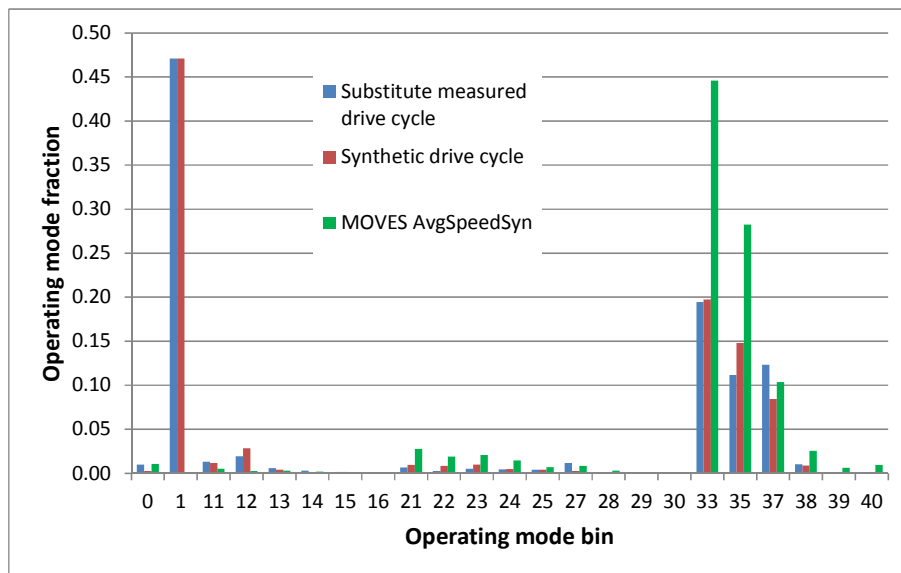


Figure 46 Operating mode bin distribution for the original, synthetic, and MOVES average speed cycles

6.3. Summary and Conclusions of the MOVES analysis

Four areas were investigated with the MOVES modeling activity in this project: (1) second-by-second emission estimates from MOVES were compared to emission measurements conducted during a dynamometer drive cycle; (2) emissions estimates using a real world drive cycle from a HD diesel truck were compared with emissions estimates from a representative synthetic drive cycle in order to validate the synthetic drive cycle analysis methodology; (3) advanced efficiency technologies for class 8 long-haul

trucks were assessed in terms of the emission reductions that can be achieved when implementing the technologies; and (4) emissions predictions based on default drive cycles in MOVES were compared to those using the synthetic drive cycle corresponding to the overall usage of the HTDC driving data.

Primary findings from the MOVES analysis include the following:

- Emission estimates of CO and HC using the MOVES model did not match measured emissions as well as those for NO_x and PM_{2.5}, and the predictions of CO and HC emissions reductions also showed less sensitivity to vehicle configuration changes than did the NO_x and PM emissions.
- MOVES emission estimates using a synthetic drive cycle were confirmed to agree very closely with those obtained from an original drive cycle that the synthetic cycle represents, and the predicted emissions reductions corresponding to vehicle configuration changes matched to within 1.5% for all of the cases evaluated.
- MOVES can be used to quantify the emissions reductions achievable with various fuel efficiency technologies, such as those associated with rolling resistance, aerodynamic drag, and weight reduction, by adjusting parameters contained in the input database. Individual technologies and combinations of these technologies were assessed using MOVES for the vehicle usage measured during ORNL's previous Heavy Truck Duty Cycle (HTDC) project.

The comparison of second-by-second emission estimates between the dynamometer test from a typical freeway-based drive cycle and those predicted by MOVES for the same cycle showed general agreement for NO_x emissions. However, CO and HC emissions did not show good agreement with the measured data. Nonetheless, the model compared favorably when aggregated emissions were compared to measured emissions even though the model was not designed for generating emissions for a single truck.

A synthetic drive cycle generated from measured driving data for a complete day of driving was evaluated for its ability to accurately represent the original drive cycle data. In particular, we compared MOVES estimated emission reductions that result when variations in vehicle parameters, corresponding to the implementation of advanced efficiency technologies, are made to the MOVES model. The validation study demonstrated that the results using the synthetic drive cycle compared very favorably with the MOVES predictions made with the original data on which the synthetic cycle was based. The results of the validation synthetic drive cycle matched the original cycle's MOVES predictions for emissions reductions to within 1.5% for all of the cases considered. This validation gives a high degree of confidence to the relevance of MOVES estimates made using a synthetic drive cycle.

The level of emission reductions for changes in vehicle parameters that are believed to be appropriate for real technology modifications including low rolling resistance tires, aerodynamic drag, and vehicle light-weighting were calculated using the MOVES model. These results, evaluated using a synthetic drive cycle developed to represent the overall usage of a class 8 tractor-trailer truckload delivery fleet, are representative of the emissions reductions that would be achieved overall in the fleet studied if the technologies are implemented for all vehicles in service. This was the key result for this analysis, and the emissions reductions estimated with MOVES for this evaluation are presented in Table 18. Since the MOVES emissions rates are typically used to evaluate emissions for the broader U.S. trucking fleet, we

can conclude that the predicted emissions reductions are appropriate to all class 8 tractor-trailers if this fleet's usage is typical of most fleets operating in the same vehicle application. Further research is needed to determine if this usage is relevant to other class 8 trucking fleets.

7. Recommendations for Future Research

The results of the tractive energy analysis showed fuel savings as high as 10% from a regenerative braking system in the class 8 freight delivery application evaluated. Although fuel savings of 20-30% are realized with medium duty hybrid trucks using regenerative braking in operations for which considerable stop and go activity is present, the conventional belief is that hybridization will not generate significant savings for class 8 tractor-trailers. The drive cycle for the fleet studied showed intermediate occurrences of low deceleration levels at speeds below 50 mph, in addition to a relatively high occurrence of low to moderate decelerations at highway speeds. An understanding of how a class 8 hybrid system could be implemented to recover the braking energy for such a drive profile is needed to determine if the fuel savings predicted using the tractive energy model could be achieved in practice. Detailed modeling studies of class 8 tractor trailers using a realistic regenerative braking configuration and employing a drive cycle that is highly representative of class 8 freight operations (such as the synthetic drive cycle developed for this project) would help determine if the assumptions used in this study are reasonable. A characterization of heavy duty truck regenerative braking systems, including their power and energy storage limitations, would also help define a more realistic set of assumptions to use when conducting a tractive energy analysis.

There is a need to confirm that the overall usage from the fleet evaluated in this study is typical of class 8 freight transport operations. Detailed drive cycle evaluations in other class 8 shipping fleets would be helpful to verify that the fuel efficiency gains predicted in this study are representative of the broader U.S. fleet. This application consumes more fuel than any other in U.S. trucking so it is important to understand where the greatest opportunities for fuel savings exist. On the other hand, there are many other trucking applications for which the typical usage is very poorly understood. Studies to quantify the usage across the full spectrum of U.S. trucking operations would allow much better decisions to be made regarding appropriate fuel efficiency technologies to implement in the other applications.

The results presented in section 6 of this report showed some weaknesses in the MOVES model in terms of how the usage is selected using the built-in drive cycles. MOVES currently will select drive cycles from a finite set of basis drive cycle segments, and it weights these to achieve the same average speed as what the user inputs when running the model. Alternative approaches or the development of additional basis drive cycles should be considered so that real usage cases can be better represented when using the average speed method for MOVES simulations. Different usage scenarios should be studied in MOVES to determine how to best represent a particular usage using the average speed and other characteristics of a fleet's operations. Even for freeway-dominant drive cycles, there needs to be some weighting of non-freeway operations, and the evaluation of several different fleets and applications could be pursued to generate a more accurate methodology for default drive cycle generation.

References:

1. Capps, G., O. Franzese, B. Knee, M.B. Lascurain, and P. Otaduy, *Class-8 Heavy Truck Duty Cycle Project Final Report*. Report No. ORNL/TM-2008/122. Oak Ridge National Laboratory, 2008.
2. LaClair, T., "Application of a Tractive Energy Analysis to Quantify the Benefits of Advanced Efficiency Technologies for Medium- and Heavy-Duty Trucks Using Characteristic Drive Cycle Data," *SAE Int. J. Commer. Veh.* 5(1):141-163, 2012, doi:10.4271/2012-01-0361.
3. M.D. Surcel, "Energotest 2007: Fuel Consumption Test for Evaluating Freight Wing Trailer Side Skirts," Internal Report IR-2007-11-28D, FP Innovations. <http://www.freightwing.com/docs/IR-2007-11-28D-MSL-Energotest2007-FreightWing.pdf>, Accessed November 1, 2012.
4. Clark, N.N., Gautum, M., Bata, R.M., Loth, J., Palmer, G.M., Wang, W.G., and Lyons, D.W., "Design and Operation of a New Transportable Laboratory for Emissions Testing of Heavy Duty Trucks and Buses," *International Journal of Vehicle Design (Heavy Vehicle Systems)*, Vol. 2, Nos. 3/4, 1995, pp. 285-299.
5. DeLorme GPS Community Forum, "Why is DeLorme Vertically or Horizontally inaccurate?" <http://forum.delorme.com/viewtopic.php?t=11777>, accessed 10/15/2012.
6. American Association of State Highway and Transportation Officials (AASHTO), *A Policy on Geometric Design of Highways and Streets*, 6th Edition, AASHTO, 2011.
7. Argonne National Laboratory, *Autonomie*, <http://www.autonomie.net>, accessed October 15, 2012.
8. Barth, M.; An, F.; Norbeck, J.; Ross, M. "Modal emissions modeling: a physical approach," *Transportation Research Record*, 1520, pp. 81-88, 1996.
9. Kean, A.J.; Harley, R.A.; Kendal, G.R. "Effects of vehicle speed and engine load on motor vehicle emissions," *Environmental Science and Technology*, 37(17), pp. 3739-3746, 2003.
10. Zhang, K.; Frey, H.C. "Road grade estimation for on-road vehicle emissions modeling using LIDAR data," *Journal of the Air and Waste Management Association*, 56(6), pp. 777-788, 2006.
11. Jimenez-Palacios, J.L. *Understanding and quantifying motor vehicle emissions with vehicle specific power and TILDAS remote sensing*, Ph.D. Thesis, Massachusetts Institute of Technology, Cambridge, MA. 1999.
12. U.S. Environmental Protection Agency, MOVES web site, www.epa.gov/otaa/models/moves/index.htm, accessed November 1, 2012.
13. U.S. Environmental Protection Agency, *Development of emission rates for heavy-duty vehicles in the Motor Vehicle Emissions Simulator MOVES2010 - Final Report*, Assessment and Standards Division, Office of Transportation and Air Quality, EPA-420-B-12-049, August 2012.
14. U.S. Environmental Protection Agency, *Diesel retrofits: Quantifying and using their benefits in SIPs and conformity - Guidance for State and Local Air and Transportation Agencies*, Transportation and Regional Programs Division and Compliance and Innovative Strategies Division, Office of Transportation and Air Quality. EPA-420-B-06-005, June 2006.
15. U.S. Environmental Protection Agency, *SmartWay SIP and transportation conformity guidance: Accounting for NO_x reductions from trailer aerodynamic kits and low rolling resistance tires - Guidance for State and Local Air and Transportation Agencies*, Transportation and Regional Programs Division, Office of Transportation and Air Quality. EPA-420-B-07-004, June 2007.

16. U.S. Environmental Protection Agency, *Development of emission rates for light-duty vehicles in the Motor Vehicle Emissions Simulator MOVES2009 - Draft Report*. Assessment and Standards Division, Office of Transportation and Air Quality, EPA-420-P-09-002, August 2009.

APPENDIX – Table of the synthetic drive cycle representing the full usage of HTDC drive data

Time (s)	Speed (mph)	Elevation (m)
1	0.00	200.0
2	0.00	200.0
3	0.00	200.0
4	0.00	200.0
5	0.00	200.0
6	0.00	200.0
7	0.00	200.0
8	0.00	200.0
9	0.00	200.0
10	0.00	200.0
11	0.00	200.0
12	0.00	200.0
13	0.00	200.0
14	1.43	200.0
15	1.60	200.0
16	1.67	200.0
17	1.41	200.0
18	1.38	200.0
19	1.35	200.0
20	1.43	200.0
21	1.47	200.0
22	2.29	200.0
23	2.31	200.0
24	2.30	200.0
25	2.36	200.0
26	2.38	200.0
27	2.48	200.0
28	3.75	200.0
29	3.85	200.0
30	3.80	200.0
31	4.33	200.0
32	4.41	200.0
33	4.46	200.0
34	4.37	200.0
35	4.28	200.0
36	4.20	200.0
37	4.33	200.0
38	4.35	200.0
39	4.13	200.0
40	5.59	200.0
41	5.73	200.0
42	5.78	200.0
43	6.48	200.0
44	7.07	200.0
45	7.22	200.0
46	7.20	200.0
47	7.27	200.0
48	7.31	200.0
49	8.46	200.0
50	8.63	200.0
51	9.07	200.0
52	9.03	200.0

Time (s)	Speed (mph)	Elevation (m)
53	8.95	200.0
54	8.35	200.0
55	8.12	200.0
56	7.51	200.0
57	7.35	200.0
58	7.26	200.0
59	6.94	200.0
60	6.85	200.0
61	6.81	200.0
62	6.80	200.0
63	5.43	200.0
64	5.29	200.0
65	5.22	200.0
66	5.17	200.0
67	5.14	200.0
68	4.61	200.0
69	4.44	200.0
70	3.90	200.0
71	3.73	200.0
72	3.65	200.0
73	3.69	200.0
74	3.65	200.0
75	2.96	200.0
76	2.52	200.0
77	2.37	200.0
78	2.31	200.0
79	2.24	200.0
80	1.93	200.0
81	1.83	200.0
82	1.88	200.0
83	1.83	200.0
84	1.77	200.0
85	0.96	200.0
86	0.00	200.0
87	0.00	200.0
88	0.00	200.0
89	0.00	200.0
90	0.00	200.0
91	0.00	200.0
92	0.00	200.0
93	0.00	200.0
94	0.00	200.0
95	0.00	200.0
96	0.00	200.0
97	0.00	200.0
98	0.00	200.0
99	0.00	200.0
100	0.00	200.0
101	0.00	200.0
102	0.00	200.0
103	0.00	200.0
104	0.00	200.0

Time (s)	Speed (mph)	Elevation (m)
105	0.00	200.0
106	0.00	200.0
107	0.00	200.0
108	0.00	200.0
109	0.00	200.0
110	0.00	200.0
111	0.00	200.0
112	0.00	200.0
113	0.00	200.0
114	0.00	200.0
115	0.00	200.0
116	0.00	200.0
117	0.00	200.0
118	0.00	200.0
119	0.00	200.0
120	0.00	200.0
121	0.00	200.0
122	0.00	200.0
123	0.00	200.0
124	0.00	200.0
125	0.45	200.0
126	1.37	200.0
127	2.57	200.0
128	2.86	200.0
129	3.36	200.0
130	3.43	200.0
131	3.51	200.0
132	4.84	200.0
133	5.52	200.0
134	5.57	200.0
135	5.61	200.0
136	6.10	200.0
137	6.30	200.0
138	6.35	200.0
139	6.39	200.0
140	6.49	200.0
141	7.76	200.0
142	8.38	200.0
143	8.42	200.0
144	8.66	200.0
145	9.35	200.0
146	9.57	200.0
147	9.64	200.0
148	10.70	200.0
149	10.84	200.0
150	10.79	200.0
151	10.82	200.0
152	11.74	200.0
153	11.76	200.0
154	11.68	200.0
155	11.52	200.0
156	11.93	200.0
157	11.45	200.0
158	12.34	200.0
159	12.87	200.0
160	12.88	200.0

Time (s)	Speed (mph)	Elevation (m)
161	13.14	200.0
162	13.22	200.0
163	13.21	200.0
164	14.31	200.0
165	14.45	200.0
166	14.49	200.0
167	15.10	200.0
168	15.43	200.0
169	16.60	200.0
170	17.25	200.1
171	17.71	200.2
172	17.72	200.4
173	18.00	200.6
174	19.09	200.9
175	19.15	201.1
176	20.14	201.4
177	20.91	201.7
178	21.67	202.0
179	21.70	202.3
180	22.38	202.5
181	23.05	202.7
182	23.48	202.9
183	23.65	203.0
184	23.72	203.0
185	24.80	203.0
186	24.82	203.1
187	26.26	203.1
188	26.28	203.1
189	27.54	203.2
190	28.56	203.3
191	28.60	203.3
192	29.42	203.5
193	30.18	203.6
194	30.18	203.6
195	30.67	203.8
196	31.14	203.9
197	31.38	204.1
198	31.43	204.1
199	31.98	203.7
200	32.27	203.4
201	33.01	203.2
202	33.02	203.2
203	33.38	202.9
204	33.93	202.6
205	35.00	202.3
206	35.04	202.3
207	36.16	202.1
208	37.17	201.9
209	37.19	201.9
210	38.13	201.7
211	38.50	201.6
212	38.50	201.6
213	38.85	201.6
214	38.94	201.6
215	39.20	201.3
216	39.54	201.1

Time (s)	Speed (mph)	Elevation (m)
217	40.01	200.7
218	40.27	200.3
219	39.65	199.8
220	39.63	199.4
221	39.72	199.3
222	40.09	199.3
223	41.19	199.3
224	41.49	199.4
225	41.48	199.5
226	41.49	199.5
227	41.65	199.5
228	42.01	199.5
229	42.00	199.6
230	42.09	199.8
231	42.57	199.8
232	43.17	199.8
233	43.51	199.8
234	43.76	199.8
235	44.08	199.7
236	44.12	199.5
237	44.03	199.1
238	43.94	198.8
239	43.78	198.5
240	43.58	198.3
241	43.13	198.3
242	43.27	198.0
243	43.99	197.7
244	44.55	197.5
245	44.71	197.3
246	45.47	197.0
247	45.58	196.6
248	45.58	196.3
249	45.83	196.3
250	46.03	196.3
251	46.38	196.0
252	46.61	195.8
253	46.79	195.8
254	47.02	195.6
255	47.17	195.4
256	47.16	195.4
257	47.12	196.1
258	46.96	196.7
259	46.88	197.4
260	47.78	197.3
261	48.74	197.3
262	49.02	197.3
263	49.24	197.4
264	49.08	197.3
265	49.00	197.3
266	48.82	197.3
267	48.75	197.3
268	48.84	197.3
269	49.21	196.9
270	49.75	196.5
271	49.82	196.1
272	49.96	196.1

Time (s)	Speed (mph)	Elevation (m)
273	50.15	195.9
274	50.31	195.7
275	50.81	195.7
276	51.19	195.3
277	51.47	194.9
278	51.64	194.8
279	51.54	195.0
280	51.51	195.1
281	51.49	195.5
282	51.20	196.1
283	50.88	196.5
284	50.94	196.5
285	50.97	195.7
286	52.05	195.7
287	52.96	195.7
288	53.16	195.7
289	53.07	195.7
290	53.05	195.6
291	53.17	195.6
292	53.25	195.5
293	53.34	195.5
294	53.44	195.5
295	53.47	195.4
296	53.18	195.5
297	51.92	196.1
298	52.26	196.4
299	52.48	196.3
300	52.62	195.9
301	52.46	196.0
302	52.22	196.1
303	52.00	196.4
304	52.09	196.6
305	52.17	196.6
306	52.62	196.7
307	53.03	196.9
308	53.67	197.0
309	54.33	197.1
310	54.29	197.1
311	54.42	196.1
312	54.92	195.2
313	55.01	194.3
314	55.17	194.3
315	55.06	194.3
316	55.05	194.3
317	55.02	194.2
318	55.01	194.2
319	55.14	194.2
320	55.67	194.1
321	55.98	194.0
322	56.23	193.9
323	55.85	193.9
324	55.48	195.0
325	55.02	196.1
326	54.49	197.1
327	54.42	197.1
328	54.42	197.0

Time (s)	Speed (mph)	Elevation (m)
329	54.77	196.8
330	54.91	196.6
331	55.16	196.4
332	55.33	196.1
333	55.42	195.8
334	55.69	195.5
335	56.38	195.3
336	57.10	195.1
337	57.77	194.9
338	58.41	194.7
339	58.59	194.6
340	58.65	194.4
341	58.65	194.2
342	58.62	194.0
343	58.61	193.9
344	58.57	193.7
345	58.98	193.7
346	59.44	193.8
347	59.99	193.9
348	59.99	193.9
349	59.99	193.9
350	59.64	193.9
351	59.22	193.9
352	58.79	193.9
353	58.27	193.9
354	57.98	193.9
355	57.76	193.9
356	57.05	193.9
357	56.78	193.9
358	56.67	193.9
359	56.59	193.9
360	56.60	194.0
361	56.71	194.1
362	56.71	194.2
363	56.78	194.3
364	57.06	194.4
365	57.40	194.6
366	57.59	194.8
367	57.61	195.0
368	57.80	195.1
369	57.83	195.3
370	57.84	195.4
371	58.16	195.5
372	58.71	195.7
373	59.08	195.8
374	59.44	195.8
375	60.12	195.8
376	60.01	195.8
377	59.95	195.8
378	59.91	195.8
379	59.88	195.8
380	59.81	195.8
381	59.88	195.8
382	59.91	196.0
383	59.94	196.4
384	59.95	196.7

Time (s)	Speed (mph)	Elevation (m)
385	60.10	196.9
386	60.72	196.9
387	61.34	196.9
388	61.92	196.8
389	62.48	196.7
390	62.09	196.7
391	61.73	197.3
392	61.47	197.9
393	61.88	197.9
394	62.24	197.9
395	62.32	197.8
396	62.41	197.6
397	63.02	197.2
398	63.78	196.7
399	64.63	196.2
400	65.48	195.6
401	66.09	195.1
402	66.31	194.5
403	66.35	194.0
404	66.42	193.5
405	66.49	193.2
406	66.57	192.9
407	66.66	192.7
408	66.73	192.7
409	66.80	192.7
410	66.81	192.7
411	66.75	192.7
412	66.69	192.7
413	66.63	192.7
414	66.75	192.7
415	66.81	192.7
416	66.84	192.6
417	66.88	192.4
418	66.93	192.2
419	67.01	192.0
420	67.07	191.7
421	67.16	191.4
422	67.25	191.1
423	67.32	190.8
424	67.38	190.5
425	67.38	190.3
426	67.35	190.1
427	67.35	190.0
428	67.40	190.0
429	67.48	190.0
430	67.58	190.0
431	67.67	190.0
432	67.81	189.9
433	67.89	189.8
434	67.96	189.7
435	68.00	189.6
436	68.02	189.5
437	68.09	189.5
438	68.01	189.5
439	68.02	189.5
440	68.66	189.5

Time (s)	Speed (mph)	Elevation (m)
441	69.32	189.1
442	69.91	188.7
443	69.63	188.7
444	69.44	188.8
445	69.44	188.9
446	69.44	189.2
447	69.45	189.6
448	69.63	190.1
449	69.74	190.6
450	69.79	191.0
451	69.89	191.5
452	69.94	191.9
453	69.97	192.3
454	70.00	192.7
455	70.01	193.0
456	70.00	193.3
457	70.00	193.6
458	70.00	193.9
459	69.96	194.3
460	69.91	194.6
461	69.83	195.1
462	69.65	195.5
463	69.44	196.1
464	69.29	196.7
465	69.03	197.4
466	68.82	198.1
467	68.72	198.9
468	68.43	199.7
469	68.28	200.6
470	68.00	201.5
471	67.88	202.5
472	67.62	203.4
473	67.48	204.4
474	67.24	205.4
475	67.13	206.3
476	66.93	207.2
477	66.86	208.1
478	66.83	208.9
479	66.83	209.6
480	66.86	210.3
481	66.92	210.9
482	67.07	211.4
483	67.28	211.9
484	67.50	212.3
485	67.74	212.7
486	68.13	212.9
487	68.43	213.1
488	68.92	213.3
489	69.22	213.3
490	69.43	213.3
491	69.65	213.3
492	69.80	213.3
493	69.93	213.3
494	70.19	213.3
495	70.38	213.3
496	70.44	213.3

Time (s)	Speed (mph)	Elevation (m)
497	70.59	213.3
498	70.58	213.2
499	70.58	213.1
500	70.58	213.1
501	70.64	213.0
502	70.73	212.9
503	70.81	212.9
504	70.84	212.9
505	70.87	212.9
506	70.96	212.8
507	71.05	212.7
508	71.11	212.7
509	71.14	212.6
510	71.17	212.5
511	71.17	212.4
512	71.17	212.4
513	71.17	212.4
514	71.13	212.4
515	71.08	212.4
516	71.05	212.4
517	71.09	212.4
518	71.11	212.4
519	71.23	212.4
520	71.26	212.4
521	71.26	212.4
522	71.28	212.4
523	71.21	212.4
524	71.22	212.4
525	71.18	212.4
526	71.17	212.4
527	71.40	212.4
528	71.65	212.4
529	72.06	212.4
530	72.15	212.5
531	72.30	212.5
532	72.38	212.5
533	72.31	212.5
534	72.24	212.5
535	72.18	212.5
536	72.16	212.5
537	72.68	212.6
538	73.12	211.8
539	73.41	211.0
540	73.13	210.4
541	72.79	210.0
542	72.44	209.6
543	72.00	209.4
544	71.47	209.4
545	71.19	209.4
546	70.82	209.3
547	70.47	209.3
548	69.90	209.1
549	69.23	209.0
550	68.73	208.8
551	68.05	208.5
552	67.33	208.2

Time (s)	Speed (mph)	Elevation (m)
553	66.95	207.8
554	66.94	207.4
555	66.94	207.0
556	66.97	206.5
557	67.22	205.9
558	67.38	205.4
559	67.77	204.9
560	67.99	204.4
561	68.28	203.9
562	68.41	203.5
563	68.66	203.0
564	68.79	202.6
565	68.94	202.1
566	69.01	201.7
567	69.03	201.3
568	69.21	200.9
569	69.37	200.5
570	69.40	200.1
571	69.46	199.7
572	69.64	199.3
573	69.70	198.9
574	69.91	198.5
575	70.13	198.1
576	70.35	197.6
577	70.45	197.2
578	70.51	196.7
579	70.52	196.1
580	70.52	195.5
581	70.51	194.9
582	70.49	194.1
583	70.46	193.4
584	70.35	192.4
585	70.20	191.4
586	70.03	190.3
587	69.94	189.0
588	69.85	187.7
589	69.72	186.3
590	69.63	184.7
591	69.59	183.0
592	69.55	181.3
593	69.39	179.7
594	69.36	178.1
595	69.36	176.6
596	69.36	175.2
597	69.37	173.9
598	69.38	172.6
599	69.39	171.4
600	69.41	170.1
601	69.41	168.9
602	69.42	167.7
603	69.45	166.5
604	69.46	165.3
605	69.47	164.1
606	69.50	163.0
607	69.51	161.8
608	69.48	160.6

Time (s)	Speed (mph)	Elevation (m)
609	69.44	159.5
610	69.34	158.5
611	69.28	157.6
612	69.02	156.9
613	68.77	156.2
614	68.63	155.7
615	68.50	155.3
616	68.50	155.0
617	68.50	154.8
618	68.64	154.6
619	68.87	154.5
620	68.96	154.5
621	69.11	154.4
622	69.14	154.2
623	69.19	154.1
624	69.25	153.9
625	69.27	153.8
626	69.31	153.7
627	69.44	153.6
628	69.48	153.6
629	69.53	153.6
630	69.72	153.5
631	70.00	153.3
632	70.22	153.1
633	70.49	152.9
634	70.68	152.5
635	70.90	152.1
636	70.91	151.5
637	70.94	150.9
638	70.95	150.3
639	70.98	149.6
640	70.98	148.9
641	70.97	148.1
642	70.95	147.4
643	70.96	146.6
644	70.94	145.8
645	70.89	145.0
646	70.83	144.3
647	70.78	143.6
648	70.62	142.9
649	70.55	142.9
650	70.47	142.9
651	70.22	142.2
652	70.04	141.7
653	69.87	141.2
654	69.46	140.8
655	69.30	140.5
656	69.22	140.5
657	69.14	140.5
658	69.05	140.5
659	68.97	140.5
660	68.34	140.3
661	67.57	140.2
662	66.88	140.2
663	66.70	140.2
664	66.49	140.2

Time (s)	Speed (mph)	Elevation (m)
665	66.21	140.3
666	66.08	140.4
667	66.14	140.6
668	66.13	140.9
669	66.08	141.2
670	66.04	141.6
671	65.96	142.1
672	65.92	142.4
673	65.87	142.7
674	65.84	142.9
675	65.84	143.0
676	65.79	143.1
677	65.67	143.1
678	65.70	143.1
679	65.86	143.1
680	65.84	143.1
681	65.84	143.1
682	65.76	143.1
683	65.43	143.1
684	65.00	143.1
685	64.57	143.1
686	64.49	143.1
687	64.41	143.1
688	64.32	143.1
689	63.59	143.1
690	62.85	143.1
691	62.50	143.1
692	62.31	143.0
693	62.30	142.9
694	62.63	142.3
695	62.88	142.0
696	63.18	141.7
697	63.49	141.4
698	63.75	141.0
699	64.10	140.6
700	64.33	140.1
701	64.60	139.7
702	64.87	139.3
703	65.10	138.8
704	65.33	138.4
705	65.57	138.0
706	65.65	137.6
707	65.72	137.1
708	65.81	136.7
709	65.99	136.3
710	66.08	136.0
711	66.13	135.7
712	66.21	135.4
713	66.37	135.2
714	66.20	135.2
715	66.05	135.5
716	65.90	136.0
717	65.66	136.7
718	65.58	137.4
719	65.32	138.0
720	65.06	138.6

Time (s)	Speed (mph)	Elevation (m)
721	65.06	139.1
722	65.14	139.3
723	65.22	139.5
724	65.30	139.7
725	65.36	139.8
726	65.72	140.1
727	65.99	140.4
728	66.32	140.4
729	66.58	140.4
730	66.86	140.3
731	67.43	140.2
732	67.89	140.0
733	68.44	140.0
734	67.99	140.2
735	67.79	140.9
736	67.52	141.8
737	67.33	142.6
738	66.97	143.1
739	66.89	143.1
740	66.86	143.0
741	66.74	142.6
742	66.39	142.1
743	66.14	141.7
744	66.02	141.4
745	65.91	141.1
746	65.62	140.9
747	64.86	140.7
748	64.69	140.7
749	64.74	140.7
750	64.75	140.8
751	64.67	141.0
752	64.50	141.1
753	64.48	141.2
754	64.55	141.3
755	64.72	141.4
756	64.89	141.4
757	65.32	141.5
758	65.66	141.5
759	65.38	141.7
760	65.14	142.4
761	64.86	143.4
762	64.62	144.4
763	64.38	145.4
764	64.14	146.3
765	63.85	147.2
766	63.62	148.0
767	63.50	148.7
768	63.42	149.4
769	63.33	150.0
770	63.32	150.5
771	63.33	150.9
772	63.35	151.3
773	63.36	151.5
774	63.47	151.7
775	63.56	151.8
776	63.47	151.8

Time (s)	Speed (mph)	Elevation (m)
777	63.44	151.8
778	63.44	151.9
779	63.39	152.0
780	63.35	152.1
781	63.31	152.4
782	63.08	152.7
783	62.81	153.1
784	62.56	153.6
785	62.30	154.1
786	62.18	154.8
787	61.96	155.5
788	61.79	156.3
789	61.70	157.1
790	61.57	157.9
791	61.44	158.7
792	61.35	159.5
793	61.23	160.3
794	61.14	161.1
795	60.97	161.9
796	60.91	162.6
797	60.99	163.2
798	61.17	163.6
799	61.51	164.0
800	61.77	164.2
801	62.46	164.2
802	62.77	164.2
803	62.86	163.9
804	62.97	163.0
805	63.12	162.2
806	63.22	161.3
807	63.71	160.4
808	63.83	159.5
809	63.91	158.6
810	63.91	157.7
811	63.77	157.2
812	63.65	157.1
813	63.74	157.1
814	63.91	157.1
815	64.04	157.1
816	64.16	157.0
817	64.24	156.9
818	64.30	156.7
819	64.35	156.5
820	64.40	156.3
821	64.42	156.0
822	64.43	155.8
823	64.43	155.5
824	64.42	155.2
825	64.42	154.9
826	64.42	154.6
827	64.41	154.3
828	64.39	153.9
829	64.36	153.6
830	64.31	153.3
831	64.26	153.0
832	64.24	152.7

Time (s)	Speed (mph)	Elevation (m)
833	64.20	152.4
834	64.13	152.2
835	64.04	151.9
836	63.90	151.8
837	63.84	151.6
838	63.76	151.4
839	63.52	151.3
840	62.85	151.2
841	62.51	151.2
842	62.40	151.1
843	62.29	151.1
844	62.22	151.2
845	62.20	151.3
846	62.28	151.5
847	62.15	151.5
848	62.13	151.7
849	62.12	152.0
850	62.12	152.2
851	62.12	152.5
852	62.20	152.8
853	62.28	152.8
854	62.47	152.8
855	62.60	152.8
856	63.04	152.9
857	63.49	153.0
858	63.57	153.0
859	64.19	153.0
860	64.63	153.0
861	64.89	153.1
862	65.07	153.2
863	65.15	153.2
864	65.24	153.3
865	65.32	153.3
866	65.40	153.3
867	65.40	153.3
868	65.39	153.3
869	65.38	153.3
870	65.36	153.3
871	64.81	153.2
872	64.47	153.2
873	64.28	153.2
874	64.01	153.2
875	63.72	153.7
876	63.31	154.3
877	63.08	154.9
878	63.04	154.9
879	63.05	154.8
880	63.05	154.7
881	63.21	154.7
882	63.30	154.7
883	63.56	154.7
884	64.28	154.7
885	64.64	154.7
886	64.86	154.8
887	65.01	154.9
888	65.07	154.9

Time (s)	Speed (mph)	Elevation (m)
889	65.15	155.0
890	65.21	155.1
891	65.07	155.1
892	64.93	155.1
893	64.79	155.1
894	64.65	155.2
895	64.62	155.3
896	64.63	155.5
897	64.68	155.7
898	64.75	155.8
899	64.83	156.0
900	64.91	156.2
901	64.99	156.3
902	65.08	156.4
903	65.20	156.5
904	65.75	156.5
905	66.20	156.3
906	66.38	156.2
907	66.50	156.1
908	66.32	156.1
909	65.68	156.1
910	65.55	156.1
911	65.40	156.1
912	65.35	156.0
913	65.24	156.0
914	65.23	156.0
915	65.23	155.9
916	65.23	155.9
917	65.33	155.8
918	65.50	155.8
919	65.97	155.8
920	66.34	155.8
921	66.71	155.9
922	67.00	155.9
923	67.39	156.0
924	67.39	156.0
925	67.30	156.0
926	67.35	156.0
927	67.50	156.0
928	67.72	156.2
929	67.96	156.3
930	68.09	156.6
931	68.13	156.9
932	68.14	157.3
933	68.14	157.8
934	68.06	158.4
935	67.98	159.1
936	67.92	159.8
937	67.84	160.5
938	67.78	161.3
939	67.72	162.0
940	67.66	162.8
941	67.59	163.5
942	67.53	164.2
943	67.37	164.8
944	67.24	165.5

Time (s)	Speed (mph)	Elevation (m)
945	67.16	166.1
946	66.91	166.7
947	66.83	167.2
948	66.76	167.7
949	66.76	168.1
950	66.77	168.7
951	66.87	168.9
952	67.10	169.0
953	67.39	169.0
954	67.05	169.0
955	66.38	169.0
956	66.19	169.1
957	66.07	169.1
958	65.70	169.2
959	65.69	169.2
960	65.69	169.3
961	65.75	169.3
962	66.65	169.1
963	67.53	168.8
964	67.88	168.8
965	67.88	168.8
966	67.88	169.1
967	67.35	169.5
968	66.76	170.1
969	66.26	170.8
970	65.71	171.7
971	65.19	172.6
972	64.72	173.6
973	64.35	174.4
974	64.11	175.3
975	64.01	176.0
976	63.98	176.7
977	63.98	177.3
978	63.99	177.8
979	64.09	178.2
980	64.11	178.5
981	64.14	178.7
982	64.31	178.8
983	64.57	179.0
984	64.88	179.0
985	64.53	178.9
986	63.62	178.8
987	62.60	178.7
988	62.77	178.7
989	62.99	178.7
990	63.57	178.7
991	64.24	178.6
992	64.78	178.6
993	65.22	178.5
994	65.46	178.4
995	65.62	178.2
996	66.27	178.1
997	66.92	177.9
998	67.59	177.7
999	68.07	177.5
1000	68.19	177.4

Time (s)	Speed (mph)	Elevation (m)
1001	68.35	177.2
1002	68.41	177.0
1003	68.48	176.9
1004	68.63	176.7
1005	68.77	176.6
1006	68.86	176.5
1007	68.94	176.3
1008	69.47	176.2
1009	70.06	176.1
1010	70.59	176.0
1011	71.16	175.8
1012	71.68	175.6
1013	72.27	175.5
1014	72.33	175.3
1015	72.33	175.1
1016	72.34	174.9
1017	72.34	174.8
1018	72.34	174.6
1019	72.33	174.4
1020	72.34	174.3
1021	72.34	174.1
1022	72.34	173.9
1023	72.33	173.7
1024	72.32	173.6
1025	72.26	173.4
1026	72.15	173.3
1027	72.05	173.1
1028	72.01	173.0
1029	71.84	172.9
1030	71.57	172.9
1031	71.49	172.9
1032	71.43	172.9
1033	71.74	172.9
1034	71.91	173.0
1035	71.98	173.0
1036	72.43	173.0
1037	72.73	172.9
1038	73.00	172.6
1039	73.04	172.3
1040	73.11	172.2
1041	73.29	171.7
1042	73.46	171.0
1043	73.81	170.2
1044	74.65	169.2
1045	74.98	168.2
1046	75.42	167.2
1047	75.51	166.4
1048	75.59	165.8
1049	75.67	165.3
1050	75.58	165.3
1051	75.50	165.3
1052	75.54	165.3
1053	75.67	165.3
1054	75.91	164.7
1055	76.41	164.1
1056	76.56	163.5

Time (s)	Speed (mph)	Elevation (m)
1057	76.54	162.8
1058	76.51	162.8
1059	76.53	162.8
1060	76.62	162.2
1061	76.81	161.4
1062	76.88	160.7
1063	76.97	159.9
1064	77.06	158.9
1065	77.05	158.9
1066	77.19	158.1
1067	77.39	157.3
1068	78.01	156.7
1069	78.03	156.3
1070	77.24	155.9
1071	76.24	155.6
1072	76.07	155.4
1073	75.98	155.4
1074	75.90	155.4
1075	75.82	155.4
1076	75.62	155.4
1077	75.28	155.4
1078	74.85	155.4
1079	74.77	155.4
1080	74.74	155.4
1081	74.76	155.4
1082	74.43	155.6
1083	73.99	155.9
1084	73.93	156.0
1085	73.78	156.1
1086	73.73	156.1
1087	73.74	156.2
1088	73.77	156.3
1089	73.79	156.3
1090	73.82	156.5
1091	73.83	156.5
1092	73.85	156.7
1093	73.87	157.0
1094	73.87	157.0
1095	73.95	157.3
1096	74.02	157.4
1097	74.08	157.5
1098	73.92	157.6
1099	74.00	157.7
1100	74.21	157.9
1101	74.41	158.1
1102	74.49	158.3
1103	74.58	158.5
1104	74.66	158.6
1105	74.74	158.7
1106	74.82	158.7
1107	74.98	158.7
1108	75.13	158.7
1109	75.21	158.6
1110	75.34	158.5
1111	75.43	158.4
1112	75.49	158.1

Time (s)	Speed (mph)	Elevation (m)
1113	75.48	157.9
1114	75.30	157.6
1115	75.15	157.3
1116	74.96	157.1
1117	74.90	156.8
1118	74.88	156.5
1119	74.88	156.2
1120	74.86	155.9
1121	74.84	155.7
1122	74.84	155.4
1123	74.87	155.1
1124	74.88	154.8
1125	74.90	154.5
1126	74.90	154.2
1127	74.88	154.0
1128	74.79	153.8
1129	74.65	153.7
1130	74.47	153.6
1131	74.38	153.5
1132	74.25	153.5
1133	74.07	153.5
1134	74.00	153.5
1135	73.91	153.5
1136	73.82	153.5
1137	73.62	153.5
1138	73.37	153.6
1139	73.34	153.7
1140	73.34	153.8
1141	73.34	153.8
1142	73.51	153.8
1143	73.59	153.8
1144	73.09	153.8
1145	72.56	154.0
1146	72.49	154.4
1147	72.22	154.9
1148	71.98	155.6
1149	71.87	156.4
1150	71.47	157.2
1151	71.09	158.2
1152	70.68	159.2
1153	70.35	160.4
1154	70.00	161.5
1155	69.68	162.7
1156	69.25	163.9
1157	68.97	165.0
1158	68.69	166.0
1159	68.54	167.0
1160	68.54	167.8
1161	68.54	168.4
1162	68.55	168.8
1163	68.98	169.2
1164	67.89	169.2
1165	68.09	169.3
1166	68.46	169.8
1167	68.65	170.3
1168	69.01	170.7

Time (s)	Speed (mph)	Elevation (m)
1169	69.28	171.1
1170	69.58	171.5
1171	70.00	171.8
1172	69.94	171.8
1173	69.94	171.4
1174	69.93	171.2
1175	69.91	170.9
1176	69.88	170.5
1177	69.89	170.2
1178	69.87	170.0
1179	69.86	169.7
1180	69.85	169.5
1181	69.82	169.3
1182	69.78	169.0
1183	69.76	168.8
1184	69.79	168.5
1185	69.83	168.3
1186	69.90	168.0
1187	69.93	167.6
1188	69.97	167.2
1189	69.93	166.8
1190	69.92	166.3
1191	69.89	165.8
1192	69.88	165.2
1193	69.93	165.2
1194	70.33	165.3
1195	70.67	165.3
1196	70.99	165.4
1197	71.41	165.6
1198	71.62	165.8
1199	71.70	166.0
1200	71.79	166.2
1201	71.83	166.4
1202	71.91	166.6
1203	71.98	166.8
1204	72.01	167.1
1205	72.05	167.2
1206	72.05	167.4
1207	72.04	167.6
1208	71.99	167.8
1209	71.82	168.0
1210	71.56	168.1
1211	71.22	168.3
1212	70.95	168.3
1213	70.69	168.4
1214	70.60	168.4
1215	70.53	168.4
1216	70.47	168.5
1217	70.51	168.7
1218	70.47	168.7
1219	70.46	168.7
1220	70.59	168.9
1221	70.68	169.4
1222	70.77	169.8
1223	70.85	170.2
1224	70.98	170.6

Time (s)	Speed (mph)	Elevation (m)
1225	71.11	171.1
1226	71.28	171.5
1227	71.40	171.9
1228	71.54	172.4
1229	71.61	173.2
1230	71.62	173.6
1231	71.59	174.0
1232	71.58	174.4
1233	71.64	175.0
1234	71.69	175.3
1235	71.76	175.6
1236	71.87	175.8
1237	71.92	176.1
1238	71.92	176.4
1239	71.86	176.8
1240	71.80	177.2
1241	71.72	177.7
1242	71.46	178.2
1243	71.12	178.8
1244	70.94	179.4
1245	70.64	180.0
1246	70.40	180.7
1247	69.88	181.4
1248	69.62	182.1
1249	69.53	182.8
1250	69.26	183.5
1251	68.90	184.1
1252	68.52	184.8
1253	68.33	185.4
1254	68.08	185.9
1255	67.91	186.5
1256	67.87	187.0
1257	67.86	187.6
1258	67.76	188.1
1259	67.76	188.6
1260	67.79	189.1
1261	67.85	189.6
1262	67.92	190.1
1263	67.95	190.6
1264	67.96	191.0
1265	67.91	191.4
1266	67.85	191.6
1267	67.79	191.7
1268	67.74	191.7
1269	67.80	191.7
1270	68.07	191.8
1271	68.11	192.0
1272	68.15	192.2
1273	68.18	192.4
1274	68.23	192.6
1275	68.25	192.8
1276	68.21	193.0
1277	68.18	193.1
1278	68.15	193.1
1279	68.36	193.1
1280	68.69	193.1

Time (s)	Speed (mph)	Elevation (m)
1281	69.06	193.1
1282	68.89	193.1
1283	68.85	193.4
1284	68.79	193.6
1285	68.75	193.9
1286	68.70	194.1
1287	68.59	194.3
1288	68.54	194.4
1289	68.54	194.5
1290	68.54	194.6
1291	68.45	194.6
1292	68.04	194.6
1293	67.62	194.6
1294	67.46	194.7
1295	67.38	194.7
1296	67.30	194.7
1297	67.23	194.7
1298	66.82	194.8
1299	66.47	195.0
1300	66.27	195.2
1301	66.23	195.4
1302	66.23	195.6
1303	66.23	195.8
1304	66.38	196.0
1305	66.57	196.1
1306	66.80	196.1
1307	66.97	196.2
1308	68.00	195.7
1309	69.09	195.2
1310	69.01	195.2
1311	68.97	195.2
1312	68.96	195.2
1313	68.96	195.0
1314	68.99	194.8
1315	69.00	194.5
1316	69.00	194.2
1317	68.99	193.9
1318	68.95	193.5
1319	68.95	193.1
1320	68.95	192.6
1321	68.78	192.6
1322	68.54	192.1
1323	68.34	191.6
1324	67.99	191.3
1325	68.00	191.3
1326	68.07	190.3
1327	69.33	190.3
1328	70.63	189.3
1329	70.75	189.3
1330	70.92	189.6
1331	71.33	189.8
1332	71.68	190.1
1333	71.63	190.4
1334	70.93	190.7
1335	70.85	190.9
1336	70.29	190.9

Time (s)	Speed (mph)	Elevation (m)
1337	70.03	190.9
1338	70.36	190.8
1339	71.08	190.7
1340	71.16	190.7
1341	71.25	190.7
1342	71.33	190.7
1343	71.63	190.7
1344	71.81	190.8
1345	71.87	190.8
1346	71.91	190.7
1347	71.99	190.7
1348	72.07	190.6
1349	72.25	190.4
1350	72.33	190.2
1351	72.48	190.0
1352	72.60	189.7
1353	72.70	189.3
1354	72.74	188.9
1355	72.74	188.6
1356	72.74	188.2
1357	72.70	187.8
1358	72.63	187.4
1359	72.61	187.0
1360	72.55	186.7
1361	72.45	186.4
1362	72.22	186.2
1363	72.23	186.2
1364	72.38	186.2
1365	72.48	186.1
1366	72.48	185.8
1367	72.36	185.4
1368	72.33	185.0
1369	72.25	184.6
1370	72.19	184.1
1371	72.15	183.6
1372	72.13	183.1
1373	72.11	182.6
1374	72.05	182.1
1375	72.01	181.5
1376	71.94	181.0
1377	71.92	180.5
1378	71.91	180.1
1379	71.90	179.6
1380	71.90	179.2
1381	71.90	178.7
1382	71.88	178.4
1383	71.80	178.0
1384	71.69	177.6
1385	71.61	177.3
1386	71.58	177.0
1387	71.58	176.7
1388	71.58	176.5
1389	71.60	176.2
1390	71.67	176.0
1391	71.77	175.8
1392	71.82	175.6

Time (s)	Speed (mph)	Elevation (m)
1393	71.89	175.4
1394	71.92	175.2
1395	71.94	175.0
1396	71.95	174.9
1397	71.96	174.7
1398	71.95	174.3
1399	71.94	174.2
1400	71.92	174.0
1401	71.89	173.8
1402	71.89	173.6
1403	71.89	173.4
1404	71.88	173.3
1405	71.97	173.1
1406	72.06	173.0
1407	72.05	173.0
1408	72.04	172.8
1409	72.09	172.3
1410	72.16	171.6
1411	72.18	170.9
1412	72.18	170.1
1413	72.19	169.3
1414	72.09	168.6
1415	71.96	167.8
1416	71.82	167.2
1417	71.66	166.6
1418	71.61	166.1
1419	71.46	165.7
1420	71.34	165.4
1421	71.32	165.2
1422	71.32	165.1
1423	71.40	165.0
1424	71.57	165.0
1425	71.80	165.0
1426	72.07	165.0
1427	72.18	165.0
1428	72.18	165.0
1429	72.13	164.9
1430	72.07	164.9
1431	72.04	164.8
1432	72.02	164.7
1433	72.01	164.7
1434	72.02	164.6
1435	72.09	164.4
1436	72.17	164.4
1437	72.24	164.3
1438	72.27	164.2
1439	72.18	164.2
1440	72.00	164.1
1441	71.81	164.1
1442	71.89	164.1
1443	71.96	164.1
1444	72.04	164.1
1445	72.12	164.1
1446	72.24	164.1
1447	72.43	164.1
1448	72.62	164.0

Time (s)	Speed (mph)	Elevation (m)
1449	72.80	164.0
1450	73.00	163.9
1451	73.26	163.9
1452	73.48	163.8
1453	73.62	163.8
1454	73.70	163.8
1455	74.06	163.7
1456	73.99	163.8
1457	73.87	164.0
1458	73.87	164.4
1459	73.85	164.5
1460	73.85	164.6
1461	73.90	164.6
1462	73.97	164.6
1463	74.01	164.6
1464	74.05	164.5
1465	74.06	164.4
1466	74.06	164.3
1467	74.07	164.3
1468	74.08	164.2
1469	74.07	164.1
1470	74.07	164.0
1471	74.06	163.9
1472	74.06	163.8
1473	74.05	163.8
1474	74.04	163.8
1475	74.01	163.8
1476	73.93	163.9
1477	73.90	164.1
1478	74.07	164.5
1479	74.21	164.8
1480	74.29	165.1
1481	74.63	165.4
1482	74.81	165.5
1483	74.89	165.6
1484	75.24	165.6
1485	75.51	165.5
1486	75.61	165.4
1487	75.62	165.3
1488	75.55	165.1
1489	75.48	164.8
1490	75.40	164.6
1491	75.29	164.4
1492	75.20	164.2
1493	75.16	164.1
1494	75.12	163.9
1495	75.10	163.7
1496	75.09	163.5
1497	75.08	163.3
1498	75.13	163.0
1499	75.17	162.8
1500	75.23	162.5
1501	75.24	162.2
1502	75.24	161.9
1503	75.24	161.6
1504	75.24	161.4

Time (s)	Speed (mph)	Elevation (m)
1505	75.25	161.1
1506	75.26	160.9
1507	75.27	160.6
1508	75.30	160.4
1509	75.32	160.3
1510	75.32	160.2
1511	75.32	160.1
1512	75.30	160.1
1513	74.33	160.1
1514	73.29	160.1
1515	72.86	160.1
1516	72.26	160.1
1517	71.69	160.1
1518	71.13	160.0
1519	70.63	160.0
1520	70.55	160.0
1521	70.47	160.5
1522	70.52	161.0
1523	70.53	161.5
1524	70.53	161.5
1525	70.52	161.4
1526	70.57	161.3
1527	70.61	161.1
1528	70.65	160.8
1529	70.70	160.4
1530	70.75	159.9
1531	70.75	159.3
1532	70.63	158.0
1533	70.54	157.3
1534	70.50	156.5
1535	70.41	155.8
1536	70.33	154.3
1537	70.19	153.7
1538	69.45	153.1
1539	68.08	152.6
1540	67.49	152.1
1541	67.28	151.7
1542	67.22	151.4
1543	67.22	150.8
1544	67.56	150.6
1545	67.96	150.4
1546	68.02	150.2
1547	68.03	150.0
1548	68.03	149.8
1549	67.83	149.4
1550	67.19	149.2
1551	66.02	149.0
1552	64.82	148.8
1553	64.19	148.6
1554	63.73	148.4
1555	62.36	148.2
1556	62.32	148.2
1557	62.45	148.2
1558	62.56	147.8
1559	62.56	147.4
1560	62.56	146.9

Time (s)	Speed (mph)	Elevation (m)
1561	62.44	146.5
1562	62.02	146.0
1563	61.88	145.6
1564	61.88	145.1
1565	61.88	144.7
1566	62.25	144.3
1567	62.60	143.9
1568	62.62	143.6
1569	62.62	143.3
1570	62.79	143.1
1571	62.81	142.9
1572	62.81	142.8
1573	62.89	142.6
1574	63.25	142.5
1575	63.50	142.4
1576	63.72	142.4
1577	63.30	142.4
1578	63.26	142.4
1579	63.27	142.2
1580	63.12	141.9
1581	62.28	141.6
1582	62.16	141.3
1583	62.16	140.9
1584	62.16	140.5
1585	62.63	140.5
1586	62.89	140.8
1587	63.06	140.8
1588	63.15	140.8
1589	63.24	140.8
1590	63.32	141.1
1591	63.58	141.1
1592	64.03	141.3
1593	63.42	141.7
1594	62.83	142.4
1595	62.77	143.1
1596	62.29	143.7
1597	61.79	144.2
1598	61.44	144.5
1599	61.03	144.5
1600	60.69	144.4
1601	60.68	144.4
1602	60.68	144.3
1603	60.75	144.3
1604	61.45	144.3
1605	62.11	144.2
1606	62.03	144.2
1607	61.38	144.5
1608	60.89	145.2
1609	60.53	145.8
1610	60.11	146.5
1611	59.85	147.1
1612	59.59	147.7
1613	59.52	148.3
1614	59.52	148.8
1615	59.52	149.3
1616	59.58	149.7

Time (s)	Speed (mph)	Elevation (m)
1617	59.75	150.1
1618	60.01	150.4
1619	60.28	150.6
1620	60.39	150.8
1621	60.60	150.8
1622	60.84	150.9
1623	60.90	151.3
1624	60.90	152.1
1625	61.05	153.0
1626	61.26	154.0
1627	61.28	155.1
1628	61.28	156.1
1629	61.28	157.2
1630	61.26	158.2
1631	61.20	159.1
1632	61.05	159.9
1633	61.04	160.6
1634	61.04	161.3
1635	61.05	161.8
1636	61.06	162.3
1637	61.06	162.7
1638	61.06	162.9
1639	60.91	162.9
1640	60.36	162.9
1641	60.34	163.0
1642	60.34	163.1
1643	60.45	163.2
1644	60.81	163.4
1645	61.11	163.6
1646	61.36	163.8
1647	61.53	164.1
1648	61.61	164.3
1649	61.64	164.4
1650	61.69	164.6
1651	61.85	164.7
1652	61.63	164.7
1653	61.54	164.7
1654	61.50	164.7
1655	61.49	164.6
1656	61.49	164.6
1657	60.77	164.5
1658	60.59	164.5
1659	60.50	164.3
1660	60.35	164.2
1661	60.14	164.0
1662	59.99	163.8
1663	59.88	163.6
1664	59.71	163.4
1665	59.59	163.2
1666	59.41	163.2
1667	59.11	163.5
1668	58.90	164.0
1669	58.77	164.7
1670	58.57	165.4
1671	58.44	166.2
1672	58.42	166.9

Time (s)	Speed (mph)	Elevation (m)
1673	58.42	167.6
1674	58.44	168.2
1675	58.63	168.8
1676	58.74	169.1
1677	58.75	169.7
1678	58.75	170.3
1679	58.69	171.0
1680	58.50	171.9
1681	58.22	172.9
1682	57.98	173.9
1683	58.23	174.9
1684	57.71	176.0
1685	57.27	176.8
1686	57.20	176.8
1687	57.11	176.8
1688	56.67	176.8
1689	56.41	176.7
1690	56.18	176.5
1691	55.98	176.2
1692	56.16	175.8
1693	56.30	175.3
1694	56.66	174.9
1695	56.99	174.6
1696	57.41	174.4
1697	57.37	174.4
1698	56.85	174.9
1699	56.78	175.5
1700	56.79	176.9
1701	56.80	177.3
1702	56.91	177.3
1703	56.99	177.6
1704	57.10	177.9
1705	57.02	177.9
1706	56.93	178.6
1707	56.85	179.0
1708	56.76	179.4
1709	56.59	179.5
1710	56.52	179.6
1711	56.44	179.6
1712	56.35	179.9
1713	56.27	180.3
1714	56.18	180.6
1715	56.09	181.4
1716	56.01	182.7
1717	55.87	183.3
1718	55.81	183.9
1719	55.77	183.9
1720	55.20	183.9
1721	54.45	183.1
1722	53.54	182.4
1723	52.74	181.9
1724	52.82	181.9
1725	52.90	181.9
1726	52.94	181.9
1727	52.91	181.8
1728	52.90	181.8

Time (s)	Speed (mph)	Elevation (m)
1729	52.90	181.7
1730	52.49	181.7
1731	51.73	181.6
1732	50.81	181.5
1733	49.81	181.5
1734	49.59	181.4
1735	49.59	181.4
1736	49.59	181.4
1737	49.81	181.4
1738	50.17	181.4
1739	50.60	181.4
1740	50.93	181.3
1741	51.16	181.3
1742	51.17	181.2
1743	51.17	181.1
1744	51.11	181.0
1745	50.99	180.8
1746	50.98	180.6
1747	50.98	180.4
1748	51.21	180.2
1749	51.70	179.9
1750	52.29	179.7
1751	52.82	179.5
1752	53.30	179.4
1753	53.63	179.2
1754	53.94	179.2
1755	54.13	179.1
1756	53.73	179.1
1757	53.72	178.3
1758	53.71	177.6
1759	53.42	177.0
1760	53.33	176.2
1761	53.17	175.5
1762	53.96	174.6
1763	54.23	173.5
1764	54.31	172.2
1765	54.37	170.8
1766	54.42	168.1
1767	54.47	166.8
1768	54.98	165.7
1769	55.60	164.7
1770	55.59	163.8
1771	55.38	161.4
1772	55.11	161.1
1773	54.98	161.2
1774	54.65	161.2
1775	54.52	161.2
1776	54.45	161.3
1777	54.36	161.3
1778	54.77	161.4
1779	55.17	161.5
1780	55.52	161.6
1781	55.60	161.6
1782	55.68	161.6
1783	55.77	161.6
1784	55.85	161.6

Time (s)	Speed (mph)	Elevation (m)
1785	55.94	161.6
1786	56.47	161.5
1787	57.05	161.2
1788	57.54	160.9
1789	58.01	160.6
1790	58.36	160.3
1791	58.58	160.0
1792	58.67	159.8
1793	58.67	159.9
1794	58.67	160.2
1795	58.69	160.6
1796	58.85	161.0
1797	59.06	161.4
1798	59.34	161.7
1799	59.66	161.8
1800	60.02	161.9
1801	60.45	161.9
1802	60.95	161.9
1803	61.37	161.9
1804	60.61	161.9
1805	60.59	161.9
1806	60.58	162.3
1807	60.57	162.8
1808	60.60	163.3
1809	60.61	163.7
1810	60.66	164.2
1811	60.68	164.6
1812	60.71	165.0
1813	60.77	165.4
1814	60.86	165.7
1815	61.02	166.0
1816	60.95	166.0
1817	60.95	165.9
1818	60.95	165.8
1819	60.73	165.8
1820	60.42	165.7
1821	59.91	165.7
1822	59.66	165.7
1823	59.06	165.7
1824	59.07	165.7
1825	59.27	165.8
1826	59.46	165.8
1827	59.61	165.9
1828	58.99	165.9
1829	58.99	165.9
1830	58.99	165.9
1831	58.99	165.6
1832	58.89	165.4
1833	58.89	165.4
1834	59.06	165.4
1835	59.17	165.4
1836	59.23	165.3
1837	59.23	165.2
1838	59.23	165.1
1839	59.30	165.0
1840	59.24	165.0

Time (s)	Speed (mph)	Elevation (m)
1841	59.17	165.0
1842	59.15	165.0
1843	59.11	165.0
1844	57.81	165.0
1845	57.73	165.0
1846	57.65	165.0
1847	57.37	165.0
1848	57.37	165.1
1849	57.51	165.5
1850	57.60	166.0
1851	57.63	166.5
1852	57.63	167.1
1853	57.63	167.7
1854	57.52	168.3
1855	57.44	168.9
1856	57.35	170.1
1857	57.25	170.7
1858	57.10	171.3
1859	55.85	171.9
1860	54.99	172.5
1861	54.80	173.1
1862	54.39	173.6
1863	53.29	174.1
1864	52.95	174.5
1865	52.50	175.0
1866	51.82	175.5
1867	51.23	176.0
1868	50.55	176.6
1869	50.51	177.0
1870	50.26	177.3
1871	48.86	177.7
1872	47.43	178.3
1873	46.61	178.9
1874	45.97	179.4
1875	46.94	179.4
1876	45.86	179.4
1877	45.72	179.5
1878	45.71	180.0
1879	46.39	180.3
1880	46.77	180.6
1881	47.05	181.0
1882	46.96	181.4
1883	46.99	181.4
1884	47.07	181.4
1885	47.16	181.4
1886	47.05	181.4
1887	47.59	181.4
1888	48.13	181.9
1889	48.73	182.4
1890	48.99	183.1
1891	48.99	183.8
1892	48.99	184.5
1893	48.11	185.1
1894	45.96	185.6
1895	43.47	185.9
1896	41.26	186.2

Time (s)	Speed (mph)	Elevation (m)
1897	40.55	186.5
1898	40.51	186.9
1899	38.97	187.4
1900	38.57	188.0
1901	36.82	188.4
1902	36.50	188.8
1903	36.49	189.2
1904	35.83	189.6
1905	35.75	189.9
1906	34.96	190.2
1907	34.73	190.4
1908	34.69	190.6
1909	33.27	190.8
1910	33.10	191.0
1911	32.08	191.1
1912	32.04	191.3
1913	31.75	191.4
1914	30.84	191.6
1915	30.48	191.7
1916	30.41	191.9
1917	29.77	192.1
1918	29.15	192.2
1919	29.06	192.4
1920	28.52	192.6
1921	28.26	192.8
1922	28.09	193.0
1923	27.30	193.2
1924	27.26	193.4
1925	26.43	193.6
1926	26.39	193.8
1927	25.22	194.0
1928	23.53	194.2
1929	23.49	194.3
1930	22.08	194.5
1931	22.04	194.7
1932	21.91	194.9
1933	21.87	195.0
1934	20.79	195.2
1935	20.26	195.2
1936	20.21	195.2
1937	19.50	195.2
1938	19.37	195.2
1939	19.05	195.2
1940	18.61	195.2
1941	18.52	195.2
1942	17.46	195.2
1943	16.75	195.2
1944	16.14	195.2
1945	15.55	195.2
1946	15.52	195.2
1947	14.95	195.2
1948	14.81	195.2
1949	13.71	195.2
1950	12.27	195.2
1951	12.23	195.2

Time (s)	Speed (mph)	Elevation (m)
1952	11.50	195.2
1953	10.97	195.2
1954	9.79	195.2
1955	8.25	195.2
1956	7.39	195.2
1957	6.65	195.2
1958	5.59	195.2
1959	4.66	195.2
1960	3.99	195.2
1961	2.91	195.2
1962	1.65	195.2
1963	0.26	195.2
1964	0.00	195.2
1965	0.00	195.2
1966	0.00	195.2
1967	0.00	195.2
1968	0.00	195.2
1969	0.00	195.2
1970	0.00	195.2
1971	0.00	195.2
1972	0.00	195.2
1973	0.00	195.2
1974	0.00	195.2
1975	0.00	195.2
1976	0.00	195.2
1977	0.00	195.2
1978	0.00	195.2
1979	0.00	195.2
1980	0.00	195.2
1981	0.00	195.2
1982	0.00	195.2
1983	0.00	195.2
1984	0.00	195.2
1985	0.00	195.2
1986	0.00	195.2
1987	0.00	195.2
1988	0.00	195.2
1989	0.00	195.2
1990	0.00	195.2
1991	0.00	195.2
1992	0.00	195.2
1993	0.00	195.2
1994	0.00	195.2
1995	0.00	195.2
1996	0.00	195.2
1997	0.00	195.2